PURSUIT-EVASION GAMES IN MOBILE NETWORKS

BY

SOURABH BHATTACHARYA

DISSERTATION

Submitted in partial fulfillment of the requirements
for the degree of Doctor of Philosophy in Electrical and Computer Engineering
in the Graduate College of the
University of Illinois at Urbana-Champaign, 2010

Urbana, Illinois

Doctoral Committee:

Professor Seth A. Hutchinson, Chair
Professor Tamer Başar
Associate Professor Daniel M. Liberzon
Professor Naira Hovakimyan
Assistant Professor Dušan M. Stipanović

ABSTRACT

In the last two decades, there has been an enormous effort to deploy a network of autonomous mobile platforms in various scenarios related to military as well as civilian applications. Interesting research problems related to security range from the development of secure communication protocols for a network of autonomous mobile agents to the development of novel deployment algorithms for a group of mobile agents trying to secure a network or an area from malicious intruders.

In this thesis, we investigate the interaction between the mobile agents and an intruder in the environment or the communication network. In contradistinction to the previous research in this area, we model the intrusion as a pursuit-evasion game in continuous time and space. We model the intruder as an antagonistic agent and apply tools from differential game theory in order to obtain the optimal motion strategies for the agents to track the intruder as well as evade intrusion.

To my parents, for their love and support.

ACKNOWLEDGMENTS

I am grateful to Professor Seth Hutchinson and Professor Tamer Başar for giving me freedom and useful advice regarding the research in my dissertation. This dissertation would not have been possible without their support. I am also thankful to my committee members Professor Naira Hovakimyan, Professor Dušan Stipanović, and Professor Daniel Liberzon for helpful discussions. In addition, I would also like to thank Professor Steven LaValle and Professor Rafael Murrieta-Cid for providing useful insights and directions at the beginning of this research.

I would also like to thank Becky Lonberger and Sharon Collins for their help regarding administrative matters.

Finally, I would like to thank my parents and sister for their love and support.

TABLE OF CONTENTS

LIST OF FIGURES

CHAPTER 1

INTRODUCTION

Pursuit-evasion games are a special class of problems that belong to the category of zero-sum games. In the classical setting, there are two players having conflicting objectives. One player is called the *pursuer* and the other player is called the *evader*. In a *game of kind*, the objective of one player (generally the pursuer) is to steer the system to a terminal set whereas the objective of the other player (generally the evader) is to steer the system away from the terminal set. In a *game of degree*, each player receives a payoff based on the outcome of the game. The objective of one of the players is to increase the outcome whereas the other player wants to decrease it. The specific role played by the pursuer or the evader depends on the game and its formulation. This idea of modeling conflict scenarios has been extended to include more than two players. In a multi-player setting, there are teams of players having conflicting objectives. In general, the role of each player and his/her payoff in a team depends on the game under consideration and the capabilities of the player.

In this thesis, we address two problems that arise in different scenarios in mobile platforms. The first problem is regarding visibility-based target tracking and the second problem is regarding motion strategies to evade jamming in communication networks. A common theme underlying both parts is the formulation of the problems as continuous time pursuit-evasion games. The constraints of visibility and communication on the vehicles manifest as a constraint in the state space. The theory of differential games provides tools to obtain the necessary conditions for the optimal strategies. In Part I, we deal with a two-player pursuit-evasion game. An extensive analysis is performed by formulating the problem of visibility-based target tracking among obstacles as a *game of degree* as well as a *game of kind*. Part II of the thesis deals with multi-player differential games. We use tools from differential game theory and algebraic graph theory to analyze the problem of jamming in mobile communication networks.

The first part of the thesis is regarding visibility-based target tracking in the

presence of obstacles. Target tracking is an interesting class of motion planning problems that considers motion strategies for a mobile robot to track a moving target among obstacles. In case of an antagonistic target, the problem lies in the framework of pursuit-evasion which belongs to a special class of problems in game theory. The goal of the pursuer is to maintain a line of sight to the evader that is not occluded by any obstacle. The goal of the evader is to escape the visibility region of the pursuer (and break this line of sight) at any instant of time.

Most of the classical problems in pursuit-evasion deal with players in obstacle-free space having either constraints on their motion or constraints on their control due to under-actuation. Research in robotics is concerned with planning feasible motion strategies for complex mechanical systems under various constraints imposed either by the internal restrictions in the motion of the robot or the geometry of the external environment due to the presence of obstacles. Complex environments impose geometric free space constraints, and pursuit-evasion problems in these environment inherit the complexity of motion planning. An additional source of complexity is visibility. If the players have a line-of-sight visibility, then they can exploit occlusions in the environment. Therefore, geometric complexity also imposes restrictions on the information available to the players. Addressing these issues requires an understanding of the combinatorial aspects of the game.

In Chapter 2, we formulate the problem of target tracking as a *game of kind*. We use the *method of explicit strategies* to completely solve the game in the presence of a corner. We extend this solution to multiple obstacles in an environment and obtain a lower bound for the size for the *escape* and the *capture set*. Furthermore, we also present bounds on the size of the escape and capture set for the case of a circular obstacle and provide an algorithm to address the problem in the presence of non-polygonal obstacles. This work has appeared in parts in [1] and [2].

In Chapter 3, we formulate the problem of target tracking as a *game of degree*. We perform the regular analysis and obtain saddle point strategies for the players. Using these strategies we provide the optimal trajectories for the players near the termination situations. Finally, we perform the singular analysis and compute the dispersal surfaces that arise when optimal trajectories from two different termination situations intersect in an environment containing two point obstacles. We extend this technique to provide an algorithm to compute the dispersal surfaces arising due to two corners in the presence of multiple obstacles. We conclude by providing an insight to extending the previous results to compute all possible dispersal surfaces in a polygonal environment containing multiple obstacles. This

work has appeared in parts in [3], [4] and [5].

The second part of the thesis addresses the problem of jamming in mobile networks. We analyze the behavior of multiple vehicles in cooperative as well as non-cooperative scenarios in the presence of a malicious intruder in the communication network. We envision a scenario in which a mobile jammer intrudes upon the communication channel in a multiple vehicle formation. In particular, we are interested in computing strategies for spatial reconfiguration of a formation in the presence of an intruder to reduce the jamming on the communication channel.

In Chapter 4, we analyze a multi-player differential game between two UAVs and an aerial jammer. The jamming, communication and mobility models for the UAVs are presented. Based on the aforementioned models, a multi-player pursuit-evasion game is analyzed. In the first problem, we assume that the two UAVs are not communicating initially. The goal of the jammer is to jam the communication channel for the maximum amount of time possible and the goal of the UAVs is to restore the communication as soon as possible. In the second problem, we assume that the UAVs are initially communicating. The goal of the jammer is to jam the communication channel in the minimum amount of time possible and the goal of the UAVs is to communicate for the maximum amount of time. Optimal strategies are obtained that guarantee a minimum payoff for each player. This work has appeared in parts in [6].

In Chapter 5, we extend the problem of jamming to address the case in which the mobile network has heterogeneous dynamics. The nodes are modeled either as aerial vehicles (unmanned aerial vehicles) or terrestrial vehicles (autonomous ground vehicles) having constraints in their configuration space and control. Optimal strategies are provided for each kind of vehicle depending on the objective of the vehicle. This work has appeared in parts in [7].

In Chapter 6, we analyze the problem of maintaining connectivity in a network of mobile agents in the presence of a jammer. This is a variation of the standard connectivity maintenance problem in which the issue arises due to limitations in communications and sensing model for each agent. In our work, the limitations in communications are due to the presence of a jammer in the vicinity. In the beginning, we present a differential game-theoretic formulation of the problem and provide the necessary conditions for optimal controls for each agent. Then we present a model that constructs a state-dependent graph based on the state-space of the agents. We use tools from algebraic-graph theory on the state-dependent graph in order to provide locally optimal control laws for the agents in the formation.

Finally, we present some simulations to validate the proposed control scheme. Parts of the this work are in [8].

In Chapter 7, we present some future research directions related to each chapter.

Part I

Visibility-Based Pursuit Evasion

CHAPTER 2

TARGET-TRACKING: A GAME OF KIND

In this work we model the target-tracking problem as a *game of kind*. In a *game of kind*, there are only two possible outcomes at the end of the game. The pursuer favors one of the possible outcomes and the evader favors the other possible outcome. The set of initial positions of the players that leads to a favorable outcome for the pursuer is called the *capture set*. The set of initial positions of the players that leads to a favorable outcome for the evader is called the *escape set*.

In this chapter, we exploit the geometry of the environment in order to provide lower bounds on the size of the *capture set* and *escape set*. In the beginning, we provide a complete spatial decomposition of the workspace for a simple environment based on the *method of explicit policy* [9]. Extending these strategies to the general environment provides us with a lower bound on the size of the *escape set* and the *capture set* [10]. The main contributions in this chapter along with the organization of the sections are as follows. First, we show in Section 2.2 that in an environment with one corner, the target-tracking problem is completely decidable. Second, we prove in Section 2.3 that in an environment containing obstacles, the initial positions of the pursuer from which it can track the evader are bounded. Though this result is trivially true for a bounded workspace, for an unbounded workspace it is intriguing. Third, while the general problem of deciding whether the evader can escape or the pursuer can track the evader forever in any arbitrary polygonal environment is still, so far as we know, an open problem, we offer partial solutions to it. In Section 2.3, we provide polynomial-time approximation schemes to bound the set of initial positions of the pursuer from which it might be able to track successfully. If the initial position of the pursuer lies outside this region, the evader escapes. The size of the region depends on the geometry of the environment and the ratio of the maximum evader speed to the maximum pursuer speed. Fourth, in Section 2.4, we present a sufficient condition for tracking. Based on this sufficient condition we provide a region around the initial position of the evader from which the pursuer can track the evader. Fifth,

in Section 2.5, we address the problem of target tracking in an environment containing non-polygonal obstacles. In the past, researchers [11] have addressed the problem of searching an evader in non-polygonal environments. However, we do not know of any prior work that addresses the problem of tracking an evader in non-polygonal environments.

In the next section, we provide a brief introduction to the problem of target tracking.

2.1 Introduction

Target tracking involves maintaining knowledge of the current location of a target. In case of visibility-based target tracking, an observer must constantly maintain a line of sight with a target. A challenging problem in this scenario is to plan motion strategies for the observer in the presence of environmental occlusions. Complex environments impose geometric free space constraints, and pursuit-evasion problems in these environment inherit the complexity of motion planning. An additional source of complexity is visibility. If the players have a line-of-sight visibility, then they can exploit occlusions in the environment. Therefore, geometric complexity also imposes restrictions on the information available to the players. Addressing these issues requires an understanding of the combinatorial aspects of the game. In this chapter, we address the problem of a mobile observer trying to maintain a line of sight with a mobile target in the presence of obstacles in the environment. Both the observer and the target are holonomic and have bounded speeds. The observer has no knowledge about the future actions of the target. In this scenario, we address the following problem: Given an initial position of the observer and the target, is it possible for the observer to track the target forever, and if so, what should be its strategy?

Target tracking is related to the game of pursuit-evasion. The goal of the pursuer is to maintain a line of sight to the evader that is not occluded by any obstacle. The goal of the evader is to escape the visibility polygon of the pursuer (and break this line of sight) at any instant of time. Apart from surveillance applications, a mobile robot might be required to continuously follow and monitor at a distance a target performing a task not necessarily related to the target tracking game such as relaying signals to and from the target [12]. The observer may also be monitoring the target for quality control, verifying the target does not perform some undesired

behavior, or ensuring that the target is not in distress. In applications that involve automated processes that need to be monitored, such as in an assembly work cell, parts or sub-assemblies might need to be verified for accuracy or are determined to be in correct configurations. Visual monitoring tasks are also suitable for mobile robot applications [13]. In home care settings, a tracking robot can follow elderly people and alert caregivers of emergencies [14]. Target-tracking techniques in the presence of obstacles have been proposed for the graphic animation of digital actors, in order to select the successive viewpoints under which an actor is to be displayed as it moves in its environment [15]. In surgical applications, controllable cameras could keep a patient's organ or tissue under continuous observation, despite unpredictable motions of potentially obstructing people and instruments. In wildlife monitoring applications, autonomous underwater vehicles use target-tracking algorithms to navigate in cluttered environments while tracking marine species.

Target-tracking using sonar and infrared sensors has been studied traditionally in the field of automatic control for naval and missile applications [16]. With the emergence of computer vision, a combination of vision and control techniques were used to design control laws to track a target using vision sensors [17, 18, 19, 20]. A major drawback of pure control approaches is that they are local by nature and it is difficult to take into account the global structure of the environment such as the configuration of workspace obstacles.

In case of a completely predictable target, the problem can be addressed using techniques from optimization. Such techniques have been used in [21] and [22] to provide algorithms for an observer to track a predictable target among obstacles. In case of an unpredictable target the hardness of the problem increases due to the lack of information about the current as well as the future strategies of the target. A plausible way to reduce the hardness of the problem is to solve the problem for specific environments. For instance, [23] solves the problem of target-tracking around a regular polygonal obstacle for a specific initial position of the observer and the target. In a similar vein, in this work we have shown that for an environment having a single corner, the problem is completely decidable [24]. Although many computationally intensive approximation and heuristic techniques [14, 25] have been used to address the target-tracking problem, the decidability in general environment still remains an open question.

In the past, various techniques have been proposed to devise strategies for an observer that optimizes a local cost function based on the current configuration

of the target and observer in the environment. In [26, 27, 28, 29], the authors formulate a risk function that takes into account the position of the target and the observer with respect to the occluding vertices of the environment. The strategy for the observer is to move in a direction that minimizes the risk function at every instant. In [30], the authors design a planner for target-tracking that takes into account the positioning uncertainty of an observer that has a map of the environment. The observer tries to minimize a utility function that maximizes the probability of future visibility of the target and minimizes the uncertainty in its own position. In [31], a motion strategy for the observer is obtained by maximizing the target's *shortest distance to escape* from the observer's field of view. Due to the greedy nature of the above techniques, the resulting strategies are not guaranteed to be optimal for the observer.

Maintaining visibility of a moving target can also be cast as a connectivity problem on a graph that encodes a pertinent cell decomposition of the workspace. In [32], the authors draw the similarity between the target-tracking problem and piano-mover's problem. They extend the three-dimensional cellular decomposition of Schwartz and Sharir [33] to represent the four-dimensional configuration space of an observer trying to maintain a fixed distance from a target. The authors reduce the problem to a recursive update and reachability problem on a graph that is constructed using the cellular decompositions. In [34], the authors introduce the notion of *strong mutual visibility* and *accessibility*. Using these two notions, they model the problem of maintaining visibility of a moving evader by means of a pair of graphs. They show that the decision problem of whether a pursuer is able to maintain *strong mutual visibility* of the evader is NP-complete. In this work, we present a complete cell decomposition of the free workspace around a single-corner and extend these decompositions to general environments. Hence we feel that the underlying theme of our work belongs to this category.

There have been some efforts in the past to address the target-tracking problem in the scenario where multiple observers try to track multiple targets. In [35], the authors present a method of tracking several evaders with multiple pursuers. Unlike our work, they do not view the problem from the perspective of computing geometric visibility. Instead they investigate the power of a weighted force vector approach distributed across robot teams in simple, uncluttered environments that are either obstacle free or have a random distribution of simple convex obstacles. In [36], the problem of tracking multiple targets is addressed using a network of communicating robots and stationary sensors. A region-based approach is in-

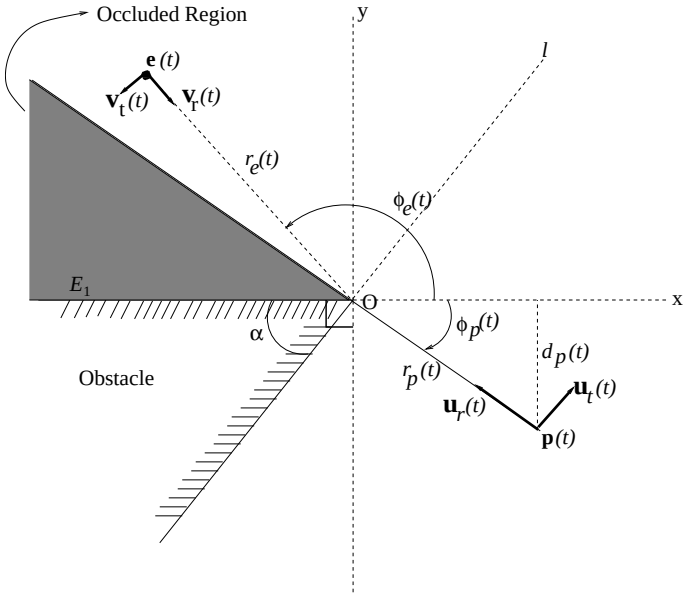

Figure 2.1: The problem environment.

troduced which controls robot deployment at two levels, namely, a coarse deployment controller and a target-following controller. In [37] and [38], authors present a behavior-based solution to the the problem of observing multiple targets using multiple robots. They propose a distributed behavior-based control system where robots share workload by assuming responsibilities concerning the observation of certain targets. In [39], the authors investigate the scenario in which the number of trackers is strictly less than the number of targets. A gradient-approximation algorithm is proposed to generate paths for mobile agents to traverse a sequence of target points. In [40], the authors propose centralized algorithms for many mobile agents to stay within an "observation range" of as many targets as possible in the absence of sensing constraints. The algorithms are based on K-means clustering and hill-climbing algorithms. None of these works (except [36]) consider the effect of occlusion in visibility due to the presence of obstacles.

In the next section, we analyze the problem of target-tracking in an environment containing a single corner.

2.2 Analysis of a Corner

In this section, we address the problem of target-tracking in a simple environment containing one corner. The workspace contains a semi-infinite obstacle with one

corner that restricts pursuer and evader motions and may occlude the pursuer's line of sight to the evader. Without loss of generality, this corner is placed at the origin and one of the sides lies along the -x axis as shown in Figure 2.1. A mobile pursuer and evader exist on a plane and move with velocities $\mathbf{u}$ and $\mathbf{v}$, respectively. Their speeds are bounded by $\overline{v}_p$ and $\overline{v}_e$, respectively. The positions of the pursuer and the evader are expressed in polar coordinates as $\mathbf{p}(t) = (r_p(t), \phi_p(t))$ and $\mathbf{e}(t) = (r_e(t), \phi_e(t))$, respectively. They can also be expressed in Cartesian coordinates as $\mathbf{p}(t) = (x_p(t), y_p(t))$ and $\mathbf{e}(t) = (x_e(t), y_e(t))$, respectively. Let the initial position of the pursuer and the evader be denoted by $\mathbf{p}_0$ and $\mathbf{e}_0$. The tangential velocities of the pursuer and the evader are denoted as $\mathbf{u}_t(t)$ and $\mathbf{v}_t(t)$, respectively. The tangential velocities are considered to be positive in the direction shown in the figure. $\mathbf{u}_r(t)$ and $\mathbf{v}_r(t)$ describe the radial velocities of the pursuer and the evader respectively. The radial velocities are considered to be positive if they point away from the origin. In Figure 2.1, the radial velocities of the pursuer and the evader are in the negative direction. The pursuer and the evader know each other's current position as long as they can see each other. Moreover the pursuer knows the evader's current velocity. The initial position of the pursuer and the evader is such that they are visible to each other. Both the players have a complete map of the environment.

The unshaded region is the visibility region of the pursuer. Visibility extends uniformly in all directions and is only terminated by workspace obstacles (omnidirectional, unbounded visibility). To prevent the evader from escaping, the pursuer must keep the evader in its visibility polygon, $V(\mathbf{p}(t))$. The visibility polygon of the pursuer is the set of points from which a line segment from the pursuer to that point does not intersect the obstacle region. The evader escapes if at *any* instant of time it can break the line of sight to the pursuer.

The two obstacle edges meeting at this corner are considered to extend for an infinite length, so that there is no other geometry that the evader can hide behind in the workspace. The two sides of the obstacle form an angle α. If $\alpha \geq \pi$ then every point in the free workspace is visible to every other point and the pursuer will trivially be able to track the evader indefinitely. Thus, we only consider obstacles where $\pi > \alpha \geq 0$.

Analogous to a star domain [41] in computational geometry, we define the *star region* associated with a vertex as the region in the free workspace bounded by the lines supporting the vertex of the obstacle. The shaded region in Figure 2.2 shows the star region associated with the vertex v. The concept of star region is

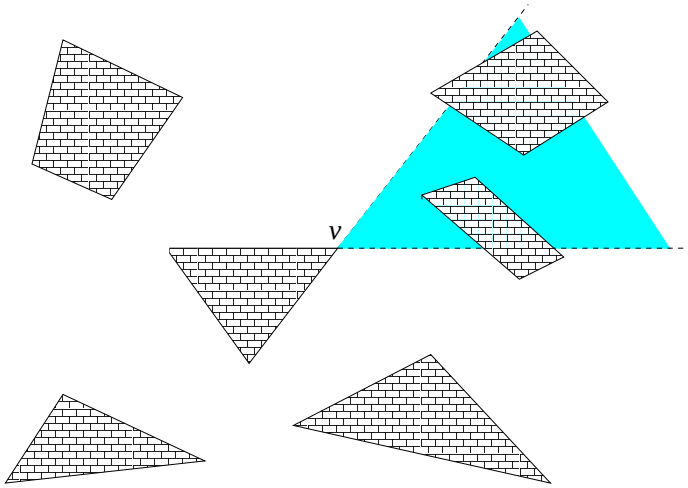

Figure 2.2: *Star region* associated with the vertex.

only applicable for a convex vertex (a vertex of angle less than π). As can be seen in Figure 2.1, in the case of a semi-infinite obstacle having a single corner, the star region extends outward from the corner of the obstacle. It is semi-infinite and bounded by the ray l and the x-axis. In case of a single corner, the entire free space is visible from any point in the star region. If the pursuer can enter the star region before losing sight of the evader, it will trivially be able to track the evader at all future times.

In this setting, we address the following problem. Given $\mathbf{p}_0$, $\mathbf{e}_0$, $\overline{v}_e$ and $\overline{v}_p$, does there exist a policy for the evader to escape the visibility region of the pursuer in finite time, or does there exist a policy for the pursuer to track the evader for all time? In the following sections, we present a partition of the workspace for an environment having a single corner so that we can answer the above question depending on the ratio $\frac{\overline{v}_e}{\overline{v}_p}$, $\mathbf{p}_0$ and $\mathbf{e}_0$.

2.2.1 Pursuer-based partition

We now present a decomposition of $V(\mathbf{p}(0))$, the visibility region of the pursuer at initial position, into regions in which the evader may lie based on the outcome of the game. These partitions can be constructed at any time during the game with the current knowledge of the pursuer's position. Depending on the partition in which the evader lies currently, we present instantaneous strategies for the winner of the game.

The number of partitions and their geometry depend on the initial position of

the pursuer. If the initial position of the pursuer is in the star region of the corner, the pursuer can see the entire workspace at all times. Hence for any initial position of the evader, the pursuer wins the game. In the remaining section, we consider the initial positions of the pursuer in which it does not lie inside the star region. Due to symmetry of the environment, the analysis is the same if the initial position of the pursuer lies below the x-axis or if it lies in the left half-space of l. Without loss of generality, we analyze the former situation.

Let us first consider the case of a corner for which $\alpha < \frac{\pi}{2}$ and $\mathbf{p}_0 = (r_p(0), \phi_p(0))$ is such that $\phi_p(0) \in \left[-\frac{\pi}{2}, 0\right)$. Define $a = \overline{v}_e/\overline{v}_p$ and let $d_p(t)$ denote the minimum distance of the pursuer from x-axis. Let $d = d_p(t) \mid_{t=0}$.

Let $\mathbf{x}= (x, y) \in \mathbb{R}^2$. We define the minimum distance from $\mathbf{x}$ to a segment, ray or line as $d(\mathbf{x}, E) = \min_{\mathbf{y}\in E} \mid\mid \mathbf{x} - \mathbf{y} \mid\mid_2$, where E denotes an edge, ray or line.

Figure 2.3 shows the partition of $V(\mathbf{p}(t))$ and Figure 2.4 shows the geometry of the partitions. $V(\mathbf{p}(t))$ is decomposed into the following regions:

1. Region 1$= \{\mathbf{x} \mid d(\mathbf{x}, E_1) \leq ad_p(t)\}$.
2. Region 2$= \{\mathbf{x} \mid d(\mathbf{x}, E_2) \geq ad_p(t)\}$.
3. Region 3$= \{\mathbf{x} \mid d(\mathbf{x}, E_2) \leq ad_p(t), \quad \mid\mid \mathbf{x} \mid\mid_2 \geq ar_p(t), \quad x \leq -ar_p(t)\}$.
4. Region 4$= \{\mathbf{x} \mid d(\mathbf{x}, E_2) \leq ad_p(t), \quad \mid\mid \mathbf{x} \mid\mid_2 \leq ar_p(t), \quad d(\mathbf{x}, E_1) \geq ad_p(t)\}$.
5. Region 5$= \{\mathbf{x} \mid d(\mathbf{x}, E_2) \leq ad_p(t), \quad x \leq -ar_p(t)\}$.

Further, we define Region 6 as the set of points in the free workspace not belonging to $V(\mathbf{p}(t))$. Before we give a set of propositions that define the winning strategy for each region in the partition, these strategies are summarized in Table 2.1.

Proposition 1: If the evader lies in Region 1 of $V(\mathbf{p}_0)$ and follows Policy A, no pursuer policy exists that can prevent the escape of the evader.

Proof. If the evader lies in Region 1, the maximum time required by the evader to reach E_1 by following Policy A is $t_e < \frac{ad}{\overline{v}_e} = \frac{d}{\overline{v}_p}$. The minimum time required by the pursuer to reach x-axis with any policy is at least $t_p > \frac{d}{\overline{v}_p}$. Since $t_p > t_e$ the evader reaches E_1 before the pursuer can reach the x-axis. If the evader lies on

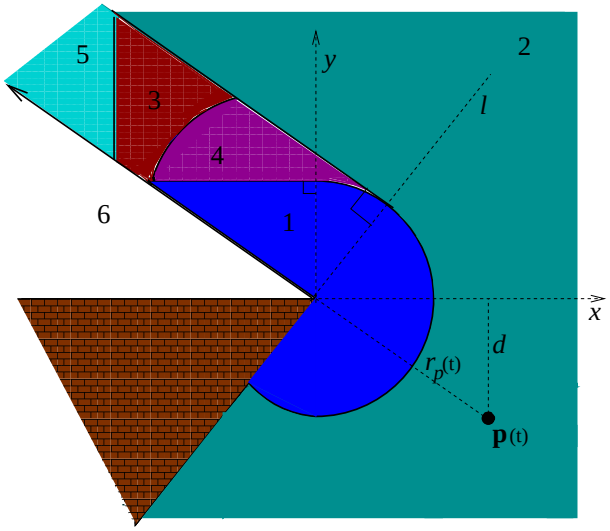

Figure 2.3: Pursuer-based partition.

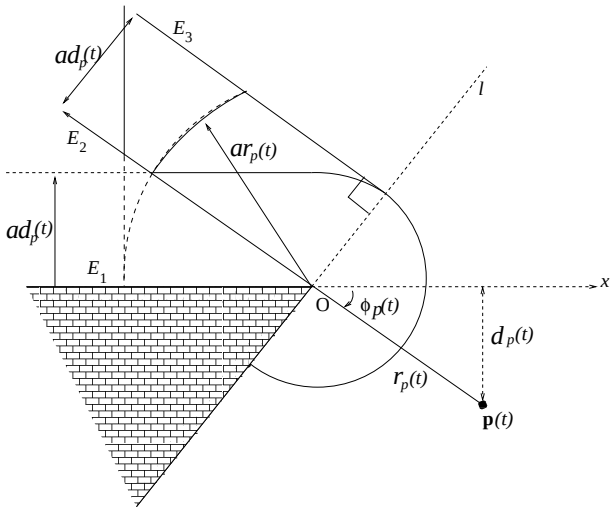

Figure 2.4: The geometry of the partition.

Table 2.1: Policies of the winner in the partitions

Evader Policies	Evader Region	Control Law
A	1 and $\phi_e \in [\alpha - \pi, \frac{\pi}{2}]$ 1 and $\phi_e \in [\frac{\pi}{2}, \pi + \phi_p]$	$\dot{r}_e(t) = -\overline{v}_e$ $\dot{y}_e(t) = -\overline{v}_e$
Pursuer Policies	**Evader Region**	**Control Law**
B	2, 4	$\dot{y}_p(t) = \overline{v}_p$
C	3	$\mathbf{u}_t(t) = \frac{r_p(t)}{r_e(t)} \lvert\mathbf{v}_t(t)\rvert$ $\mathbf{u}_r(t) = -\frac{r_p(t)}{r_e(t)} \lvert\mathbf{v}_r(t)\rvert$
D	5	$\mathbf{u}_t(t) = \overline{v}_p$

E_1 and the pursuer has not yet reached the x-axis, the evader will be outside the visibility region of the pursuer. Hence the evader escapes. □

Proposition 2: If the evader lies in Region 2 of $V(\mathbf{p}_0)$ and the pursuer follows Policy B, no evader policy exists that can escape the visibility region of the pursuer.

Proof. The time required by the pursuer to reach the x-axis by following Policy B is $t_p = \frac{d}{\overline{v}_p}$. If the evader lies in Region 2, the minimum time required by the evader to reach E_2 is $t_e > \frac{ad}{\overline{v}_e} = \frac{d}{\overline{v}_p}$. Thus, $t_e \geq t_p$. If the pursuer follows Policy B, $V(\mathbf{p}_0) \subset V(\mathbf{p}(t)) \mid_{t>0}$; i.e., the visibility region for the pursuer is monotonically increasing during the execution of this policy. Since the evader cannot reach E_2, the only free boundary of $V(\mathbf{p}_0)$, before the pursuer reaches the boundary of the star region, $\mathbf{e}(t) \in V(\mathbf{p}(t)) \quad \forall t \in [0, t_p]$. Once the pursuer reaches the x-axis, the entire free workspace belongs to $V(\mathbf{p}(t_p))$ and the evader remains in sight of the pursuer for all future times. □

Proposition 3: For all initial positions of the evader in Regions 3 and 4 of V($\mathbf{p}_0$), the pursuer can track the evader by following a reactive motion and switching between policies B, C and D appropriately.

Proof. In order to prove the Proposition, we need the following Lemmas.

Lemma 1: If the evader lies in Region 3 of $V(\mathbf{p}(t))$ and the pursuer follows Policy C, for every evader policy the evader can either stay in Region 3 or move to

region 2 or region 5 of $V(\mathbf{p}(t))$.

Proof. If the pursuer follows Policy C, then it follows both the radial and angular movements of the evader. According to the control law of the pursuer in Region 3, $\mid \mathbf{u} \mid \;=\; \mid \mathbf{v} \mid \frac{r_p(t)}{r_e(t)}$. The maximum speed of the evader is $\overline{v}_e$ and the geometry of Region 3 is such that $\frac{r_p(t)}{r_e(t)} \leq \frac{1}{a}$. Hence $\mid \mathbf{u} \mid \leq \frac{\overline{v}_e}{a} = \overline{v}_p$. Thus, the pursuer velocities of Policy C are always attainable in Region 3.

If order to keep the evader in the visibility polygon of the pursuer and prevent it from entering Region 6, the following inequality must hold at all times before the pursuer can enter the *star region*:

$$\phi_e(t) - \phi_p(t) \;\leq\; \pi$$

If the evader lies in Region 3, from the geometry of Region 3 we can see that $\phi_e(t) > \phi_p(t)$. The tangential component of the control law implies the following:

$$\frac{\mid \mathbf{v}_t(t) \mid}{r_e(t)} = \frac{\mathbf{u}_t(t)}{r_p(t)}$$

The right-hand side of the above equation is the angular velocity of the pursuer and the left-hand side is the absolute value of the angular velocity of the evader.

$$\mid \dot{\phi}_e(t) \mid \;=\; \dot{\phi}_p(t)$$

Integrating both sides of the equation gives us the following equations, and further using the fact that $\left|\int_0^t \dot{\phi}_e(t)dt\right| \;\leq\; \int_0^t \mid \dot{\phi}_e(t) \mid dt$, we obtain the following:

$$\begin{aligned} \left|\int_0^t \dot{\phi}_e(t)dt\right| &\leq \int_0^t \dot{\phi}_p(t)dt \\ \Rightarrow \quad \mid \phi_e(t) - \phi_e(0) \mid &\leq \phi_p(t) - \phi_p(0) \end{aligned}$$

Since $\phi_e(t) - \phi_e(0) \;\leq\; \mid \phi_e(t) - \phi_e(0) \mid$

$$\Rightarrow \phi_e(t) - \phi_e(0) \;\leq\; \phi_p(t) - \phi_p(0)$$

$$\Rightarrow \phi_e(t) - \phi_p(t) \;\leq\; \phi_e(0) - \phi_p(0)$$

From the assumption that the pursuer and the evader are visible to each other at

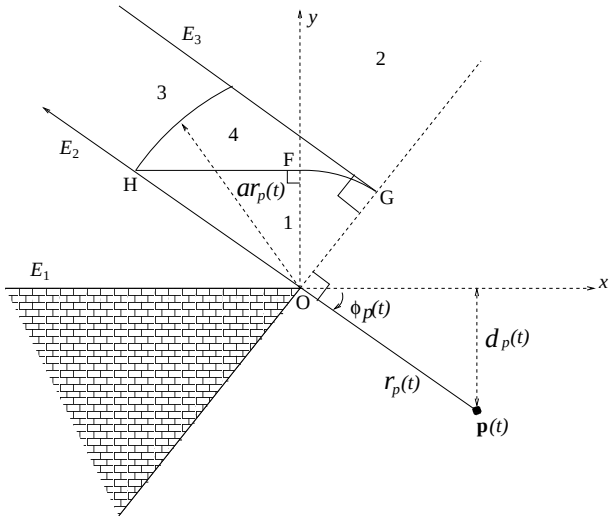

Figure 2.5: Geometry of Region 4.

the beginning of the game, we obtain the following:

$$\phi_e(0) - \phi_p(0) \quad \leq \quad \pi$$

This leads to

$$\phi_e(t) - \phi_p(t) \quad \leq \quad \pi$$

Hence the evader cannot escape the visibility region of the pursuer if the pursuer follows Policy C. The radial component of the control law implies

$$\begin{aligned} \frac{|\,\dot{r}_e(t)\,|}{r_e(t)} &= -\frac{\dot{r}_p(t)}{r_p(t)} \\ \Rightarrow \frac{\dot{r}_e(t)}{r_e(t)} &\geq \frac{\dot{r}_p(t)}{r_p(t)} \\ \Rightarrow \frac{r_e(t)}{r_p(t)} &\geq \frac{r_e(0)}{r_p(0)} \geq a \end{aligned}$$

Thus, the evader cannot enter Region 4. Hence for any policy the evader can either stay in Region 3 or it can enter Region 2 or Region 5 of $V(\mathbf{p}(t))$. □

Lemma 2: If the evader lies in Region 4 of $V(\mathbf{p}(t))$ and the pursuer follows Policy B, for every evader policy the evader can either stay in Region 4 or move to regions 2 or 3 of $V(\mathbf{p}(t))$.

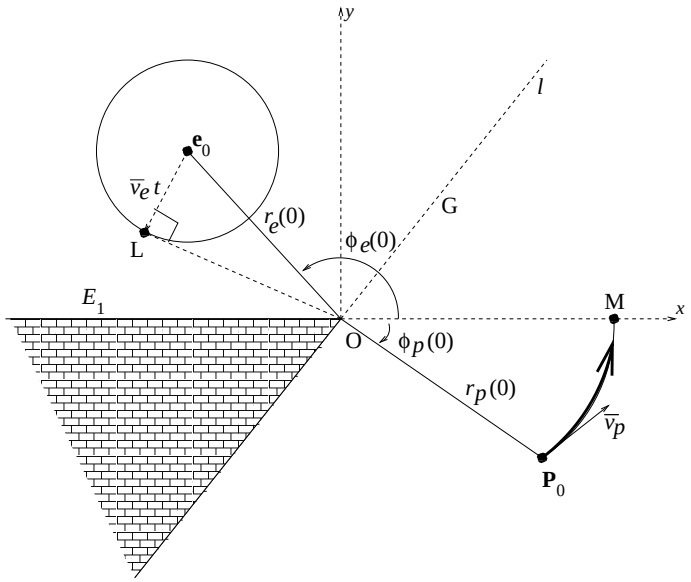

Figure 2.6: Evader in Region 5.

Proof. Refer to Figure 2.5. If the pursuer follows Policy B, all points on segment HF move with velocity $a\overline{v}_p = \overline{v}_e$ towards the edge E_1. Similarly, all points on the arc FG move with radial velocity $\overline{v}_e$ toward O. In order to enter Region 1 from Region 4, the evader must move toward the boundary of Region 1 with a velocity greater than the velocity at which the boundary is receding away from the evader. That is not possible since the boundary of Region 1 moves with velocity $\overline{v}_e$, the maximum possible evader velocity, away from the evader. Hence the evader cannot enter Region 1 from Region 4. Hence for all evader policies, the evader can only reach Region 3 or Region 2 from Region 4. □

Lemma 3: For all initial positions of the evader in Region 5 of V($\mathbf{p}_0$), the pursuer can track the evader by following policy D.

Proof. Refer to Figure 2.6. After time t, the evader lies in the closure of a circle of radius $\overline{v}_e t$ centered at $\mathbf{e}_0$. Let OL denote the tangent from the origin to the circle. A sufficient condition for the pursuer to keep the evader in sight for all future times is to keep the magnitude of the angular velocity of the line of the sight, OP, to be greater than the magnitude of the angular velocity of the line tangent to the growing circle, OL, for all future time until the pursuer reaches the *star region*. The pursuer moves in a circle of radius $r_p(0)$ with tangential velocity of $\overline{v}_p$ while it follows policy D. Hence the magnitude of the angular velocity of

the line OP is given by $\omega_p = \frac{\overline{v}_p}{r_p(0)}$. The magnitude of the angular velocity of OL is given by $\omega_{OL} = \frac{-\overline{v}_e}{OL}$. ω_{OL} is maximum when the radial distance of L is minimum. This happens when the circle touches the edge OA. This length is given by $r_e(0)\cos(\phi_e(0))$. Hence the maximum value of ω_{OL} is given by $\omega^*_{OL} = \frac{-\overline{v}_e}{r_e(0)\cos(\phi_e(0))}$. Solving for $\omega_p \geq \omega^*_{OL}$ leads to the following condition.

$$r_e(0) \geq -\frac{ar_p(0)}{\cos(\phi_e(0))}$$

Since $\cos(\phi_e(0)) \leq 0$, we obtain the following condition:

$$x_e(0) \leq -ar_p(0)$$

which is satisfied for all points in Region 5. □

Returning now to Proposition 3, if the evader starts in Region 3 and remains in Region 3, then we have proved in Lemma 1 that Policy C for the pursuer can keep the evader in sight for all future time. While the pursuer is following policy C, if the evader enters Region 2, by Proposition 2, the pursuer can track the evader indefinitely by following Policy B, whereas if the evader enters region 5, from Lemma 3, the pursuer can keep track of the evader by following policy D. Hence the pursuer can keep sight of the evader for all future time.

If the evader starts in Region 4 and remains in Region 4, then Lemma 2 proves that Policy B for the pursuer can keep the evader in sight for all future time. While the pursuer is following policy B, the evader can move to Region 3 or Region 2. If the evader moves to Region 3, the strategy provided in the previous paragraph can keep the evader in sight for all future times. On the other hand, while the pursuer is following policy B, if the evader moves to Region 2, by Proposition 2, the pursuer can indefinitely track the evader by following Policy B. Thus, the pursuer will keep the evader in sight for all future time. □

Figure 2.7 summarizes Propositions 2 and 3. Each state is the region in the partition of $V(\mathbf{p}(t))$ in which the evader lies. The arrows show the allowable transitions of the evader under the respective policy of the pursuer. Hence given the initial position of the pursuer and the evader, we can construct the partition of $V(\mathbf{p}_0)$ and use Figure 2.7 to obtain the instantaneous strategy of the pursuer if it can track the evader.

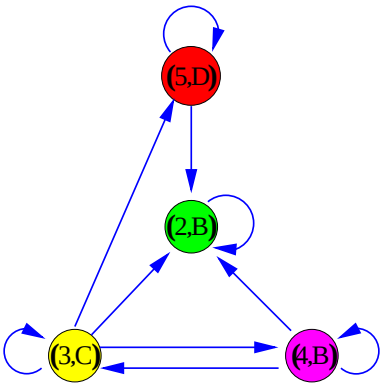

Figure 2.7: Regions and their control laws.

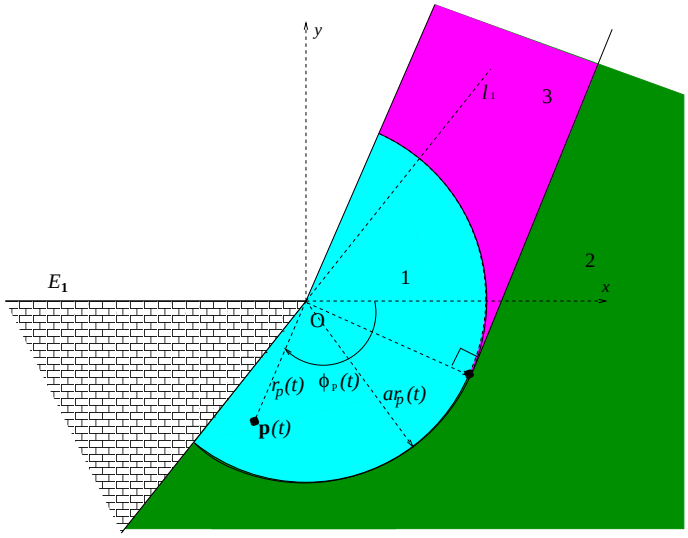

Figure 2.8: The partition of V(**p**(t)) when $\phi_p(t) < -\frac{\pi}{2}$.

The above analysis was for the case when $\phi_p(0) \in \left[-\frac{\pi}{2}, 0\right)$. For the case when $\phi_p(0) < -\frac{\pi}{2}$, the analysis still holds. The only changes are that Region 1 expands, the area of Region 4 is reduced to zero and Region 5 ceases to exist. Figure 2.8 shows the partition of the visibility region of the pursuer in this case.

The analysis we have presented so far assumed that $\alpha \in \left[0, \frac{\pi}{2}\right]$. Refer to Figure 2.1. If $\alpha \in \left[\frac{\pi}{2}, \pi\right]$, then $\phi_p(0)$ must lie in the fourth quadrant and hence $\phi_p(0)$ must be greater than $-\frac{\pi}{2}$. Hence it reduces to the problem we analyzed in this section.

We now provide a decomposition of $V(\mathbf{e}_0)$ into regions in which the pursuer may lie based on the outcome of the game.

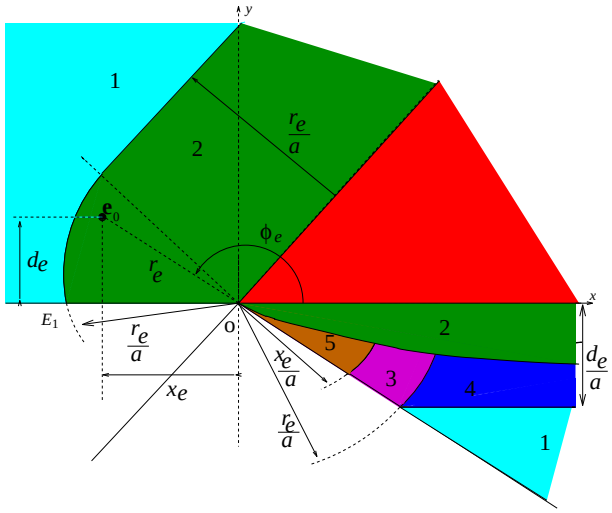

Figure 2.9: The evader is nearer to the side of the obstacle than the corner.

2.2.2 Evader-based partition

In the previous subsection, a partition of $V(\mathbf{p}_0)$ has been given based on the policies used by the players to win the game. In this subsection, we use the same policies as used by the players in Table 2.1. We fix the position of the evader and compute the boundaries across which the policies of the winner change. These curves partition $V(\mathbf{e}_0)$ into regions in which the pursuer may lie depending on the policy of the winner. The geometry of the partitions is a function of the velocity ratio between the pursuer and the evader.

To determine the partition of $V(\mathbf{e}_0)$, we must consider three cases depending on whether (a) the closest point to the evader on the obstacle lies on the corner, (b) the closest point belongs uniquely to one of the sides, or (c) the evader lies inside the star region. Figure 2.9 shows the partition of $V(\mathbf{e}_0)$ for the case when the closest point to the evader on the obstacle belongs to the side AO. In the rest of this section, we analyze this case.

Since we are considering the inverse of the problem addressed in the previous subsection, the geometry of the regions in this case is different from that given in Table 2.1. Moreover, in the previous subsection, we saw that the result of the game depends on the initial position of the pursuer and the evader. Hence the configuration variables in this subsection denote their values at the beginning of the game.

First, let us consider the case in which the pursuer lies in the star region. In this case, the entire free workspace is visible to the pursuer and it can track the evader

by remaining stationary. Hence if the pursuer lies in the star region, it wins the game and its policy is to remain stationary. Now we present the derivation of each region of the partition in the remaining part of $V(\mathbf{e}_0)$.

Region 1

From the previous subsection, Region 1 consists of all those points in $V(\mathbf{p}_0)$ from which the evader wins the game irrespective of the pursuer's policy.

First, let us consider the case in which the pursuer lies below the x-axis. The strategy of the evader is to move directly towards the obstacle so that it can reach AO before the pursuer can reach the boundary of the star region, which is the x-axis in this case. Since we are considering the case where the closest point to the evader on the obstacle belongs to side AO, the evader lies in Region 1 of $V(\mathbf{p}_0)$ if $d_e \leq ad_p \Rightarrow d_p \geq \frac{d_e}{a}$.

Now let us consider the case in which the pursuer lies above the x-axis and outside the star region. In this case, the evader wins the game if the time taken by the evader to reach the corner is less than the time taken by the pursuer to reach the star region. Let d_e denote the perpendicular distance of the evader from the edge AO. Hence Region 1 consists of points such that $r_e < ad_p \Longrightarrow d_p > \frac{r_e}{a}$.

Region 2

Let us first consider the case in which the pursuer lies below the x-axis. Refer to Figure 2.4. We can see that the evader lies in Region 2 of $V(\mathbf{p}_0)$ if the least distance of the evader from line OB is greater than ad_p. From Figure 2.10, we can see that the least distance of the evader from line OB is $r_e \sin(\phi_e - \phi_p)$.

$$-ar_p \sin\phi_p \leq r_e \sin(\phi_e - \phi_p)$$

Since $\phi_p < 0$, the above equation can be written as

$$\begin{aligned} r_p &\leq -\frac{r_e \sin(\phi_e - \phi_p)}{a \sin\phi_p} \\ \Rightarrow r_p &\leq \frac{r_e \sin\phi_e(\cot\phi_e - \cot\phi_p)}{a} \end{aligned}$$

Now let us consider the case when the pursuer lies above the x-axis and outside

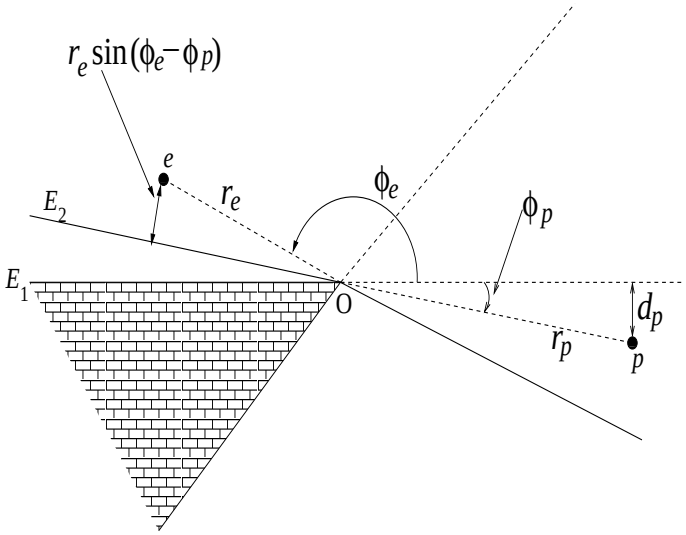

Figure 2.10: Distance of evader from line of sight of the pursuer.

the star region. From Figures 2.4 and 2.8, we can conclude that the evader lies in Region 2 of $V(\mathbf{p}_0)$ if $r_e \geq a \min\{r_p, d_p\} \Rightarrow \frac{r_e}{a} \geq \min\{r_p, d_p\}$.

Region 3

Refer to Figure 2.4. The evader lies in Region 3 of $V(\mathbf{p}_0)$ if $r_e \geq ar_p$, $x_e \geq -ar_p$ and least distance of the evader from line OB is less than ad_p. This implies that $r_p \leq \frac{r_e}{a}$, $r_p \geq -\frac{x_e}{a}$ and $r_p \geq \frac{r_e \sin\phi_e(\cot\phi_e - \cot\phi_p)}{a}$. Hence $\max\{-\frac{x_e}{a}, \frac{r_e \sin\phi_e(\cot\phi_e - \cot\phi_p)}{a}\} \leq r_p \leq \frac{r_e}{a}$.

Region 4

From Figure 2.4, we see that the evader lies in Region 4 of $V(\mathbf{p}_0)$ if $r_e \leq ar_p$, $\min\{d_e, r_e\} \geq ad_p \Rightarrow \min\{d_e, r_e\} \geq -ar_p \sin\phi_p$ and the least distance of the evader from line OB is less than ad_p. This leads to the following condition:

$$-\frac{\min\{d_e, r_e\}}{a \sin\phi_p} \geq r_p \geq \max\{\frac{r_e}{a}, r_e \sin\phi_e(\cot\phi_e - \cot\phi_p)\}$$

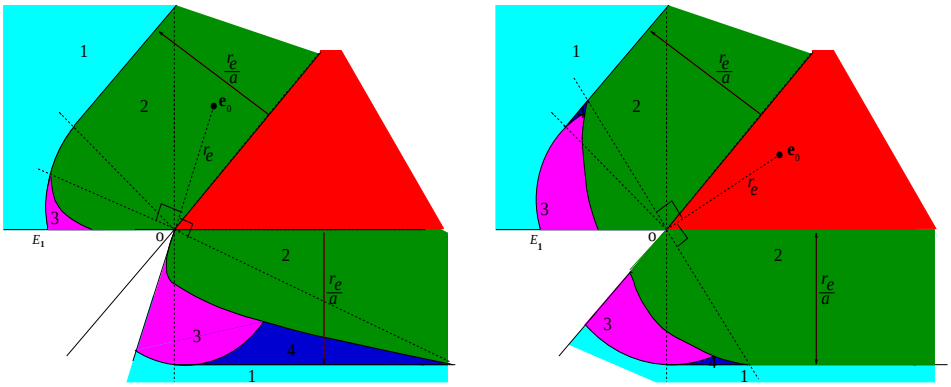

(a) $\mathbf{e}_0$ outside the star region. **(b) $\mathbf{e}_0$ inside the star region.**

Figure 2.11: Evader-based partitions.

Region 5

From Figure 2.4, we see that the evader lies in Region 5 of $V(\mathbf{p}_0)$ if $x_e \leq -ar_p \Rightarrow r_p \leq \frac{-x_e}{a}$.

All the above partitions are shown in Figure 2.9. Figure 2.2.2 (a) shows the partition of $V(\mathbf{e}_0)$ when the nearest point of the obstacle to the evader is corner O but the evader is outside the star region, and Figure 2.2.2 (b) shows the partition of $V(\mathbf{e}_0)$ when the evader is in the star region.

Based on the partition of $V(\mathbf{e}_0)$, we present a sufficient condition of escape for the evader in the next section that is used to bound the set of initial positions of the pursuer from which it might win the game.

2.3 Approximation Schemes for Polygonal Environment

In the previous section, we provided a partition of $V(\mathbf{e}_0)$ to decide the outcome of the target tracking game. From the previous section, we can conclude that if the pursuer lies in Region 1 of $V(\mathbf{e}_0)$, then the evader has a strategy to win irrespective of the pursuer's strategy. The presence of other obstacles does not affect this result. This leads to the following sufficient condition for escape of the evader in any general environment.

Sufficient Condition: If the time required by the pursuer to reach the star region

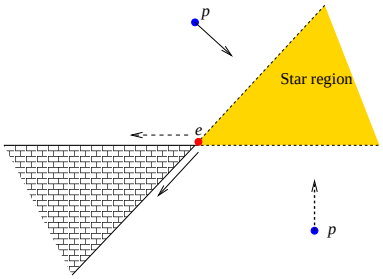

Figure 2.12: Sufficient condition for escape.

associated with a vertex is greater than the time required by the evader to reach the vertex, the evader has a strategy to escape the pursuer's visibility region.

The relation between the time taken by the pursuer and evader can be expressed in terms of the distances traveled by the pursuer and the evader and their speeds. In a general environment, if d_e is the length of the shortest path of the evader from a corner, d_p is the length of the shortest path of the pursuer from the star region associated with the corner and a is the ratio of the maximum speed of the evader to that of the pursuer, then the sufficient condition can also be expressed in the following way:

SC: If $s_e < as_p$, the evader wins the game.

The sufficient condition arises from the fact that if the evader reaches the corner before the pursuer can reach the star region associated with the corner, the evader may escape to the side of the obstacle hidden from the pursuer. This is illustrated in Figure 2.12. In the figure, the evader, **e**, is at the corner while the pursuer, **p**, is yet to reach the star region associated with the corner. If the pursuer approaches the star region from the left side as shown by the solid arrow, the evader can escape the visibility region of the pursuer by moving in the direction of the solid arrow. On the other hand, if the pursuer approaches the star region from the right side as shown by the dotted arrow, the evader can escape the visibility region of the pursuer by moving in the direction of the dotted arrow.

For convenience, we refer to the sufficient condition as SC in the rest of the paper. Using the SC, we show that in any environment containing polygonal obstacles, the set of initial positions from which a pursuer can track the evader is bounded. First, we prove the statement for an environment containing a single convex polygonal obstacle. Then we extend the results to a general polygonal environment containing multiple obstacles. This leads to our first approximation

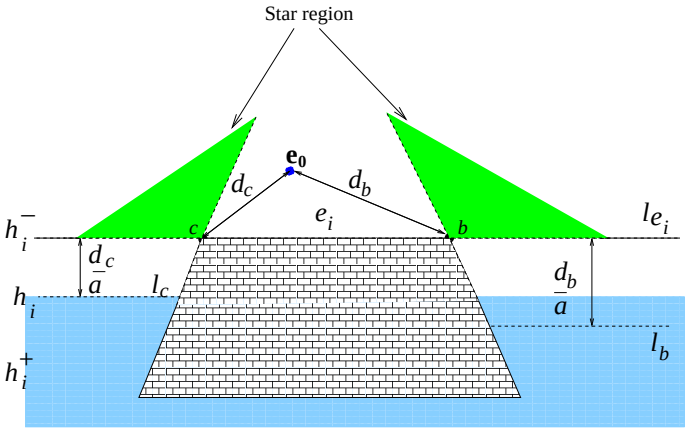

Figure 2.13: Proof of Lemma 1.

scheme.

Consider an evader in an environment with a single convex polygonal obstacle having n edges $E_1, E_2 \cdots E_n$. Every edge E_i is a line segment that lies on a line l_{E_i} in the plane. Let $\{h_i\}_1^n$ denote a family of lines, each given by the equation $h_i(x, y, \mathbf{e}_0, a) = 0$. The presence of the terms $\mathbf{e}_0$ and a in the equation implies that the equation of the line depends on the initial position of the evader and the speed ratio respectively. Each line h_i divides the plane into two half-spaces, namely, $h_i^+ = \{(x, y) \mid h_i(x, y, \mathbf{e}_0, a) > 0\}$ and $h_i^- = \{(x, y) \mid h_i(x, y, \mathbf{e}_0, a) < 0\}$. Now we use the SC to prove a property related to the edges of the obstacle.

Lemma 4: For every edge E_i, there exists a line h_i parallel to E_i and a corresponding half-space h_i^+ such that the pursuer loses the game if $\mathbf{p}_0 \in h_i^+$.

Proof. Consider an edge E_i of a convex obstacle as shown in Figure 2.13. Since the obstacle is convex, it lies in one of the half-spaces generated by the line l_{E_i}. Without loss of generality, let the obstacle lie in the half-space below the line l_{E_i}. Let d_c and d_b be the length of the shortest path of the evader from vertices c and b of the edge e_i respectively. Since the obstacle lies in the lower half-space of l_{E_i}, the star regions associated with vertices c and b are in the upper half-space of l_{E_i} as shown by the green shaded region. Let l_c and l_b be the lines at distances of $\frac{d_c}{a}$ and $\frac{d_b}{a}$, respectively, from the line l_{E_i}. If the pursuer lies at a distance greater than $\min(\frac{d_c}{a}, \frac{d_b}{a})$ below the line l_{E_i}, then the time taken by the pursuer to reach the line l_{E_i} is $t_p \geq \frac{\min(\frac{d_c}{a}, \frac{d_b}{a})}{\overline{v}_p}$. The minimum time required by the evader to reach corner c or b, whichever is nearer, is given by $t_e = \frac{\min(d_c, d_b)}{\overline{v}_p}$. From the expressions of

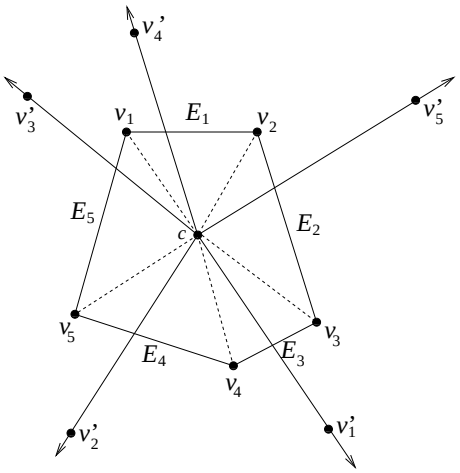

Figure 2.14: A polygon and its sectors.

t_e and t_p we can see that $t_p > t_e$. Hence the pursuer will reach the nearer of the two corners before the evader reaches line l_{e_i}. Hence from SC, we conclude that if the pursuer lies below the line h_i parallel to e_i at a distance of $\min(\frac{d_c}{a}, \frac{d_b}{a})$, then the evader wins the game by following the shortest path to the nearer of the two corners. In Figure 2.13, since $d_b > d_c$ the line h_i coincides with line l_c. □

Given an edge E_i and the initial position of the evader, the proof of Lemma 1 provides an algorithm to find the line h_i and the corresponding half-plane h_i^+ as long as the length of the shortest path of the evader to the corners of an edge is computable. For example, in the presence of other obstacles, the length of the shortest path of the evader to the corners can be obtained by Dijkstra's algorithm.

Now we present some geometrical constructions required to prove the next proposition. Refer to Figure 2.14. Consider a convex obstacle. Consider a point c strictly inside the obstacle. For each vertex v_i, extend the line segment v_ic to infinity in the direction $\vec{v_ic}$ to form the ray cv_i'. Define the region bounded by rays cv_i' and cv_{i+1}' as *sector* $v_i'cv_{i+1}'$. The $sectors$ possess the following properties:

1. Any two sectors are mutually disjoint.

2. The union of all the sectors is the entire plane.

We use this construction to prove the following proposition.

Proposition 4: In an environment containing a single convex polygonal obstacle, given the initial position of the evader, the set of initial positions of the pursuer

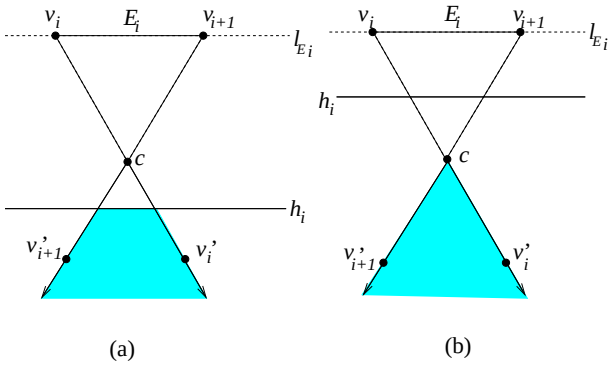

Figure 2.15: Proof of Proposition 4.

from which it can win the game is a bounded subset of the free workspace.

Proof. Refer to Figure 2.15. Consider an edge E_i of the convex obstacle with end points v_i and v_{i+1}. WLOG, the obstacle lies below l_{E_i}. Let c be a point strictly inside the convex polygon. Extend the line segments v_ic and $v_{i+1}c$ to form sector $v_i'cv_{i+1}'$. Using Lemma 1, given the initial position of the evader, we can construct a line h_i parallel to E_i such that if the initial pursuer position lies below h_i, the evader wins the game. In case the line h_i intersects sector $v_i'cv_{i+1}'$, as shown in Figure 2.15(a), the evader wins the game if the initial pursuer position lies in the shaded region. In case the line h_i does not intersect sector $v_i'cv_{i+1}'$, as shown in Figure 2.15(b), the evader wins the game if the initial pursuer position lies anywhere in the sector. Hence for every sector, there is a region of finite area such that if the initial pursuer position lies in that region then it might win the game. Every edge of the polygon has a corresponding sector associated with it. Since each sector has a region of finite area such that if the initial pursuer position lies in it, the pursuer might win the game, the union of all these regions is finite. Hence the proposition follows. □

In the proof of Proposition 4, we generate a bounded set for each convex polygonal obstacle such that the evader wins the game if the initial position of the pursuer lies outside this set. Figure 2.16 shows the evader in an environment containing a single hexagonal obstacle. The polygon in the center bounded by thick lines shows the region of possible pursuer win. In a similar way, we can generate a bounded set for a non-convex obstacle. Given a non-convex obstacle, we construct its convex-hull. We can prove that Lemma 1 holds for the convex-hull. Finally, we can use Proposition 4 to prove the existence of a bounded set.

From the previous discussions, we conclude that any polygonal obstacle, convex or non-convex, restricts the set of initial positions from which the pursuer might win the game to a bounded set. Moreover, given the initial position of the evader and the ratio of the maximum speed of the evader to that of the pursuer, the bounded set can be obtained from the geometry of the obstacle by the construction used in the proof of Proposition 4. For any polygon in the environment, let us call the bounded set generated by it the *B set*. If the initial position of the pursuer lies outside the *B set*, the evader wins the game. For an environment containing multiple polygonal obstacles, we can compute the intersection of all *B sets* generated by individual obstacles. Since each *B set* is bounded, the intersection is a bounded set. Moreover, the intersection has the property that if the initial position of the pursuer lies outside the intersection, the evader wins the game. This leads to the following proposition.

Proposition 5: Given the initial position of the evader, the set of initial positions from which the pursuer might win the game is bounded for an environment consisting of polygonal obstacles.

Proof. The bounded set referred to in this theorem is the intersection of the *B sets* generated by the obstacles. If the initial pursuer position does not lie in the intersection, it implies that it is not contained in all the *B sets*. Hence there exists at least one polygon in the environment for which the initial pursuer position does not lie in its *B set*. By Proposition 4, the evader has a winning strategy. Hence the proposition follows. □

From the above discussion, we conclude the following sufficient condition for escape: For any initial position of the pursuer outside the $Bset$, the evader wins the game.

But we still do not know the result of the game for all initial positions of the pursuer inside the intersection. However, we can find better approximation schemes and reduce the size of the region in which the result of the game is unknown. In the next subsection, we present one such approximation scheme.

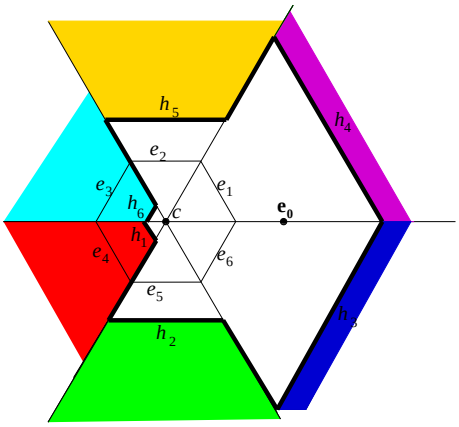

Figure 2.16: *B set* for an environment consisting of a regular hexagonal obstacle and $a = 0.5$.

2.3.1 U set

Now we present an approximation scheme that gives a tighter bound on the initial positions of the pursuer from which it might win the game. From Lemma 1, the evader wins the game if $\mathbf{p}_0 \in h_i^+$ for any edge. We can conclude that if $\mathbf{p}_0 \in \cup_{i=1}^n h_i^+$, the evader wins the game. Since $(\cup_{i=1}^n h_i^+)^c = \cap_{i=1}^n (h_i^+)^c = \cap_{i=1}^n h_i^-$, where S^c denotes the complement of set S, if $\mathbf{p}_0$ lies outside $\cap_{i=1}^n h_i^-$, the evader wins the game. Hence the set of initial positions from where the pursuer might win the game is contained in $\cap_{i=1}^n h_i^-$. We call $\cap_{i=1}^n h_i^-$ the *U set*. An important point to note is that the intersection can be taken among any number of half-spaces. If the intersection is among the half-spaces generated by the edges of an obstacle, we call it the *U set* generated by the obstacle. If the intersection is among the half-spaces generated by all the edges in an environment, we call it the *U set* generated by the environment.

The next proposition proves that the *U set* generated by a single obstacle is a subset of the *B set* and hence a better approximation.

Proposition 6: For a given convex obstacle, the *U set* is a subset of the *B set* and hence bounded.

Proof. Consider a point q that does not lie in the *B set*. From the construction of the *B set*, q must belong to some half-plane h_j^+. If $q \in h_j^+$, then $q \notin h_j^- \implies q \notin \cap_{i=1}^n h_i^-$. This implies that the complement of the *B set* is a subset of the complement of the *U set*. This implies that the *U set* is a subset of the *B set*. □

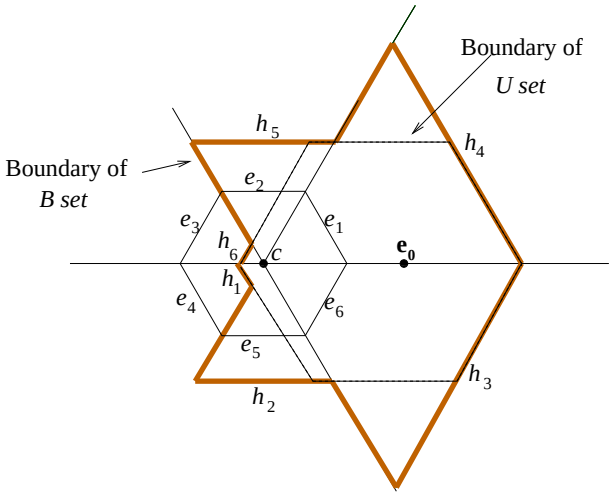

Figure 2.17: *B set* and *U set* for an environment containing of a regular hexagonal obstacle and $a = 0.5$. The polygon bounded by thick lines is the *B set* and the polygon bounded by thin lines is the *U set*.

Figure 2.17 shows the *B set* and *U set* for an environment containing a regular hexagonal obstacle. In the appendix, we present a polynomial-time algorithm to compute the *U set* for an environment with polygonal obstacles. The overall time-complexity of this algorithm is $O(n^2 \log n)$ where n is the number of edges in the environment. Figure 2.18 shows the evader in a polygonal environment. The region enclosed by the dashed lines is the *U set* generated by the environment for the initial position of the evader. The *U set* for any environment having polygonal obstacles is a convex polygon with at most n sides [41]. Figure 2.19 shows the *U set* for an environment for various ratios of the maximum speed of the evader to that of the pursuer. In Figure 2.19, it can be seen that as the speed ratio between the evader and the pursuer increases, the size of the *U set* decreases. The size of the *U set* diminishes to zero at a critical speed ratio. At speed ratios higher than the critical ratio, the evader has a winning strategy for any initial position of the pursuer.

Before we proceed to the next proposition, we prove the following Lemma.

Lemma 5: For $a \leq 1$, the evader lies inside the *U set*.

Proof. For $a \leq 1$, $\bar{v}_p \geq \bar{v}_e$. If the pursuer lies at the same position as the evader, its strategy to win is to maintain the same velocity as that of the evader. Hence if the pursuer and the evader have the same initial position, the pursuer can track

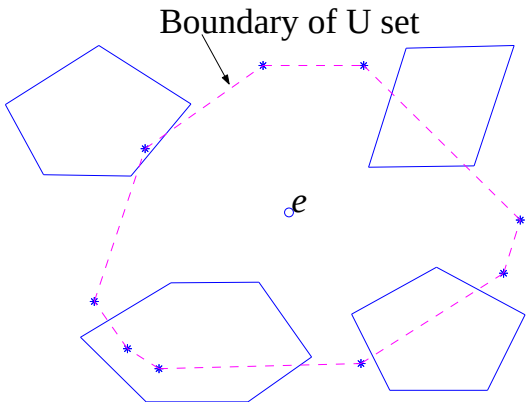

Figure 2.18: *U set* for a general environment.

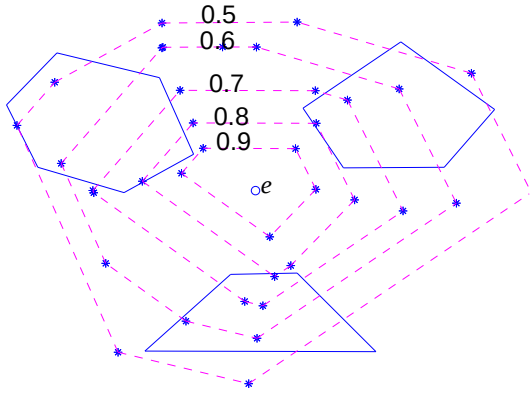

Figure 2.19: *U set* for a various speed ratios of the evader to that of the pursuer.

the evader successfully. Since all the initial positions from which the pursuer can win the game must be contained inside the *U set*, the evader position must also be inside the *U set*. □

The following proposition provides a sufficient condition for escape of the evader in an environment containing obstacles using the *U set*.

Proposition 7: If the *U set* does not contain the initial position of either the pursuer or the evader, the evader wins the game.

Proof. From the definition of the *U set*, if the pursuer lies outside the *U set*, it loses. If the evader lies outside the *U set*, Lemma 2 implies $a > 1$. If $a > 1$, $\bar{v}_e > \bar{v}_p$. If $\bar{v}_e > \bar{v}_p$, the evader wins the game in any environment containing obstacles. Its winning strategy is to move on the convex hull of any obstacle. □

2.3.2 Discussion

In the previous sections, we have provided a simple approximation scheme for computing the set of initial pursuer positions from which the evader can escape based on the intersection of a family of half-spaces. A slight modification to the proposed scheme leads to a better approximation. In the proof of Lemma 1, we presented an algorithm to find a half-space for every edge of the polygon such that if the initial position of the pursuer lies in the half-space, the evader wins the game. All the points in the half-space are at a distance greater than $\frac{d_c}{a}$ from l_{E_i}. By imposing the condition that the minimum distance of the desired set of points from l_{E_i} in the free workspace should be greater than $\frac{d_c}{a}$, we can include more points in the decidable regions as shown in Figure 2.20. The figure shows an obstacle in free space. From the proof of Lemma 1, we get the half-space shaded in red. By adding the new condition, the region shaded in green gets included. When we repeat this for every edge, the set of initial positions from which the pursuer might win the game gets reduced and leads to a better approximation. The boundary of the shaded region consists of straight lines and arc of circles. The boundary of the desired set is obtained by computing the intersections among a collection of rays and arcs of circles generated by each edge. In this case a better approximation comes at the cost of expensive computation.

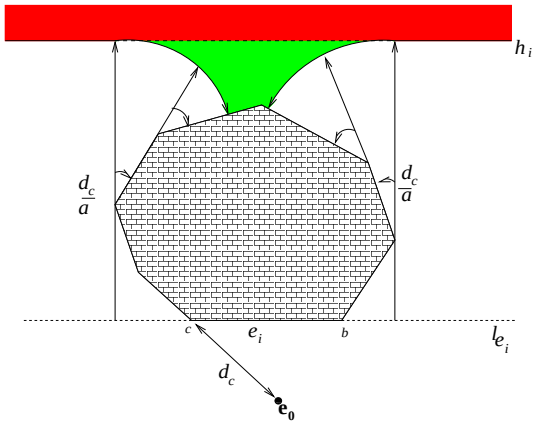

Figure 2.20: A polygon in free space. The region shaded in red is obtained by using Lemma 1. The region shaded in green gets added by using a better approximation scheme.

None of the approximation schemes we have suggested so far restricts the initial position of the pursuer to be in the evader's visibility region. This condition can be imposed by taking an intersection of the output of the approximation algorithm with the visibility polygon at the evader's initial position. Efficient algorithms exist for computing the visibility polygon of a static point in an environment [42].

In the next section we present an approximate bound on the initial positions of the pursuer from which it can track the evader.

2.4 *U Set* for Specific Environments

In the real world we encounter a lot of non-polygonal obstacles in the environment. Common obstacles in an environment are circular columns and pillars that project to a disc in a plane. In this section we compute the $Uset$ for a disc in a plane and then extend the procedure to compute the $Uset$ for obstacles whose boundaries have a well defined tangent at each point.

2.4.1 Disc in a plane

Consider an environment consisting of an obstacle in the shape of a disc of radius r in free space. Refer to Figure 2.21. Let C denote the boundary of the obstacle. Let $\mathbf{e}_0$ denote the initial position of the evader. Let O be the center of the circular obstacle. The distance between O and $\mathbf{e}_0$ is d_0. O is also the origin of the world

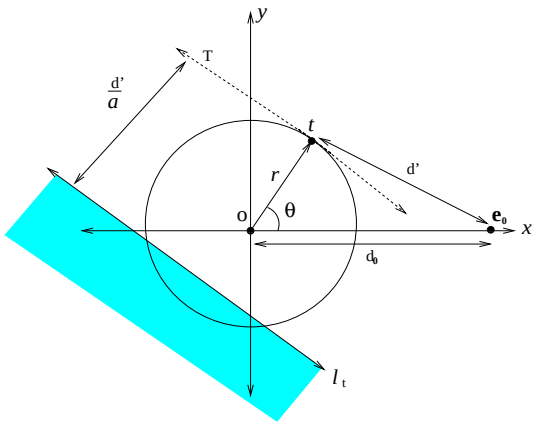

Figure 2.21: A disc-like obstacle in free space.

reference frame. The x-axis of the world reference frame passes through $\mathbf{e}_0$ and O. Let t be a point on the boundary of the obstacle such that Ot makes an angle θ with the x-axis. Let d' denote the distance between t and $\mathbf{e}_0$. Let T denote the tangent to the circle at the point t. Let l_t be a line at a distance of $\frac{d'}{a}$ from T in the same half-space of T as the obstacle. By SC, the evader will win the game if the pursuer lies in the half-space shown by the shaded region. The equation of line l_t is $y + x\cot\theta - (r - \frac{d'}{a})\csc\theta = 0$. For each point t on the circle, we can find such a line l_t and the corresponding half-space l_t^+. The *U set* is defined as $\cap_{t\in C} l_t^-$. If the initial position of the pursuer lies outside the *U set*, the evader wins the game. Let $l(x, y, \theta)$ denote the family of lines l_t generated by all points t lying on C. Due to symmetry of the environment about the x-axis, the *U set* is symmetric about the x-axis. We will construct the part of the *U set* generated as θ increases from 0 to π.

Let B denote the boundary of the *U set*.

Proposition 9: B is the envelope of the family of lines $l(x, y, \theta)$.

Proof. Consider any point q on B. The point q belongs to some line in the family of lines $l(x, y, \theta)$ since it belongs to the boundary. Let that line be l_q, which has to be tangent to the boundary B or else there is a neighborhood around q in which B lies in both the half-spaces generated by l_q. Since q is any point on B, it is true for all points q on B that the tangent to B at q belongs to the family of lines $l(x, y, \theta)$. A curve satisfying this property is the envelope to the family of lines $l(x, y, \theta)$. □

We can find the envelope of a family of lines $l(x, y, \theta)$ by solving the following

equations simultaneously:

$$l(x, y, \theta) = y + x \cot\theta - (r - \frac{d'}{a}) \csc\theta = 0 \tag{2.1}$$

$$\frac{\partial l}{\partial \theta} = 0 \tag{2.2}$$

Here, d' as a function of θ is given by

$$d'(\theta) = \begin{cases} \sqrt{r^2 + d_0^2 - 2rd_0\cos\theta} & \text{if} \quad \theta \leq \theta_0 \\ \sqrt{d_0^2 - r^2} + r(\theta - \theta_0) & \text{if} \quad \theta \geq \theta_0 \end{cases}$$

where $\theta_0 = \cos^{-1}\frac{r}{d}$.

2.4.2 Case 1 ($\theta \leq \theta_0$)

Substituting Equation (2.1) in Equation (2.2) gives

$$x = (r - \frac{\sqrt{r^2 + d_0^2 - 2rd_0\cos\theta}}{a})\cos\theta + \frac{rd_0\sin^2\theta}{a\sqrt{r^2 + d_0^2 - 2rd_0\cos\theta}}$$

$$y = (r - \frac{\sqrt{r^2 + d_0^2 - 2rd_0\cos\theta}}{a})\sin\theta - \frac{rd_0\sin\theta\cos\theta}{a\sqrt{r^2 + d_0^2 - 2rd_0\cos\theta}}$$

2.4.3 Case 2 ($\theta \geq \theta_0$)

Substituting Equation (2.1) in Equation (2.2) gives

$$x = (r - \frac{\sqrt{d_0^2 - r^2} + r(\theta - \theta_0)}{a})\cos\theta + \frac{\sin\theta}{a}$$

$$y = (r - \frac{\sqrt{d_0^2 - r^2} + r(\theta - \theta_0)}{a})\sin\theta - \frac{\cos\theta}{a}$$

Since B is symmetrical about the $x-$axis, the other half of B is obtained by reflecting the above curves about the $x-$axis. Figure 2.22 shows the boundary of the *U set* for a disc of radius 3 units. Figures 2.22 (b), (c) and (d) show the boundary of the *U set* for varying distance between the evader and the obstacle. In each of these figures, the boundary of the *U set* is shown for three different values of a. We can see that for $a \leq 1$, the evader lies inside the *U set*.

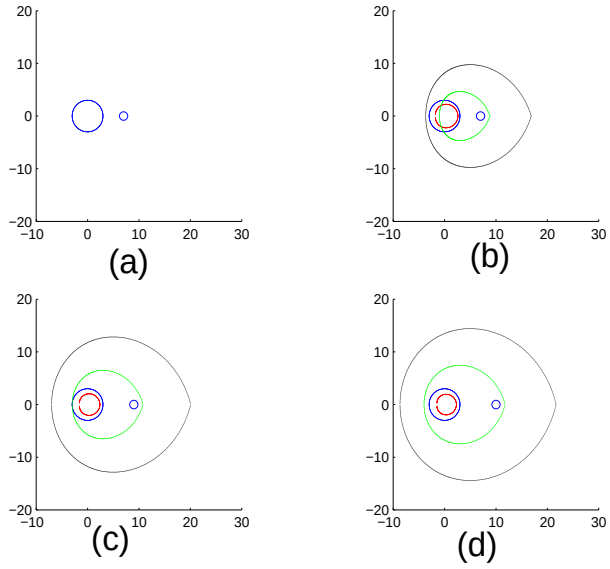

Figure 2.22: (a) Disc-like obstacle with the initial position of the evader. The smaller circle is the evader. Panels (b), (c) and (d) show the boundaries of the *U sets* for the obstacle with increasing distance between the evader and the center of the disc. In (b), (c) and (d), the black boundary is for the case when $a = 0.5$, the cyan boundary is for the case when $a = 1$ and the red boundary is for the case when $a = 10$.

The above procedure can be used to construct the *U set* for any convex obstacle whose boundary has a well defined tangent at every point. If the boundary is given by the equation $f(x, y) = 0$ where $f(x, y)$ is such that $\frac{\partial f}{\partial x}$ and $\frac{\partial f}{\partial y}$ exist for all points, the procedure to generate the boundary of the *U set* is as follows:

1. Given any point t on the boundary, find the equation of the line l_t as defined above.

2. Find the family $l(x, y, \theta)$ of lines generated by l_t as t moves on the boundary of the obstacle. θ is a parameter that defines t.

3. The envelope of the family $l(x, y, \theta)$ is the boundary of the *U set*. This is true since the proof of Proposition 3 does not depend on the shape of the obstacle and hence Proposition 3 is true for any obstacle.

In the next section we present an approximate bound on the initial positions of the pursuer from which it can track the evader.

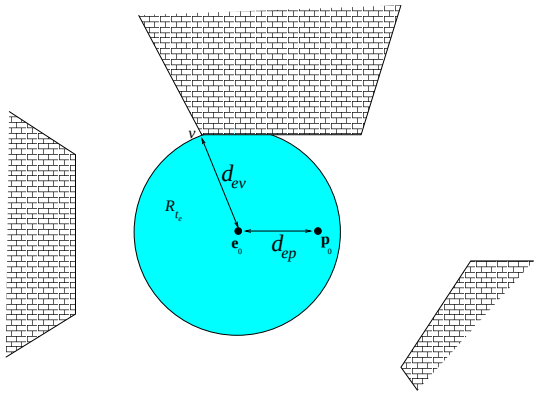

Figure 2.23: Sufficient condition for surveillance.

2.5 Sufficient Condition for Surveillance

In this section, we present a sufficient condition for a pursuer to track the evader. If $\overline{v}_e > \overline{v}_p$, the evader wins the game for any initial position of the pursuer. So a necessary condition for successful tracking is $\overline{v}_e \leq \overline{v}_p$. A plausible strategy for the pursuer to track the evader would be to catch the evader in a finite time and then move with the same velocity as the evader. The latter is possible since we assumed that the pursuer can estimate the instantaneous velocity of the evader at all times. Using the above ideas, we present the following sufficient condition for tracking.

Sufficient Condition for Tracking: Let d_{ev} denote the distance to the nearest reflex vertex from $\mathbf{e}_0$ and $d_{ep} = || \mathbf{e}_0 - \mathbf{p}_0 ||$ (Figure 2.23 shows an example). A sufficient condition for the pursuer to catch the evader is the following:

$$\min\{\frac{1-a}{a}, 1\} > \frac{d_{ep}}{d_{ev}}$$

Proof. The minimum time required by the evader to reach the nearest reflex vertex is $t_e = \frac{d_{ev}}{\overline{v}_e}$. Let R_{t_e} denote the set of points in the free workspace reachable by the evader, starting at $\mathbf{e}_0$, in time t_e; i.e., R_{t_e} consists of points $\mathbf{x} \in \mathbb{R}^2$ in free workspace such that $|| \mathbf{x} - \mathbf{e}_0 || \leq d_{ev}$.

Lemma 6: R_{t_e} is convex.

Proof. R_{t_e} cannot contain any reflex vertex of the environment in its interior as t_e is the time required by the evader to reach the nearest reflex vertex. HenceR_{t_e} is convex. □

Consider $\mathbf{p}_0 \in R_{t_e} \implies \frac{d_{ep}}{d_{ev}} < 1$. Consider a strategy for the pursuer in which it moves directly towards the evader with speed $\overline{v}_p$.

Property 1: The pursuer remains in $R_{t_e} \quad \forall \quad t \leq t_e$.

Proof. From triangular inequality, we obtain the following condition:

$$|| \mathbf{p}(t) - \mathbf{e}_0 || \leq || \mathbf{p}(t) - \mathbf{e}(t) || + || \mathbf{e}(t) - \mathbf{e}_0 ||$$

At any time t, the distance between the pursuer and the evader decreases by at most $(\overline{v}_p - \overline{v}_e)t$. Hence $|| \mathbf{p}(t) - \mathbf{e}(t) || \leq d_{ep} - (\overline{v}_p - \overline{v}_e)t$. At any time t, the evader travels a maximum distance of $\overline{v}_e t$ from its initial position. Hence $|| \mathbf{e}(t) - \mathbf{e}_0 || \leq \overline{v}_e t$.

$$\begin{aligned} \implies || \mathbf{p}(t) - \mathbf{e}_0 || &\leq d_{ep} - (\overline{v}_p - \overline{v}_e)t + \overline{v}_e t \\ &\leq d_{ep} + (2\overline{v}_e - \overline{v}_p)t_e \end{aligned}$$

Substituting $t_e = \frac{d_{ev}}{\overline{v}_e}$ in the above inequality leads to

$$\begin{aligned} || \mathbf{p}(t) - \mathbf{e}_0 || &\leq d_{ep} + (2\overline{v}_e - \overline{v}_p)\frac{d_{ev}}{\overline{v}_e} \\ &= d_{ep} + \frac{(2a-1)}{a} d_{ev} \end{aligned}$$

Using the condition $\frac{d_{ep}}{d_{ev}} < \frac{1-a}{a}$, we obtain

$$\begin{aligned} || \mathbf{p}(t) - \mathbf{e}_0 || &\leq \frac{(1-a)}{a} d_{ev} + \frac{(2a-1)}{a} d_{ev} \\ &= d_{ev} \end{aligned}$$

Hence at all times $t \leq t_e$, the pursuer remains inside R_{t_e}. □

Property 2: The pursuer can see the evader $\quad \forall \quad t \leq t_e$.

Proof. From Property 1, $\mathbf{p}(t) \in R_{t_e} \quad \forall \quad t \leq t_e$. By definition $\mathbf{e}(t) \in R_{t_e} \quad \forall \quad t \leq t_e$. Hence $\mathbf{p}(t)$ and $\mathbf{e}(t)$ are in $R_{t_e} \quad \forall \quad t \leq t_e$. Using Lemma 6, we can conclude that pursuer can see the evader $\quad \forall \quad t \leq t_e$. □

Property 3: The pursuer can catch the evader in time $t \leq t_e$.

Proof. If the pursuer follows the strategy to move directly towards the evader with speed $\overline{v}_p$, the time required by the pursuer to catch the evader is $t_p \leq \frac{d_{ep}}{\overline{v}_p - \overline{v}_e}$. The time required by the evader to reach the boundary of R_{t_e} is $t_e \geq \frac{d_{ev}}{\overline{v}_e}$. Since $\frac{d_{ep}}{d_{ev}} < \frac{1-a}{a} \quad \Longrightarrow \quad t_p \leq t_e$. Hence the property follows. □

From Property 2 and 3, the pursuer can track the evader and catch it if the following conditions are satisfied: $\mathbf{p}_0 \in R_{t_e} \quad \Longrightarrow \quad \frac{d_{ep}}{d_{ev}} < 1$ and $\frac{d_{ep}}{d_{ev}} < \frac{1-a}{a}$. This leads to the sufficient condition for tracking. □

CHAPTER 3

TARGET TRACKING: A GAME OF DEGREE

In this chapter, we analyze the problem of target tracking as a *game of degree*. We use techniques from differential game theory to compute the saddle point strategies for the players. Furthermore, we compute the optimal trajectories of the players near the termination situations. We conclude the chapter by presenting the construction of a specific kind of *singular surface*, called the *dispersal surface*, that appears in this game.

The organizations of this chapter is as follows. In Section 3.1, we provide a brief history of pursuit-evasion and differential games. In Section 3.2, we present the formulation of the target-tracking problem as a game of degree. In Section 3.3, we present the saddle-point strategies for the players. In Section 3.4, we present the construction of the optimal trajectories near the termination situations around a corner. In Section 3.5, we present the construction of the *dispersal surfaces* that appear in this game.

3.1 Pursuit-Evasion and Differential Games: A Brief History

One of the earliest works that illustrates the connection between differential games and pursuit-evasion is the seminal work of Isaacs that culminated in his book [9]. A general framework based on the concepts in classical game theory and the notion of *tenet of transition* was used to analyze pursuit-evasion problems. Classical problems like the *Lion and the Man*, *Homicidal Chauffeur* and *Maritime Dogfight* were introduced in this book. Among the many problems introduced in this book is the famous problem of *The Lady in the Lake*. A formulation of this game that appeared in the Russian translation of Isaacs work is as follows [10]:

> *The problem is about a lady E who swims (with speed $\beta < 1$) in a circular pond (with a radius of magnitude 1). A lusty man P runs*

along the circumference of the pond wishing to take the closest picture of the lady as she gets out...

The problem is to find a strategy for the lady to get out of the pond at a point farthest away from the man. Another famous game introduced in his book is the *Homicidal Chauffeur*. In this game a car strives to hit a slower but a more nimble pedestrian. The motivation for Isaacs was to model in a simplified manner a game of air combat where a slow, but more maneuverable airplane is pursued by a faster and less maneuverable craft. A complete solution to the *Homicidal Chauffeur* is spread out over [43] and [44]. In the *Obstacle Tag* problem [45], [46], a faster pursuer wants to capture a slower evader in minimum time in the presence of an obstacle. In addition to the formulation of these problems that relate to real-life scenarios, Isaacs' book also provides the necessary conditions for optimal trajectories for the players, although these were also proposed independently by Blaquiére et al. in [47]. Moreover, it is the first work that provides an extensive introduction to various kinds of *singular surfaces* that arise in pursuit-evasion games. It concludes with a brief introduction to the the theory of games with incomplete information. An elaborate history of the various generalizations and modifications of the classical problems dealt with in Isaacs' book and formulation of new problems in pursuit-evasion are presented in [48], [10].

In this chapter, we deal with continuous time formulation of the target-tracking game. It was through this type of problem (i.e., through the study of pursuit and evasion between two objects moving according to simple kinematic laws) that the theory of differential games was started in the early 1950s [48]. The theory of differential games is a blending of the notions of control theory with the decision structures and solution concepts of classical game theory. In general, we can reduce a differential game model to a control problem if we assume that only one player is active and the other is not. This also implies that the theory of differential games includes the results of the theory of optimal controls as special cases. Differential games is used for modeling conflict problems of real life in analytical fashion although it has been used in the past by researchers in control theory to form the linkage between the notion of *robust optimal control* and linear-quadratic differential games in controller design [49]. Continuous-time formulation of pursuit-evasion games belongs to the class of zero-sum differential games. An exhaustive list of solved or partly solved zero-sum differential games is given in [50].

A modification to the classical problems in differential games involves the consideration of their discrete-time versions and the application of a proper information structure to compute the value of the game. In [51], [52], a discrete-time version of a continuous-time zero-sum differential game is analyzed. Based on appropriate assumptions about the smoothness of the value function, the authors prove the convergence of the value as the time step goes to zero. Relaxing the assumption on the smoothness of the value function and restricting the cost function in addition to the dynamics of the players leads to convergence for special problems [53]. Furthermore, in [54] the authors prove the convergence of the game for all cases without the restrictions proposed in [53]. In [55], the author considers the existence of a "min-sup" strategy to a pursuit-evasion game. The author proves the existence of the solutions in case the game terminates in a finite time. In [56], the authors propose a definition of a strategy and justify it by demonstrating the existence of a saddle point. In [57], the authors analyze generalized pursuit-evasion games (games with integral-payoff). They present *modified Isaacs conditions* under which an *extended value function* exists for the players when they use *relaxed controls*. In [58], the authors extend the previous work to linear differential games and prove the existence of saddle point strategies over the set of relaxed controls.

In his work, Isaacs showed that if the values of various differential games are regular enough, then they solve the Isaacs equations that are first order PDE with "max-min" or "min-max" type nonlinearity. In many problems the value functions are not smooth enough to satisfy the Isaacs equations. Many papers have worked around this difficulty, especially Fleming [59], [54], Friedman [60], Elliott and Kalton [61], [62], Krassovski and Subbotin [63], and Subbotin [64]. In [65], the authors present a new notion of "viscosity" solution for Hamilton-Jacobi equations and prove the uniqueness of such solutions in a wide variety of situations. In [66], the author shows that the dynamic programming optimality condition for the value function in differential control theory problems implies that this value function is the viscocity solution of the associated HJB PDE. The foregoing conclusions turn out to extend to differential game theory. In [67], the authors show that in the context of differential games, the dynamic programming optimality conditions imply that the values are viscosity solutions of appropriate partial differential equations. In [68], the authors present a simplification of the previous work.

In general, the solution of optimal strategies for the pursuer and evader is reduced to the problem of solving the Hamilton-Jacobi-Isaacs (HJI) equation, which is a partial differential equation relating the value of the game to the state variables and optimal control inputs. Barring a few exceptions, for a non-linear system model with constraints in state and control inputs, the HJI is difficult to solve in closed form. This calls for the need of numerical techniques to solve the equations. In [69], the authors present various numerical techniques for two-person, zero-sum deterministic differential games for systems that are non-linear in the state variables as well as the control variables. Numerical approximations based on the idea of *reachable sets* [70] are presented in [71]. Further discussion of the advantages and limitations of various numerical techniques can be found in [71], Sec. II.C.

In the next section we formulate the problem of target tracking as a game of degree.

3.2 Formulation of the Game

We consider a mobile pursuer and an evader moving in the plane with velocities $\mathbf{u}(t) = (u_p(t), \theta_p(t))$ and $\mathbf{v}(t) = (u_e(t), \theta_e(t))$ respectively. The speeds of the pursuer and the evader are given by $u_p(t)$ and $u_e(t)$, respectively, and are bounded by $\overline{v}_p$ and $\overline{v}_e$ respectively. The directions of the velocity vectors of the pursuer and the evader are given by $\theta_p(t)$ and $\theta_e(t)$ respectively. We use a to denote the ratio of the maximum speed of the evader to that of the pursuer $a = \frac{\overline{v}_e}{\overline{v}_p}$. The players are assumed to be point robots with no constraints on their motion except for bounded speeds.

The workspace contains obstacles that restrict pursuer and evader motions and may occlude the pursuer's line of sight to the evader. The initial positions of the pursuer and the evader are such that they are visible to each other. The visibility region of the pursuer is the set of points for which a line segment from that point to the pursuer does not intersect the obstacle region. Visibility extends uniformly in all directions and is only terminated by workspace obstacles (omnidirectional, unbounded visibility). The players know each other's current position as long as they are visible to each other. Both players have a complete map of the environment.

In this setting, we consider the following game. The pursuer wants to keep the

evader in its visibility region for the maximum possible time and the evader wants to break the line of sight to the pursuer as soon as possible. If at any instant, the evader breaks the line of sight to the pursuer, the game terminates. Given the initial position of the pursuer and the evader, we want to know the equilibrium strategies used by the players to achieve their respective goals.

The positions of the pursuer and evader on the plane are given by $(x_p(t), y_p(t))$ and $(x_e(t), y_e(t))$ respectively. The state of the system is given by $\mathbf{x}(t) = [x_p(t), y_p(t), x_e(t), y_e(t)]^T$. The kinematic equations of the players are given as follows:

$$\begin{pmatrix} \dot{x}_p(t) \\ \dot{y}_p(t) \\ \dot{x}_e(t) \\ \dot{y}_e(t) \end{pmatrix} = \begin{pmatrix} u_p(t)\cos\theta_p(t) \\ u_p(t)\sin\theta_p(t) \\ u_e(t)\cos\theta_e(t) \\ u_e(t)\sin\theta_e(t) \end{pmatrix}$$

The above set of equations can also be expressed in the form $\dot{\mathbf{x}}(t) = f(\mathbf{x}(t), \mathbf{u}(t), \mathbf{v}(t))$. The presence of obstacles poses configuration and visibility constraints for certain states in $\mathbb{R}^4$. In the next section, we present the characterization of the boundaries of the state space.

3.2.1 State Space

In $\mathbb{R}^4$, the *game set* is the set of all states such that the players are in the free workspace and can see each other. The boundary of the game set consists of two kinds of configurations of the pursuer and the evader (refer to Figure 3.1). The first kind of boundary points consists of states in which either the pursuer or the evader or both lie on the boundary of the workspace. At no point in time can the state of the game cross the boundary at such a point since this results in either of the players penetrating an obstacle in the workspace. The second kind of boundary, called the *target set*, consists of states in which a boundary of an obstacle is incident on the line of sight between the pursuer and the evader. At any point in time, if the current state of the game lies on the target set, then it can cross the boundary according to the rules of the game since in the workspace this results in breaking the mutual visibility between the players which leads to termination of the game. Since we are interested in situations where the mutual visibility between the players can be broken, we are only interested in the part of

the boundary that forms the target set.

Figure 3.2 shows an instance in which the state of the system lies on the target set. Let l_p denote the distance of the vertex from the pursuer. Let l denote the distance between the pursuer and the evader. The evader can force termination if and only if the magnitude of the maximum angular velocity of the evader around the corner is greater than the magnitude of the maximum angular velocity achievable by the pursuer around the corner. This can happen if and only if the following condition holds:

$$\frac{l_p}{l} > \frac{1}{1+a} \tag{3.1}$$

Hence we can further subdivide the target set, depending on whether the evader can guarantee termination at that point. The part of the target set where the evader can guarantee termination regardless of the choice of the controls of the pursuer is called the *usable part* (UP). The remaining part of the target set outside the UP is called the *non-usable part* (NUP). Given any initial position of the pursuer and the evader, the game will always terminate on the UP.

Now we present the equations characterizing the target set around a vertex of an obstacle; see Figure 3.2. The figure shows a state of the pursuer and evader in which a vertex, v, lies on the line of sight between the pursuer and the evader. Hence the current state of the system lies on the target set. We want the equation of the hypersurface that characterizes the target set generated by v. Let $(x_p, y_p, x_e, y_e)^T$ be the state of the system on the target set and (x^o, y^o) be the coordinates of the vertex of the obstacle. We can write the following equation of constraint:

$$\frac{y^o - y_e}{x^o - x_e} = \frac{y^o - y_p}{x^o - x_p}$$

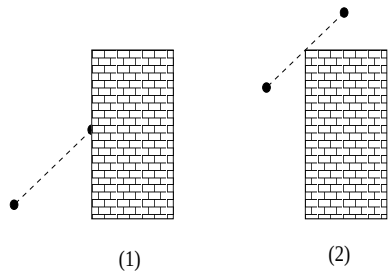

Figure 3.1: Boundary of the game set.

Hence the target set is characterized by

$$\Rightarrow F(x_p, y_p, x_e, y_e) = (y^o - y_p)(x^o - x_e) - (y^o - y_e)(x^o - x_p) = 0 \qquad (3.2)$$

Since the above equation applies to any point on the target set, Equation (3.2) also characterizes the UP of the target set. In the next section, we present the optimal strategies for the players near the termination situations.

3.3 Optimal Strategies

In order to present optimal strategies, we need to define the payoff for the players in the game. Consider a play that terminates at time t_f. Since the objective of the pursuer is to increase the time of termination, its payoff function can be considered as t_f. On the other hand, since the objective of the evader is to minimize the time of termination, its payoff can be considered to be $-t_f$. Since the payoff functions of the players add to zero, this is a *zero-sum* differential game. The time of termination is a function of the initial state $\mathbf{x_0} = \mathbf{x}(0)$ and the control history during the play, $\mathbf{u}(\cdot)$ and $\mathbf{v}(\cdot)$.

Since the players have conflicting goals, the concept of optimality involves the idea of *Nash equilibrium*. If a player follows its equilibrium strategy, it is guaranteed of a minimum outcome without any knowledge of the other player's future actions. Moreover when a pair of strategies for the players is in *Nash equilibrium* then a player cannot improve his outcome by unilateral deviation from its equilibrium strategy. Consider a situation in which the pursuer can keep the evader in sight for time t_f when the players follow their equilibrium strategies. If the evader deviates from its equilibrium strategy then the pursuer might have a strategy to track it for a time greater than t_f. On the other hand, if the pursuer deviates

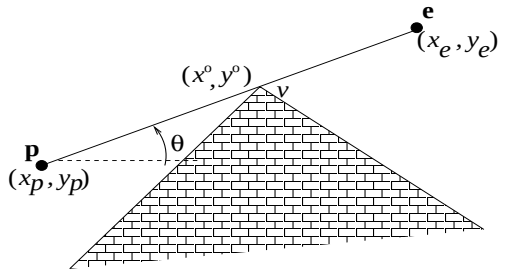

Figure 3.2: State of the system on the target set.

from its equilibrium strategy then the evader might be able to escape in time less than t_f. Hence there is no motivation for either of the players to deviate from their equilibrium strategies due to the lack of knowledge of the other player's future actions. For a pair of equilibrium strategies for the players, either the evader can escape the pursuer's sight in finite time or the pursuer can track the evader forever. Hence computing the equilibrium strategies gives the strategies that are sufficient for tracking or escape, whichever holds at a given point in the state space. In case of a *zero-sum* game, the equilibrium strategies are also referred to as the *saddle-point strategies*. In scenarios where the players have no knowledge about each other's strategies, equilibrium strategies are important since they lead to a guaranteed minimum outcome for the players in spite of the other player's strategies. In this work, *optimal strategies* refers to strategies that are in *Nash equilibrium*.

For a point $\mathbf{x}$ in the state space, $J(\mathbf{x})$ represents the outcome if the players implement their optimal strategies starting at the point $\mathbf{x}$. In this game, $J(\mathbf{x})$ is the time of termination of the game when the players implement their optimal strategies. It is also called the *value* of the game at $\mathbf{x}$. Any unilateral deviation from the optimal strategy by a player can lead to a better payoff for the other player. For example, for a game that starts at a point $\mathbf{x}$, if the evader deviates from the optimal strategy then there may be a strategy for the pursuer in which its payoff is greater than $J(\mathbf{x})$, and if the pursuer deviates from the optimal strategy then there may be a strategy for the evader in which its payoff is greater than $-J(\mathbf{x})$. Since this is a *zero-sum* game, any strategy that leads to a higher payoff for one player will reduce the payoff for the second player.

Let $\nabla J = [J_{x_e} \quad J_{y_e} \quad J_{x_p} \quad J_{y_p}]^T$ denote the gradient of the value function. The Hamiltonian, *H*, of any system is given by

$$H(\mathbf{x}, \nabla J, \mathbf{u}(t), \mathbf{v}(t)) = \nabla J \cdot f(\mathbf{x}, \mathbf{u}(t), \mathbf{v}(t)) + 1$$

Let $\mathbf{u}^*(t) = (u_p^*(t), \theta_p^*(t))$ and $\mathbf{v}^*(t) = (u_e^*(t), \theta_e^*(t))$ be the optimal controls used by the pursuer and the evader respectively. Since the pursuer is the maximizer and the evader is the minimizer, the Hamiltonian of the system satisfies the following conditions, called the *Isaacs* conditions, along the optimal trajectories [9].

1. $H(\mathbf{x}, \nabla J, \mathbf{u}(t), \mathbf{v}^*(t)) \leq H(\mathbf{x}, \nabla J, \mathbf{u}^*(t), \mathbf{v}^*(t)) \leq H(\mathbf{x}, \nabla J, \mathbf{u}^*(t), \mathbf{v}(t))$
2. $H(\mathbf{x}, \nabla J, \mathbf{u}^*(t), \mathbf{v}^*(t)) = 0$

Condition 1 implies that when the players implement their optimal strategies any

unilateral deviation by the pursuer might lead to a smaller value for the Hamiltonian and any unilateral deviation by the evader might lead to a larger value of the Hamiltonian. Moreover condition 2 implies that when the players implement their optimal controls, the Hamiltonian of the system is zero. The Isaacs conditions are an extension of *Pontryagin's principle* in optimization to a differential game [10].

The Hamiltonian of our system is given by

$$\begin{aligned} H(\mathbf{x}, \nabla J, \mathbf{u}(t), \mathbf{v}(t)) &= \nabla J \cdot f(\mathbf{x}, \mathbf{u}(t), \mathbf{v}(t)) + 1 \\ &= u_e(t)[J_{x_e} \cos\theta_e(t) + J_{y_e} \sin\theta_e(t)] \\ &\quad + u_p(t)[J_{x_p} \cos\theta_p(t) + J_{y_p} \sin\theta_p(t)] + 1 \end{aligned}$$

We can see that the Hamiltonian is *separable* in the controls $u_p(t)$ and $u_e(t)$; i.e., it can be written in the form $u_p(t)f_1(\mathbf{x}, \nabla J) + u_e(t)f_2(\mathbf{x}, \nabla J)$. Hence the *minimax* assumption [9] holds. Moreover since the set of controls for each player is compact, the optimal strategies exist. Using Isaacs' first condition, we see that the optimal $\mathbf{u}^*(t)$ and $\mathbf{v}^*(t)$ are given by the following expressions:

$$\mathbf{u}^*(t) = (u_e^*(t), \theta_e^*(t)) = \arg \min_{u_e(t), \theta_e(t)} H(\mathbf{x}, \nabla J, \mathbf{u}(t), \mathbf{v}^*(t))$$

$$\mathbf{v}^*(t) = (u_p^*(t), \theta_p^*(t)) = \arg \max_{u_p(t), \theta_p(t)} H(\mathbf{x}, \nabla J, \mathbf{u}^*(t), \mathbf{v}(t))$$

Since the Hamiltonian is separable, the optimal controls for the players are given by the following expressions in terms of the gradient of the value function:

$$(\cos\theta_p^*(t), \sin\theta_p^*(t)) \mid\mid (J_{x_p}, J_{y_p})$$

$$\implies (\cos\theta_p^*(t), \sin\theta_p^*(t)) = \left(\frac{J_{x_p}}{\sqrt{J_{x_p}^2 + J_{y_p}^2}}, \frac{J_{y_p}}{\sqrt{J_{x_p}^2 + J_{y_p}^2}}\right) \tag{3.3}$$

$$(\cos\theta_e^*(t), \sin\theta_e^*(t)) \mid\mid (-J_{x_e}, -J_{y_e})$$

$$\implies (\cos\theta_e^*(t), \sin\theta_e^*(t)) = \left(-\frac{J_{x_e}}{\sqrt{J_{x_e}^2 + J_{y_e}^2}}, -\frac{J_{y_e}}{\sqrt{J_{x_e}^2 + J_{y_e}^2}}\right) \tag{3.4}$$

$$u_e^*(t) = \overline{v}_e$$

$$u_p^*(t) = \overline{v}_p \tag{3.5}$$

In the first and second equations $||$ is used to denote parallel vectors. In case $J_{x_p} = 0$ and $J_{y_p} = 0$, then θ_p^* can take any value and the pursuer can follow any control strategy. Similarly if $J_{x_e} = 0$ and $J_{y_e} = 0$, then θ_e^* can take any value and

the evader can follow any control strategy. These conditions represent *singularity* in the Hamiltonian.

The entire state space can be partitioned into two regions depending on the value of the game. For all the initial positions of the pursuer and the evader for which the value of the game $J(\mathbf{x})$ is finite, the evader can break the line of sight in finite time by following the strategies in Equation (3.2). For all the initial positions of the pursuer and the evader for which the value of the game is infinite, the pursuer can track the evader forever if it follows the controls given in Equation (3.2).

The analysis done in this section implies that if we are given the value function $J(\mathbf{x})$, then we can compute the optimal strategies for the players from Equation (3.2).

3.4 Construction of Optimal Trajectories

In this section, we present the trajectories generated by the optimal strategies near termination situations. From Equation (3.2), we can conclude that the target set is three-dimensional and hence can be represented by three independent variables. Let the independent variables used to parametrize the target set be chosen as the following:

$$\begin{aligned} s_1 &= x_e - x^o \\ s_2 &= y_e - y^o \\ s_3 &= x_p - x^o \\ \implies y_p &= y^o + \frac{s_2 s_3}{s_1} \end{aligned}$$

The value function at every point on the UP is 0. Hence the directional derivative of the value function along s_1, s_2 and s_3 is zero. Let J^0 denote the value function on the UP of the target set.

$$J^0_{s_1} = 0 = J^0_{x_e} - J^0_{y_p} \frac{s_2 s_3}{s_1^2} \tag{3.6}$$

$$J^0_{s_2} = 0 = J^0_{y_e} + J^0_{y_p} \frac{s_3}{s_1} \tag{3.7}$$

$$J^0_{s_3} = 0 = J^0_{x_p} + J^0_{y_p} \frac{s_2}{s_1} \tag{3.8}$$

Substituting the optimal control laws from Equation (3.3) into the second Isaacs condition, we get the following condition:

$$-\overline{v}_e\sqrt{J_{x_e}^2+J_{y_e}^2}+\overline{v}_p\sqrt{J_{x_p}^2+J_{y_p}^2}+1=0 \tag{3.9}$$

Substituting Equations (3.4), (3.5) and (3.6) into Equation (3.7), we get the following expression for $J_{y_p}^0$:

$$\mid J_{y_p}^0 \mid = \frac{1}{(\sqrt{\frac{s_2^2}{s_1^2}+1})(\overline{v}_e\sqrt{\frac{s_3^2}{s_1^2}}-\overline{v}_p)} \tag{3.10}$$

From Equation (3.1), we can conclude that on the UP, $\mid \frac{s_3}{s_1} \mid > \frac{\overline{v}_p}{\overline{v}_e}$ and hence the R.H.S. of the above equation is always positive. Hence $J_{y_p}^0$ can have two possible values differing just by a sign. In the termination condition shown in Figure 3.2, $J_{y_p}^0$ is positive since the value of the game increases when we perturb the pursuer position vertically upwards. Depending on the position of the corner and the orientation of the pursuer and the evader at the termination situation, we can eliminate one of the possible values of $J_{y_p}^0$.

Now we use the following theorem to obtain the value function along the optimal trajectories backwards in time.

Theorem [9]: Along the optimal trajectory, the following equation holds:

$$\frac{d}{dt}\nabla J[\mathbf{x}(t)] = -\frac{\partial}{\partial x}H(\mathbf{x},\nabla J,\mathbf{u}^*,\mathbf{v}^*)$$

The above equation is called the *retrogressive path equation* (RPE). The retro-time (*time-to-go*) form of the RPE is

$$\frac{d}{d\tau}\nabla J[\mathbf{x}(\tau)] = \frac{\partial}{\partial x}H(\mathbf{x},\nabla J,\mathbf{u}^*,\mathbf{v}^*) \tag{3.11}$$

where $\tau = t_f - t$ is called the retro-time. t_f is the time of termination of the game.

The RPE is a differential equation for the $\nabla J(\mathbf{x})$ along the optimal trajectories in terms of the optimal controls. Substituting the optimal control of the players as a function of $\nabla J(\mathbf{x})$ from Equation (3.3) into the RPE leads to a set of ordinary differential equations for $\nabla J(\mathbf{x})$. For our system, the RPE gives the following set

of differential equations:

$$\begin{aligned}
\mathring{J}_{x_p} &= 0 \\
\mathring{J}_{y_p} &= 0 \\
\mathring{J}_{x_e} &= 0 \\
\mathring{J}_{y_e} &= 0
\end{aligned} \tag{3.12}$$

Hence ∇J remains constant along an optimal trajectory. We can obtain the values of ∇J by computing the initial conditions of RPE which are the same as the termination situations for the game in forward time. Integrating the RPE backward in time from the UP gives the following expressions of $\nabla J(\mathbf{x})$:

$$\begin{aligned}
J_{x_p} &= J^0_{x_p} \\
J_{y_p} &= J^0_{y_p} \\
J_{x_e} &= J^0_{x_e} \\
J_{y_e} &= J^0_{y_e}
\end{aligned} \tag{3.13}$$

Substituting $\nabla J(\mathbf{x})$ into the optimal controls in Equation (3.3) gives the control strategies for the players.

$$\begin{aligned}
(\cos\theta^*_p, \sin\theta^*_p) &= \left(\frac{J^0_{x_p}}{\sqrt{(J^0_{x_p})^2 + (J^0_{y_p})^2}}, \frac{J^0_{y_p}}{\sqrt{(J^0_{x_p})^2 + (J^0_{y_p})^2}}\right) \\
(\cos\theta^*_e, \sin\theta^*_e) &= \left(-\frac{J^0_{x_e}}{\sqrt{(J^0_{x_e})^2 + (J^0_{y_e})^2}}, -\frac{J^0_{y_e}}{\sqrt{(J^0_{x_e})^2 + (J^0_{y_e})^2}}\right) \\
u^*_e &= \overline{v}_e \\
u^*_p &= \overline{v}_p
\end{aligned} \tag{3.14}$$

Substituting the control laws for the players into the kinematic equation leads to the optimal trajectories in retro time. Let $(x^f_p, y^f_p, x^f_e, y^f_e)$ be the state of the system at the termination situation on the UP. From Equation (3.8), the value of $J^0_{y_p} = \overset{+}{-} c_1 cos\theta_f$, where $c_1 = \frac{1}{\overline{v}_e|\frac{x^o - x^f_e}{x^o - x^f_p}| - \overline{v}_p}$ and $\tan\theta_f = \frac{y^f_e - y^o}{x^f_e - x^o}$. The optimal trajectory of

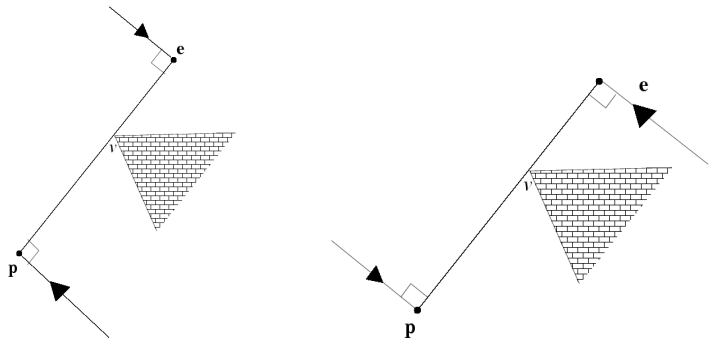

Figure 3.3: Optimal trajectories to a termination situation.

the pursuer as a function of retro-time is given by the following equations:

$$\begin{aligned} x_p(\tau) &= x_p^f \underset{-}{+} \tau \overline{v}_p \sin\theta_f \\ y_p(\tau) &= y_p^f \underset{+}{-} \tau \overline{v}_p \cos\theta_f \end{aligned} \tag{3.15}$$

The optimal trajectory of the evader as a function of retro-time is given by the following equations:

$$\begin{aligned} x_e(\tau) &= x_e^f \underset{+}{-} \tau \overline{v}_e \sin\theta_f \\ y_e(\tau) &= y_e^f \underset{-}{+} \tau \overline{v}_e \cos\theta_f \end{aligned} \tag{3.16}$$

Since ∇J is constant along an optimal trajectory, from the expression of the optimal strategies of the players, we see that they are straight lines. Moreover from Equations (3.13) and (3.14), we conclude that the players move parallel to each other in opposite directions, perpendicular to the line of sight at the termination situation. Given a termination situation, this leads to two kinds of trajectories for the players as shown in Figure 3.4. Now we show that only one of these two kinds can lead to termination.

Referring to Figure 3.4, let **p** and **e** be positions of the pursuer and the evader at a termination situation. Consider a small amount of perturbation in the pursuer's position in the positive y-direction. Let the new position of the pursuer be $\mathbf{p}'$. The value of the game at $(x_{p'}, y_{p'}, x_e, y_e)$ is greater than zero since the evader cannot terminate the game instantly. Hence J_{y_p} is greater than zero at (x_p, y_p, x_e, y_e). The velocity of the pursuer is perpendicular to the line-of-sight between the pursuer and the evader at the termination situation. $J_{y_p} > 0 \Longrightarrow \sin\theta_p^* > 0 \Longrightarrow 0 <$

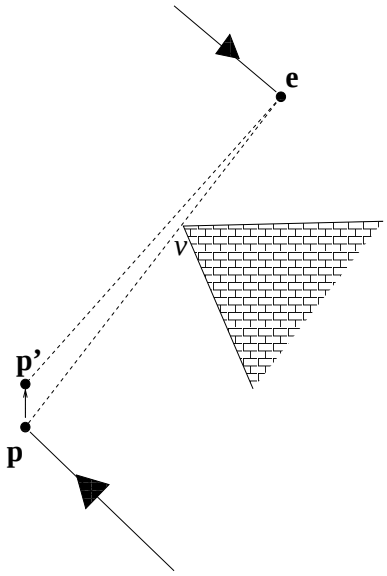

Figure 3.4: A configuration of the bar on the target set.

$\theta_p^* < \pi$ at the termination situation. Hence the pursuer approaches the termination situation in the direction shown in the figure. Since the velocity of the evader is in the opposite direction, the evader approaches the termination situation in the direction shown in the figure. Repeating the above analysis for all orientations of the termination configuration and the obstacle leads to the conclusion that at the termination situation the evader moves toward the obstacle and the pursuer moves away from the obstacle. This leads to a unique set of optimal trajectories from every point on the UP.

For a general environment in the plane, the optimal trajectories lie in $\mathbb{R}^4$. In order to depict them in $\mathbb{R}^3$, we need to consider a subspace of the optimal paths terminating at a corner. In the following examples, for each corner in the environment we show the subspace of the optimal paths that have a fixed distance of the pursuer from the corner at the termination situation. The value of the speed ratio, a, is 0.66 in all the examples. Figure 3.4 shows the optimal trajectories for the players in a simple environment containing a point obstacle at the origin. The line of sight between the pursuer and the evader is broken if it passes through the origin. The evader wants to minimize the time required to break the line of sight and the pursuer wants to maximize it. Let $(x_p^f, y_p^f, x_e^f, y_e^f)$ represent the state of the system at the termination situation. Figure 3.4(a) shows the optimal trajectories of the players for a constant value of $(x_p^f,\ y_p^f)$. Figure 3.4(b) shows the optimal trajectories for every orientation of the line-of-sight between the pursuer and the

evader at the termination situation. The z axis represents the angle that the line-of-sight makes with the horizontal axis at the termination situation. A cross-section parallel to the xy-plane gives the optimal trajectories of the players in a plane for a given θ_f. The red line in the middle denotes the point obstacle. The inner spiral is formed by the optimal trajectories of the evader and the outer spiral is formed by the optimal trajectory of the pursuer. The color of a point represents the value of the game, $J(\mathbf{x})$, at that point. The value of the game increases as the color changes from blue to red. For any point on the spiral, the value of the game is directly proportional to its radial distance from the point obstacle. Figure 3.6(a) shows a single corner in the plane. The internal angle at the corner is $\frac{2\pi}{3}$. Figure 3.6(b) shows the optimal trajectories of the players for the corner in a manner similar to Figure 3.4(b). Figure 3.4(a) shows a regular hexagon in the plane. Figure 3.4(b) shows the optimal trajectories of the players for the hexagonal obstacle in a manner similar to Figure 3.4(b).

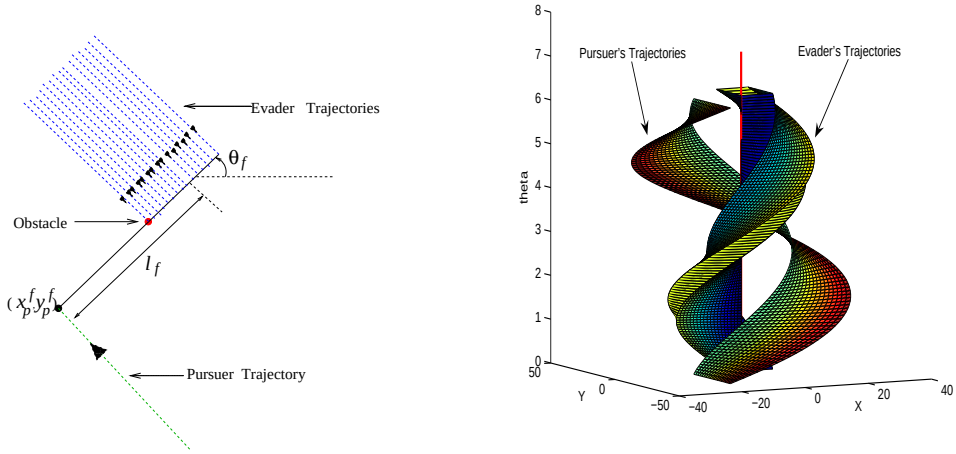

(a) Optimal trajectories in the plane. (b) Optimal trajectories across a section in $\mathbb{R}^4$.

Figure 3.5: Optimal trajectories for an environment having a single point obstacle.

3.5 Singular Surfaces

Issacs' work on two-person zero-sum differential game is mainly a study of singular surfaces (together with the fundamentals of Hamilton-Jacobi theory). An

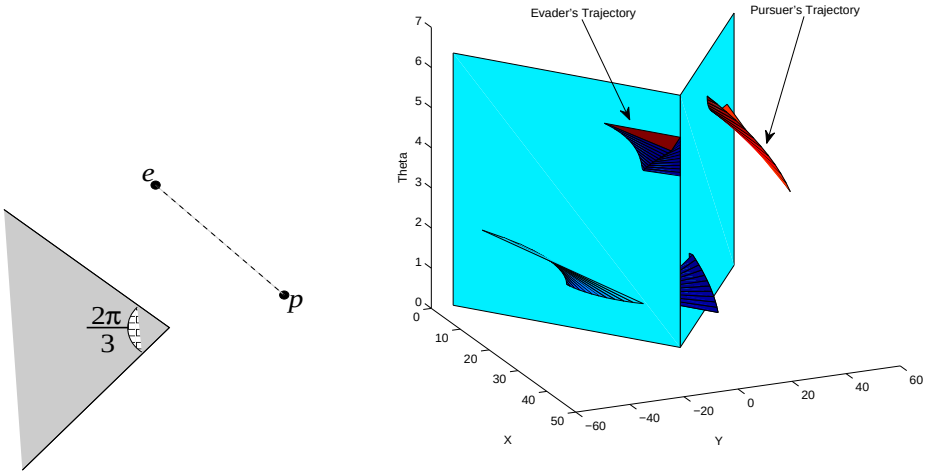

(a) A single corner in space. (b) Optimal trajectories for the players.

Figure 3.6: Optimal trajectories of the players for a corner in space.

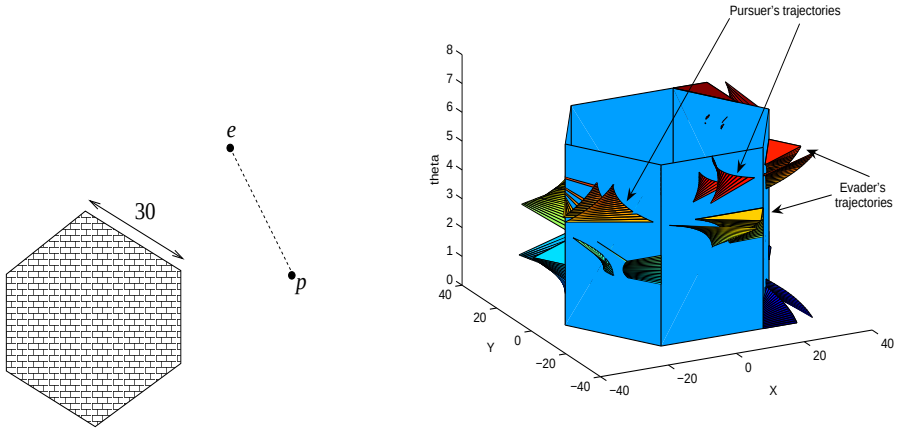

(a) A hexagonal obstacle in space. (b) Optimal trajectories for the players.

Figure 3.7: Optimal trajectories of the players for a hexagonal obstacle in space.

assumption almost always made at the outset of every pursuit-evasion game is that the state space can be split up into a number of mutually disjoint regions, the value function being continuosly differentiable in each of them. The behavior and the method of construction of the value function are well understood in such regions. The boundaries of these regions are called *singular surfaces*, or *singular lines* if they involve one-dimensional manifolds, and the value function is not continuously differentiable across them. A singular surface is a manifold on which

(i) the equilibrium strategies are not uniquely determined by Isaacs' necessary conditions, or (ii) the value function is not continuously differentiable, or (iii) the value function is discontinuous. This topic was extensively investigated by J. V. Breakwell and his students. Various kinds of singular surfaces occurring in the different kinds of pursuit-evasion games are illustrated in [10] and [48] .

From [72], we get the following definition for singular surfaces based on the regularity of the Hamiltonian (H$(\mathbf{x}, \nabla J(\mathbf{x}))$) and the value function ($J(\mathbf{x})$):

A regular point of a differential game is an internal point $\mathbf{x}^*$ *of the domain of the definition of the game value* $J(\mathbf{x})$ *such that the function* $J(\mathbf{x})$ *is twice differentiable in a neighborhood* D *of* $\mathbf{x}^*$, $J(\mathbf{x}) \in C^2(D)$, *and the Hamiltonian* $H(\mathbf{x}, \nabla J(\mathbf{x}))$ *is also twice differentiable in its arguments; i.e.,* $H(\mathbf{x}, \nabla J(\mathbf{x})) \in C^2(N)$ *where* N *is a neighborhood of the point* $(\mathbf{x}^*, \nabla J(\mathbf{x}^*))$. *A singular point is any point in the phase space which is not regular. Singular curve, surface or manifold consist of singular points.*

The above definition meets the geometrical definitions of [9], [73] and [48]. Figure 3.8 presents the qualitative behavior of the regular and singular paths for different types of singular hypersurfaces. Some of the surfaces contain singular paths, while others, like dispersal or switching surfaces, do not. Several surfaces are associated with a jump of ∇J, while others, like the switching or universal ones, are not. The classification presented in Figure 3.8 is not complete; it is a list of singularities met so far and more or less fully investigated [72].

Based on the method of singular characteristics [72], researchers have encountered singular surfaces in pursuit-evasion games related to pursuit and capture. In [74], the problem of pursuit and capture is addressed for players that lie on arbitrary manifolds. An algorithm is presented to partition the phase-space into primary and secondary domains and characterize the regular as well as the singular trajectories in each domain. In [75], [76], the techniques presented in the previous work are applied to a pursuit-evasion game on a cone. In addition to the primary and secondary domains, the authors present explicitly the construction of the equivocal and dispersal surfaces occurring in the game. In [77], the authors address a pursuit-evasion problem on second-order rotation surfaces. The authors present the solution to the pursuit problem on a two-sheet cone.

In the next section, we present an introduction to a special kind of *singular surface* called the *dispersal surface*.

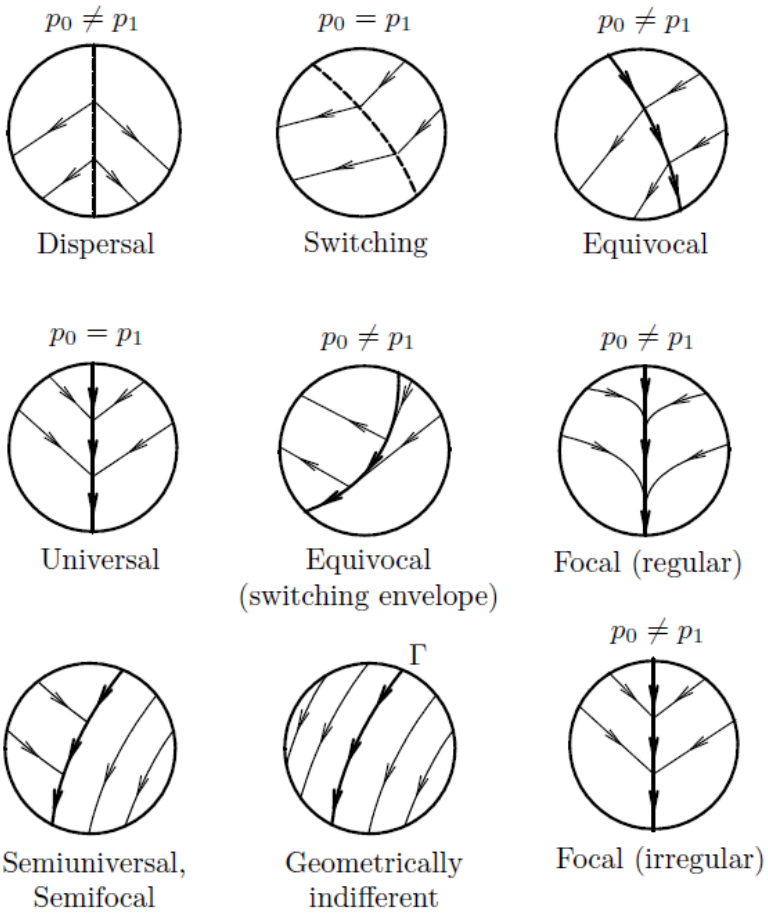

Figure 3.8: Singular surfaces.

3.5.1 Dispersal surfaces

Dispersal surfaces are commonly encountered in games of degree. These are singular surfaces on which the players have more than one saddle-point strategy that leads to the same payoff at termination. For a single-player the game reduces to an optimization problem and the player can choose either one of the strategies to achieve its optimal value. In the case of zero-sum games the choice of strategies is less obvious. In the previous section, the optimal trajectories are constructed backward in time from the termination situations. Termination situations are characterized by points in the configuration space where the evader can break the mutual line-of-sight with the pursuer irrespective of the pursuer's strategy. Since the construction of the trajectories is retrograde in time this might lead to a situation in which more than one optimal trajectory reaches a point in the configu-

ration space from different termination situations. In this work, we only consider points at which two optimal trajectories reach a point in the phase space from two different termination situations. From such a point, the players have two different pairs of strategies to terminate the game. Figure 3.9 shows such an example. The pursuer and the evader are at the end of a semi-infinite corridor. Both the players are on the line *l* that is equidistant from both the walls of the corridor. The evader can move toward C_1 or C_2 to hide from the pursuer. If the evader moves toward C_1, the optimal strategy of the pursuer is to move toward p_1 in order to keep the evader visible for the maximum amount of time. If the evader moves toward C_2, the optimal strategy of the pursuer is to move toward p_2. Hence the players can choose between either pair of the strategies to terminate the game. Moreover, the time of termination is the same for either choice.

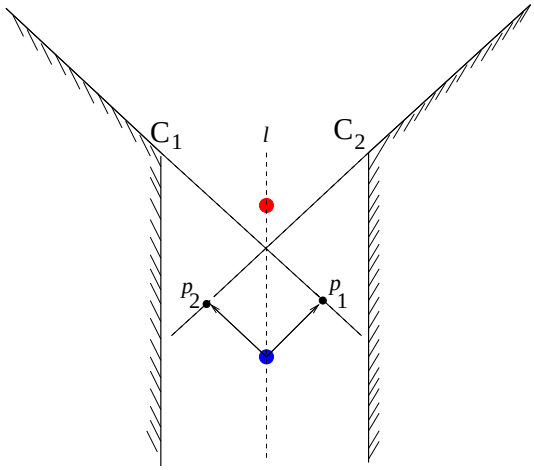

Figure 3.9: Dispersal surfaces.

If the game starts on the dispersal surface, the evader has an open-loop strategy to guarantee the payoff, but the pursuer lacks such an open-loop strategy. The pursuer has to be informationally superior in order to guarantee its payoff. In this case the pursuer must know the instantaneous velocity of the evader to guarantee its payoff. If the pursuer lacks knowledge about the evader's current strategy, then the optimal policy for the pursuer is a mixed strategy. Once the evader leaves the line l, such a situation does not exist anymore. Hence the dispersal surfaces can also be the seat of *instantaneous mixed strategy* (IMS).

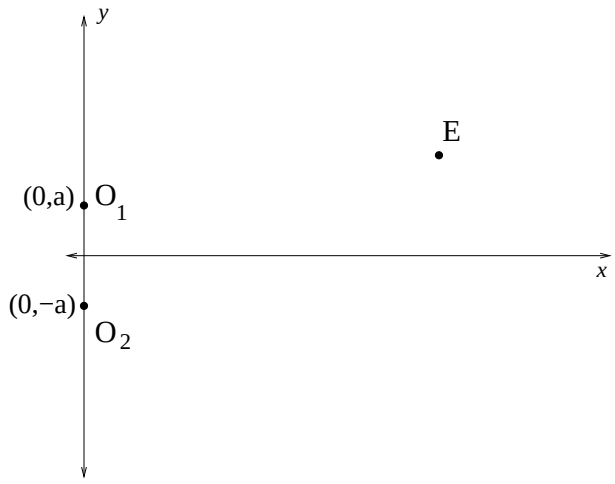

Figure 3.10: Position of obstacles and the evader.

3.5.2 Two point obstacles

In this section, we present the construction of a dispersal surface in the presence of two point obstacles in space. Refer to Figure 3.10. Let $O_1 = (0, a)$ and $O_2 = (0, -a)$ denote the position of the two point obstacles. Let E denote the initial position of the evader. Let the Cartesian coordinates of E be given by (x_e, y_e). Let t denote the time of termination of the game; i.e., if the pursuer is initially at E, it loses sight of the evader for the first time at t.

Since the maximum speed of the evader is $\overline{v}_e$ the reachable set of the evader at time t is $B_{\overline{v}_e t}[E]$ where $B_{\overline{v}_e t}[E] = \{P \in \mathbb{R}^2 \mid d(P, E) \leq \overline{v}_e t\}$. Let $\mathcal{D}$ denote $B_{\overline{v}_e t}[E]$. An infinite number of trajectories for the evader are possible that lie inside $\mathcal{D}$ and do not violate the constraints on the maximum speed of the evader. Since we are only interested in calculating the paths of the evader obtained from saddle-point strategies, this restricts the set of possible trajectories.

Lemma 7: If the game terminates at time t, then the possible positions of the evader at termination are the points of tangency of $\mathcal{D}$ from the corners O_1 and O_2 as shown in Figure 3.11.

Proof. The evader can break the line of sight only around a corner present in the environment. Therefore, the game terminates either around O_1 or O_2. Let us first consider the former case. In the previous section, it has been shown that if the evader follows its saddle-point strategy it must travel on a straight line with speed $\overline{v}_e$ before termination. Therefore, the evader lies on $\partial\mathcal{D}$ (boundary of $\mathcal{D}$) at termination. Moreover, from the previous section we also know that the straight line

on which the evader travels must be perpendicular to the line segment joining O_1 and the position of the evader at termination. This leads to two possible positions of the evader on $\partial\mathcal{D}$ at termination as shown in Figure 3.11: A and A'. The line from O_1 to A and A' is tangent to $\partial\mathcal{D}$. Moreover, from the regular analysis we can conclude that the only possible position for the evader at termination is the point A since the pursuer can avoid termination if the evader is at A'. Similarly, we can perform the analysis if the evader breaks the line of sight around O_2 and conclude that the only possible position of the evader at termination in this case is the point B. Therefore, we have shown that if the evader starts from E and follows its saddle-point strategy it can terminate the game either at A or B, both of which are points of tangency of D from O_1 and O_2. □

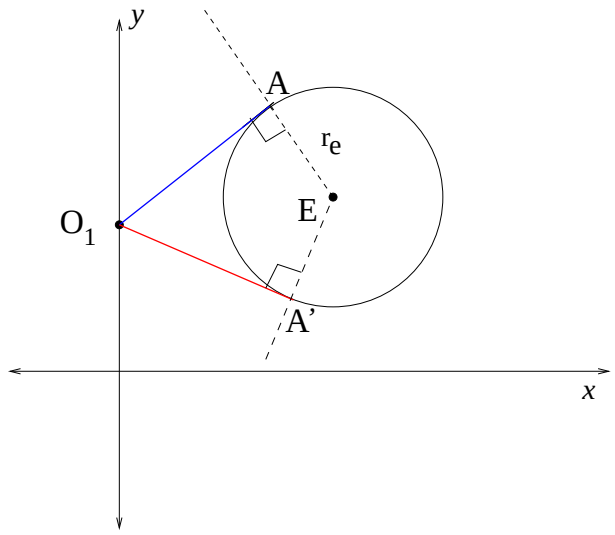

Figure 3.11: Possible positions of the evader at termination.

As t varies from 0 to t_{max}, the point A traces an arc of a circle. The center of the circle lies at the mid-point of O_1E and the radius of the circle is $\sqrt{x_e^2 + (y_e - a)^2}$. From Lemma 1 we can compute the initial positions of the pursuer. Let us consider the case when the termination occurs around O_1. From the regular analysis, we can conclude that at termination the pursuer can be anywhere on the ray DF. The saddle-point strategy of the pursuer is to follow a straight line that is perpendicular to the line joining the pursuer and the evader at termination. Since the game lasts for time t, the initial position of the pursuer can be anywhere on the ray l_1 that lies on L_1 and is parallel to the ray DF at a distance $\overline{v}_p t$. L_1 is parallel to the ray AF and therefore both have the same slope. The slope of AF can be

calculated as follows. Refer to Figure 3.12.

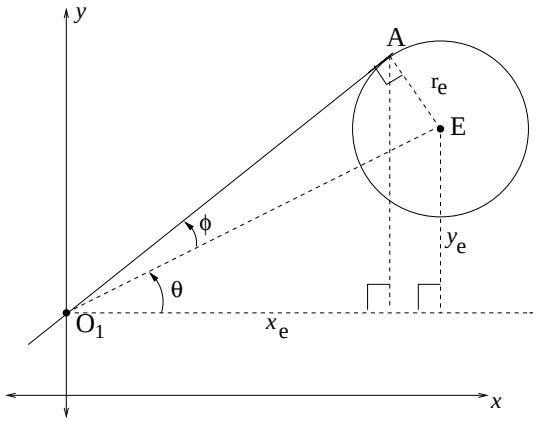

Figure 3.12: Geometry of $\mathcal{D}$ at time t.

$$\tan\theta = \frac{y_e - a}{x_e}$$

$$\tan\phi = \frac{\overline{v}_e t}{\sqrt{x_e^2 + (y_e - a)^2 - \overline{v}_e^2 t^2}}$$

$$m_1 = \tan(\theta + \phi) = \frac{\tan\theta + \tan\phi}{1 - \tan\theta\tan\phi}$$

Hence $m_1 = \frac{(y_e-a)\sqrt{x_e^2+(y_e-a)^2-\overline{v}_e^2t^2}+x_e\overline{v}_et}{x_e\sqrt{x_e^2+(y_e-a)^2-\overline{v}_e^2t^2}-(y_e-a)\overline{v}_et}$. Refer to Figure 3.13. The y-intercept of L_1 is given as follows:

$$c_1 = a + v_p t\sec\theta = a + \overline{v}_p t\sqrt{1+\tan^2\theta}$$

where θ is the angle that L_1 makes with the positive x-axis. Since m_1 is the slope of line L_1, $\tan\theta = m_1$.

$$\implies c_1 = a + \overline{v}_p t\sqrt{1+m_1^2}$$

Hence the equation of line L_1 is given by

$$y = \frac{(y_e - a)\sqrt{x_e^2 + (y_e - a)^2 - \overline{v}_e^2 t^2} + x_e\overline{v}_e t}{x_e\sqrt{x_e^2 + (y_e - a)^2 - \overline{v}_e^2 t^2} - (y_e - a)\overline{v}_e t}x + a + \overline{v}_p t\sqrt{1+m_1^2}$$

If the termination occurs around the corner O_2, the initial position of the pursuer can be anywhere on ray l_2. We can carry out an analysis as before and find the

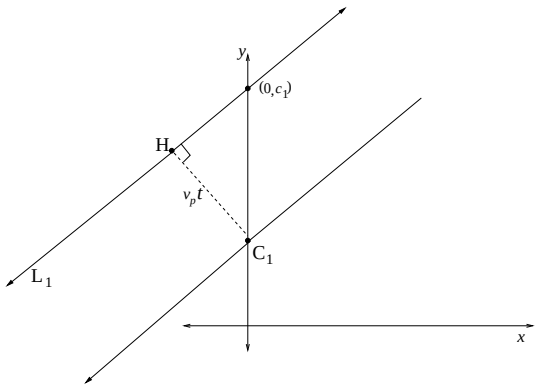

Figure 3.13: Geometry of L_1.

equation of line L_2 on which the l_2 lies. The equation of L_2 is

$$y = \frac{(y_e+a)\sqrt{x_e^2+(y_e+a)^2-\overline{v}_e{}^2t^2}-x_e\overline{v}_et}{x_e\sqrt{x_e^2+(y_e+a)^2-\overline{v}_e{}^2t^2}+(y_e+a)\overline{v}_et}x - a - \overline{v}_pt\sqrt{1+m_2^2}$$

Let P denote the point of intersection of rays l_1 and l_2. If the initial position of the pursuer is P, then the evader has two equally good choices to terminate the game. The pursuer has to make his choice based on the instantaneous velocity of the evader. The initial position of the players corresponding to this situation lies on a dispersal surface. The coordinates of P are given as follows:

$$x_p = \frac{c_2-c_1}{m_1-m_2}; \quad y_p = \frac{m_1c_2-m_2c_1}{m_1-m_2} \tag{3.17}$$

For a fixed initial position of the evader, the point P traces a curve in the plane as t varies. This curve is the one-dimensional projection of the three-dimensional dispersal surface along the initial position of the evader. In order to find the trajectory of P as t increases, the origin and the slope of rays l_1 and l_2 must be computed as a function of time. The origin of l_1 is denoted by H in Figure 3.10. Due to similarity of triangles $\triangle O_1H_1D$ and $\triangle O_1EA$, the point H_1 remains stationary in time. The coordinates of H_1 are $(-rx_e, (1+r)a - ry_e)$. As t increases, the ray l_1 rotates about H_1 with its slope equal to that of segment AF. Similarly the point O_2 leads to the point $H_2 = (-rx_e, -a(1+r) - y_e)$. If the rays l_1 or l_2 become parallel to the y axis, the point P ceases to exist after that instant. Hence the maximum time of termination for which the game allows a dispersal surface is $t_{max} = \frac{x_e}{\overline{v}_e}$.

The presence of the obstacles in the environment prevents t from taking all

values in $[0, \infty]$. If any of the corners lie inside $\mathcal{D}$ then there is no tangent from that corner to $\partial\mathcal{D}$. Hence the dispersal surface ceases to exist. If the lines tangent to $\partial\mathcal{D}$ from the corners are parallel or divergent, then L_1 and L_2 do not intersect. This shows that there is a lower bound on the size of $\mathcal{D}$ for which P exists, and therefore for P to exist $t \geq t_{min}$. Lemma 8 provides a condition for computing t_{min}. Refer to Figure 3.14.

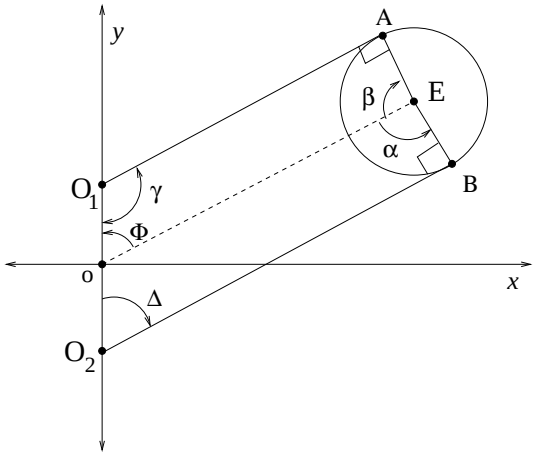

Figure 3.14: Geometry of $\mathcal{D}$.

Lemma 8: The point P exists *iff* $\alpha + \beta < \pi$

Proof. If $\gamma + \Delta > \pi$, O_1A and O_2B intersect $\Leftrightarrow$ L_1 and L_2 intersect$\Leftrightarrow$P exists. From the sum of angles of $\square$ O_1AOE, we obtain that $\gamma = 2\pi - (\phi + \frac{\pi}{2} + \beta) = \frac{3}{2}\pi - (\phi + \beta)$. From the sum of angles of $\square$ O_2OEB, we can conclude that $\Delta = 2\pi - (\pi - \phi + \frac{\pi}{2} + \alpha) = \frac{\pi}{2} - (\alpha - \phi)$. Hence $\gamma + \Delta = 2\pi - (\alpha + \beta)$. Hence the result follows. $\square$

At the moment $\alpha + \beta = \pi$, the lines O_1A and O_2B are parallel to each other and the radius of ∂D is given by $r_{min} = a \sin\phi = a\frac{x_e}{\sqrt{x_e^2+y_e^2}}$. Hence the minimum time of termination is $t_{min} = \frac{ax_e}{\overline{v}_e\sqrt{x_e^2+y_e^2}}$.

Figure 3.15 illustrates the singular surfaces for two different scenarios. The positions of the point obstacles are (0,3) and (0,-3). The maximum speed of the pursuer is assumed to be 1. In Figure 3.15(a), the dispersal surfaces are shown for four different initial positions of the evader. In Figure 3.15(b), dispersal surfaces are shown for different maximum speeds of the evader.

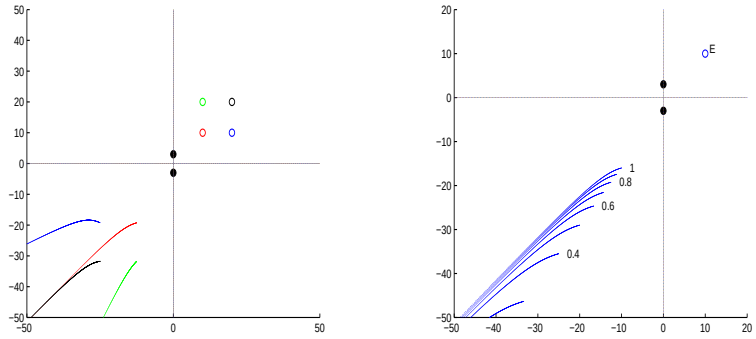

(a) Different evader positions. (b) Different evader speeds.

Figure 3.15: Singular surfaces for a point obstacle.

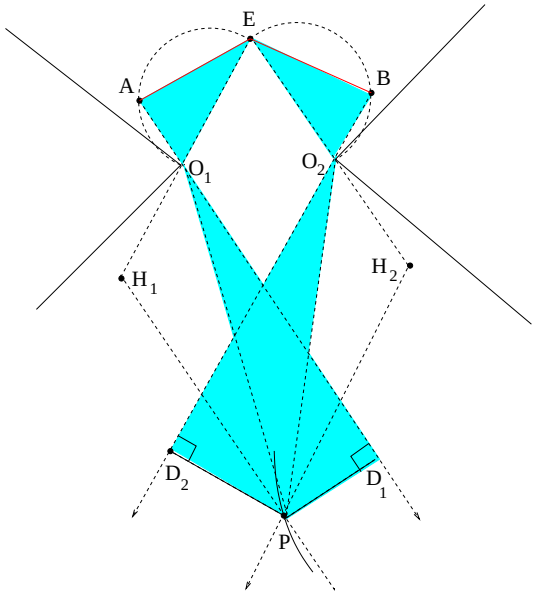

Figure 3.16: Dispersal surface in the vicinity of two corners.

3.5.3 Two corners in a general polygonal environment

In this section, we extend the previous analysis to compute the dispersal surface formed due to the intersection of the optimal paths emanating in retrograde time from two corners in the presence of other obstacles. Refer to Figure 3.16. Consider an environment having polygonal obstacles. Let E be the initial position of the evader. Let (x_e, y_e) represent the coordinates of E in the plane. Let O_1 and O_2 be corners of obstacles C_1 and C_2 in the environment that satisfy the following conditions:

1. $O_1 \in V(E)$

2. $O_2 \in V(E)$

It is not necessary for C_1 and C_2 to be distinct obstacles.

Let A be the position of the evader at termination if it breaks the line-of-sight with the pursuer around O_1. Similarly, let B be the position of the evader at termination if it breaks the line-of-sight with the pursuer around O_2. Since A is the termination position of the evader, it satisfies the following conditions:

1. A$\in W_{\text{free}}$.

2. A lies on the arc of the semi-circle with O_1E as the diameter.

3. O_1 is visible to the evader as it moves on a straight line joining E and A $\implies$ AE$\in V(O_1)$.

Similar conditions must hold for B to qualify as a terminating position for the evader around corner O_2. Let $\tilde{S}_1$ denote the set of all points A that satisfy the above conditions and $\tilde{S}_2$ denote the set of all points B that satisfy a similar set of conditions around the corner O_2.

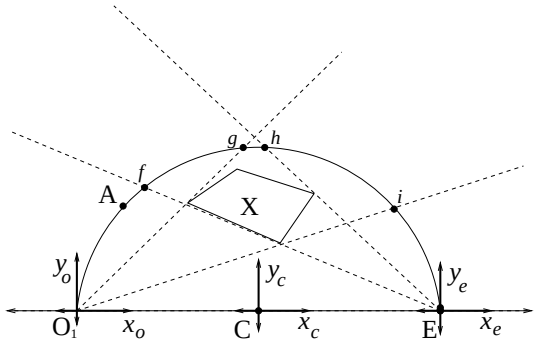

Figure 3.17: Obstacle in the vicinity of the corner and the initial evader position.

Now we present the construction of $\tilde{S}_1$ and $\tilde{S}_2$. Refer to Figure 3.17. Let E be the initial position of the evader. Let O_1 denote the corner of an obstacle. Let O_1E be the diameter of the semi-circular arc O_1AE. Let C denote the center of the semi-circular arc. We attach a coordinate frame with each of the points C, O_1 and E as shown in the figure. Angles are measured counter-clockwise with respect to the x-axis of the frame in context. Let X be an obstacle inside the closure of the semi-circular disk. Let ∂X denote the boundary of the obstacle. Let K denote the set of points on the semi-circular arc O_1AE excluding the points

O_1 and E. We exclude the points E and O_1 since E is the initial position of the evader and O_1 is a point on the obstacle. Hence we consider all games that have termination time $t > 0$ and do not terminate on the obstacle. There exists a natural bijective map $\gamma : K \rightarrow (0, \pi)$ that maps any point in K to its radial angle θ_c in the coordinate frame attached to C.

For any point $p \in K$, let P denote the position of p on the plane. Let $S \subseteq K$ such that the following properties hold for points in S:

1. $PE \subset \text{V}(O_1) \quad \forall \quad p \in S$.

2. $P \subset \text{V}(E) \quad \forall \quad p \in S$.

Let the tangents from the E to X intersect K at f and h with $\theta_c(f) > \theta_c(h)$. Let the tangents from the O_1 to X intersect K at g and i with $\theta_c(g) > \theta_c(i)$.

Lemma 9: $\gamma(S) \subset (0, \pi)$ and is a closed interval.

Proof. S is composed of all the points on the semi-circle in between f and i. Since ∂X is closed $f, i \in S$. Therefore, the boundary of S is contained in S and hence S is closed. Since γ is bijective $\gamma(S)$ is a closed interval. □

In case the obstacles have a non-empty intersection with K, we can prove Lemma 2 in a similar fashion.

Now let us consider the case when there are $n > 1$ obstacles in the closure of the semi-circular disk. For each obstacle i we can construct the the set S^i in the following manner. Construct the tangents from O_1 to the obstacle. Compute the intersection of the tangents with K. Let the points be denoted as g and i with $\theta_c(g) > \theta_c(i)$. Similarly compute the intersection of the tangents from E to K and denote the points as f and h with $\theta_c(f) > \theta_c(h)$. S^i contains the the set of points $p \in K$ such that $\theta_c(i) \leq \theta_c(p) \leq \theta_c(f)$.

Let us define $S_1 = K \setminus \cup_{i=1}^{n} S^i$.

Lemma 10: The set S_1 is a union of open intervals and hence open.

Proof. The proof follows from the definition of S_1. □

From the above Lemma, we conclude that $\gamma(S_1) = \bigcup_{i=1}^{k_1} (\theta_i, \theta_{i+1})$. If the evader starts at E, then every point in S_1 is associated with a unique termination time that is proportional to the distance of that point from E. Hence we can define a bijective map $\mathcal{I}_1 : S_1 \rightarrow R$, where $\mathcal{I}_1(p) = t_p$, where t_p is the time of termination of the game if the evader starts at E. Hence from Lemma 3 we conclude that

$\mathcal{I}_1(S_1) = \bigcup_{i=1}^{k_1}(t_i, t_{i+1})$. Since $\mathcal{I}_1$ is bijective $\mathcal{I}_1(S_1) \simeq S_1$. Similarly, we can define a set S_2 and I_2.

Every point $q \in S_1$ has a time of termination t_q associated with itself. Consider a point $q_1 \in S_1$ such that there is no corresponding point $q_2 \in S_2$ satisfying $t_{q_1} = t_{q_2}$. Let P be the initial position of the pursuer such that the game terminates in time t_{q_1} when the initial position of the evader is at E. E and P cannot be on the dispersal surface since there is no point corresponding to q_1 on the arc EBO_2 such that the evader can break the line of sight around O_2 in the same time t_{q_1}. Therefore such points should be removed from S_1. This leads us to define the following sets:

$$\tilde{S}_1 = \{q \in S_1 \mid \exists q' \in S_2 \quad \text{s.t.} \quad t_q = t_{q'}\}$$

$$\tilde{S}_2 = \{q \in S_2 \mid \exists q' \in S_1 \quad \text{s.t.} \quad t_q = t_{q'}\}$$

Hence $\tilde{S}_1$ and $\tilde{S}_2$ are the maximal subsets of S_1 and S_2 respectively such that the termination position of the players at any point in the set **might** lie on the dispersal surface.

Lemma 11: The set of points in $\tilde{S}_1$ and $\tilde{S}_2$ is a union of open intervals of the form (q_1, q_2) where $q_1, q_2 \in S_1$.

Proof. From the above Lemma, we can conclude that $\mathcal{I}_1(S_1) = \bigcup_{i=1}^{k_1}(t_i, t_{i+1})$ and $\mathcal{I}_2(S_2) = \bigcup_{i=1}^{k_2}(t_i, t_{i+1})$. Hence T= $\mathcal{I}_1(S_1) \cap \mathcal{I}_2(S_2)$ is open since it is an intersection of a finite number of open sets. Moreover it is also a union of open intervals. Since $\mathcal{I}_1$ and $\mathcal{I}_2$ are bijective, $\tilde{S}_1 = \mathcal{I}_1^{-1}(T)$ and $\tilde{S}_2 = \mathcal{I}_2^{-1}(T)$ is a union of open intervals. □

Let $\tilde{P}$ contain the initial positions of the pursuer that lie on the dispersal surface when the evader is initially at E. Now we present the construction of $\tilde{P}$ from the sets $\tilde{S}_1$ and $\tilde{S}_2$. Let $q_1 \in \tilde{S}_1$ and $q_2 \in \tilde{S}_2$ such that $t_{q_1} = t_{q_2}$. The intersection of the lines parallel to q_1O_1 from H_1 and q_2O_2 from H_2 gives the point p. In order for p to lie in $\tilde{P}$ it should satisfy the following conditions:

1. $p, D_1, D_2 \in W_{\text{free}}$
2. $p \in V(D_1) \cap V(D_2)$
3. $(1-t')p + t'D_1 \in V(t'E + (1-t')A)$ and $(1-t')p + t'D_2 \in V(t'E + (1-t')B) \quad \forall t' \in [0, t]$

Condition 3 ensures that the pursuer and the evader are visible to each other at all times $t' \leq t$. For all points $p \in \tilde{P}$, we can obtain the coordinates (x_p, y_p) using Equation (3.1).

3.5.4 General polygonal environment

In this section we extend the results of the previous section to environments containing polygonal obstacles. Consider a environment containing polygonal obstacles. Let $E = (x_e, y_e)$ denote the initial position of the evader. Construct $V(E)$. Choose two corners O_1 and O_2 of obstacles and compute the dispersal surface using the technique presented in the previous section. In order to complete the construction, the above procedure has to be repeated for every pair of corners of obstacles present in $V(E)$. This completes the construction of the dispersal surface for a given initial position of the evader E $= (x_e, y_e)$.

Part II

Communication-Based Pursuit Evasion

CHAPTER 4

JAMMING IN MOBILE NETWORKS

In this chapter, we consider a differential game theoretic approach to compute optimal strategies by a team of UAVs to evade the attack of an aerial jammer on the communication channel. We formulate the problem as a zero-sum pursuit-evasion game. The cost function is the termination time of the game. We use Isaacs' approach to derive the necessary conditions to arrive at the equations governing the saddle-point strategies of the players. We illustrate the results through simulations.

Section 4.1 presents a brief motivation and introduction to our problem. Section 4.2 presents the problem formulation. The jamming, communication and mobility models for the nodes are presented. Based on the aforementioned models, a multi-player pursuit-evasion game is analyzed in Section 4.3. Section 4.4 extends the solutions to a variant of the problem discussed in Section 4.3. Section 4.5 presents the results and the conclusion.

4.1 Introduction

In the past few years, a lot of research has been done to deploy multiple UAVs in a decentralized manner to carry out tasks in military as well as civilian scenarios. UAVs have shown promise in a wide range of applications. The recent availability of low-cost UAVs suggests the use of teams of vehicles to perform various tasks such as mapping, surveillance, search and tracking operations [78], [79]. For these applications, there has been a lot of focus to deploy teams of multiple UAVs in a cooperative or competitive manner [80], [81]. An extensive summary of important milestones and future challenges in network control of multiple UAVs is presented in [82].

In general, the mode of communication among UAVs deployed in a team mission is wireless. This renders the communication channel vulnerable to malicious

attacks from aerial intruders flying in the vicinity. An example of such an intruder is an aerial jammer. Jamming is a malicious attack whose objective is to disrupt the communication of the victim network by causing interference or collision at the receiver side. Jamming attack is a well-studied and an active area of research in wireless networks. Many defense strategies have been proposed by researchers against jamming in wireless networks. In [83], Wu et al. propose two strategies to evade jamming. The first strategy, channel surfing, is a form of spectral evasion that involves legitimate wireless devices changing the channel that they are operating on. The second strategy, spatial retreats, is a form of special evasion whereby legitimate devices move away from the jammer. In [84], Wood et al. present a distributed protocol to map the jammed region so that the network can avoid routing traffic through it. The solution proposed by Cagalj et al. [85] uses different worm holes (wired worm holes, frequency-hopping pairs, and uncoordinated channel hopping) that lead out of the jammed region to report the alarm to the network operator. In [86], Wood et al. investigate how to deliberately avoid jamming in IEEE 802.15.4 based wireless networks. In [87], Lin Chen proposes a strategy to introduce into the network a special node called the anti-jammer to drain the jammer's energy. To achieve its goal, the anti-jammer configures the probability of transmitting bait packets to attract the jammer to transmit.

For a static jammer and mobile nodes, the optimal strategy for the nodes is to retreat away from the jammer after detecting jamming. In case of an aerial jamming attack, optimal strategies for retreat are harder to compute due to the mobility of the jammer and constraints in the kinematics of the UAVs. This attack can be modeled as a zero-sum game [48] between the jammer and the UAVs. Such dynamic games governed by differential equations can be analyzed using tools from differential game theory [10],[9]. In the past, differential game theory has been used as a framework to analyze problems in multi-player pursuit-evasion games. Solutions for particular multi-player games were presented by Pashkov and Terekhov [88], Levchenkov and Pashkov [89], Hagedorn and Breakwell [90], Breakwell and Hagedorn [91] and Shankaran et al. [92]. More general treatment of multi-player differential games was presented by Starr and Ho [93], Vaisbord and Zhukovskiy [94], Zhukovskiy and Salukvadze [95] and Stipanović, Hovakimyan and Melikyan [96, 97]. The inherent difficulty of obtaining an analytical solution to the Hamilton-Jacobi-Isaacs equation has led to the development of numerical techniques for the computation of the value function. Recent efforts in this direction to compute an approximation of the reachable sets have been

provided by Mitchell and Tomlin [98], Stipanović, Hwang and Tomlin [99] and Stipanović, Shankaran and Tomlin [100].

In contradistinction, our work in this chapter analyzes the behavior of multiple UAVs in cooperative as well as non-cooperative scenarios in the presence of a malicious intruder in the communication network. In this work, we envision a scenario in which an aerial jammer intrudes upon the communication channel in a multiple UAV formation. We model the intrusion as a continuous time pursuit-evasion game between the UAV's and the aerial jammer. In contrast to the previous works in pursuit-evasion games that formulate a payoff based on a geometric quantity in the configuration space of the system, we formulate a payoff based on the capability of the players in a team to communicate among themselves in the presence of a jammer in the vicinity. In particular, we are interested in computing strategies for spatial reconfiguration of a formation of UAVs in the presence of an aerial jammer to reduce the jamming on the communication channel.

In the next section, we present the problem formulation.

4.2 Problem Formulation

In this section, we first introduce a communication model between two mobile nodes in the presence of a jammer. Then we present the mobility models for the nodes. We conclude the section by formally formulating the problems we study in the chapter.

4.2.1 Jammer and communication model

Consider a mobile node (*receiver*) receiving messages from another mobile node (*transmitter*) at some frequency. Both communicating nodes are assumed to be lying on a plane. Consider a third node that is attempting to jam the communication channel shared by the transmitter and the receiver by sending a high power noise at the same frequency. This kind of jamming is referred to as *trivial jamming*. Two other types of jamming are:

1. *Periodic jamming*: A periodic noise pulse is generated by the jammer irrespective of the packets that are put on the network.

2. *Intelligent jamming*: A jammer is put in a promiscuous mode to destroy primarily the control packets.

A variety of metrics can be used to compare the effectiveness of various jamming attacks. Some of these metrics are energy efficiency, low probability of detection, and strong *denial of service* [101], [102]. In this chapter, we use the ratio of the jamming power to the signal power (JSR) as the metric. From [103], we have the following models for the JSR (ξ) at the receiver's antenna.

1. R^n model
$$\xi = \frac{P_{J_T} G_{JR} G_{RJ}}{P_T G_{TR} G_{RT}} 10^{n \log_{10}(\frac{D_{TR}}{D_{JR}})}$$

2. Ground Reflection Propagation
$$\xi = \frac{P_{J_T} G_{JR} G_{RJ}}{P_T G_{TR} G_{RT}} (\frac{h_J}{h_T})^2 (\frac{D_{TR}}{D_{JR}})^4$$

3. Nicholson
$$\xi = \frac{P_{J_T} G_{JR} G_{RJ}}{P_T G_{TR} G_{RT}} 10^{4 \log_{10}(\frac{D_{TR}}{D_{JR}})}$$

where P_{J_T} is the power of the jammer transmitting antenna, P_T is the power of the transmitter, G_{TR} is the antenna gain from transmitter to receiver, G_{RT} is the antenna gain from receiver to transmitter, G_{JR} is the antenna gain from jammer to receiver, G_{RJ} is the antenna gain from receiver to jammer, h_J is the height of the jammer antenna above the ground, h_T is the height of the transmitter antenna above the ground, D_{TR} is the Euclidean distance between transmitter and receiver, and D_{JR} is the Euclidean distance between jammer and transmitter. All the above models are based on the propagation loss depending on the distance of the jammer and the transmitter from the receiver. In all the above models the jammer to signal ratio is dependent on the ratio $\frac{D_{TR}}{D_{JR}}$.

For digital signals, the jammer's goal is to raise the ratio to a level such that the *bit error rate* [104] is above a certain threshold. For analog voice communication, the goal is to reduce the articulation performance so that the signals are difficult to understand. Hence we assume that the communication channel between a receiver and a transmitter is considered to be jammed in the presence of a jammer if $\xi \geq \xi_{tr}$ where ξ_{tr} is a threshold determined by many factors including application scenario and communication hardware. If all the parameters except the mutual distances between the jammer, transmitter and receiver are kept constant, we can

conclude the following from all the above models: If the ratio $\frac{D_{TR}}{D_{JR}} \geq \eta$ then the communication channel between a transmitter and a receiver is considered to be jammed. Here η is a function of ξ, P_{J_T}, P_T, G_{TR}, G_{RT}, G_{JR}, G_{RJ} and D_{TR}. Hence if the transmitter is not within a disc of radius ηD_{JR} centered around the receiver, then the communication channel is considered to be jammed. We call this disc the *perception range*. The *perception range* for any node depends on the distance between the jammer and the node. For effective communication between two nodes, each node should be able to transmit as well as receive messages from the other node. Hence two nodes can communicate if they lie in each other's *perception range*.

In the rest of the chapter, we will use the above jamming and communication model.

4.2.2 System model

We now describe the kinematic model of the nodes. In our analysis, each node is a UAV. We consider two UAV's (UAV$_1$ and UAV$_2$) in the presence of a third UAV (UAV$_j$) that is trying to jam the communication link in between them. We assume that the UAVs are having a constant altitude flight. This assumption helps to simplify our analysis to a planar case. Referring to Figure 4.1, the configuration of each UAV in the global coordinate frame can be expressed in terms of the variables (x_i^g, y_i^g, ϕ_i^g). The subscript *i* is either 1, 2 or j depending on the UAV being referred to. The pair (x_i^g, y_i^g) represents the position of a reference point on UAV_i with respect to the origin of the global reference frame and ϕ_i^g denotes the instantaneous heading of the UAV$_i$ in the global reference frame. Hence the state space for UAV_i is $\mathbf{X}_i \cong \mathbb{R}^2 \times \mathrm{S}^1$. In our analysis, we assume that the UAVs are a kinematic system and hence the dynamics of the UAVs are not taken into account in the differential equation governing the evolution of the system. The kinematics of the UAVs are assumed to be the following:

$$\frac{dx_i^g}{dt} = W_i \cos\phi_i^g; \frac{dy_i^g}{dt} = W_i \sin\phi_i^g; \frac{d\phi_i^g}{dt} = \sigma_i \tag{4.1}$$

where W_i and σ_i are the speed and angular velocity of UAV$_i$, respectively. In this chapter, we assume that $\sigma_i \in [-1, +1] \quad \forall i$. Moreover, we assume that $W_i = 1 \quad \forall i$.

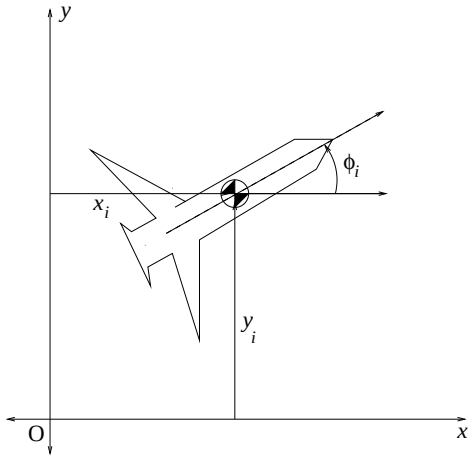

Figure 4.1: Configuration of a UAV.

The state space of the entire system is $\mathbf{X}_1 \times \mathbf{X}_2 \times \mathbf{X}_j \cong \mathbb{R}^6 \times (\mathrm{S}^1)^3$. In order to reduce the dimension of the state space we analyze the system in a coordinate frame fixed to UAV_2 as shown in Figure 4.2. In the new coordinate frame, the system can be modeled using six independent variables and the equations of motion of the UAV_1 and UAV_j with respect to the new coordinate frame are given by the following [92]:

$$\dot{x}_1 = -1 + \sigma_2 y_1 + \cos\phi_1, \dot{y}_1 = -\sigma_2 x_1 + \sin\phi_1$$
$$\dot{\phi}_1 = -\sigma_2 + \sigma_1 \tag{4.2}$$
$$\dot{x}_j = -1 + \sigma_2 y_j + \cos\phi_j, \dot{y}_j = -\sigma_2 x_j + \sin\phi_j$$
$$\dot{\phi}_j = -\sigma_2 + \sigma_j \tag{4.3}$$

In the above expressions (x_j, y_j, ϕ_j) and (x_1, y_1, ϕ_1) represent the relative position and orientation of the UAV_j and UAV_1 in the reference frame attached to UAV_2. Hence the state space of the reduced system is isomorphic to $\mathbb{R}^4 \times (\mathrm{S}^1)^2$.

4.2.3 Problem statement

From the communication and the mobility models proposed in the previous subsections, we formulate the following problems.

- *Problem 1*: Consider a situation in which UAV_1 and UAV_2 are not communicating initially in the presence of a jammer (UAV_j). The objective of the jammer is to maximize the time for which it can jam the communication

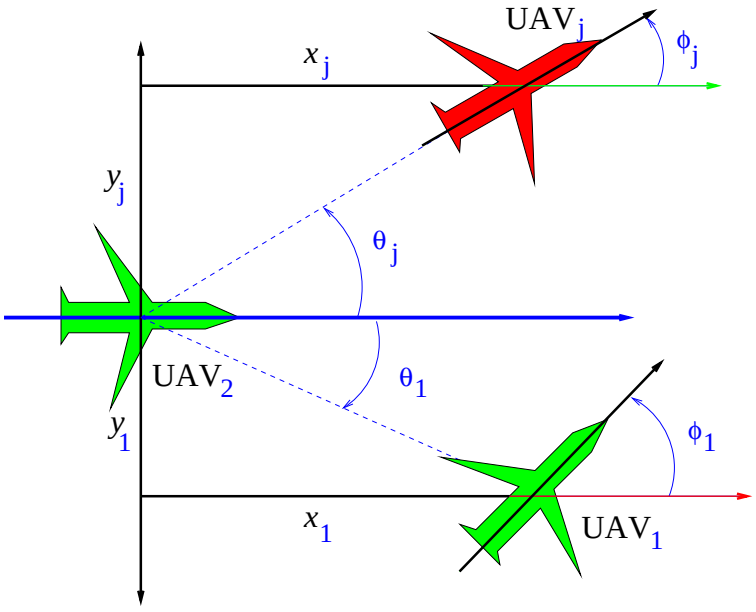

Figure 4.2: Relative configuration of UAVs.

between UAV$_1$ and UAV$_2$. The objective of UAV$_1$ and UAV$_2$ is to minimize the time for which communication remains jammed. The game terminates at the first instant at which UAV$_1$ and UAV$_2$ are in a position to communicate. We need to compute the optimal strategy for each UAV.

- *Problem 2*: Now consider a situation in which UAV$_1$ and UAV$_2$ are communicating initially in the presence of a jammer (UAV$_j$). The objective of the jammer is to minimize the time it takes to jam the communication channel between UAV$_1$ and UAV$_2$. The objective of UAV$_1$ and UAV$_2$ is to maximize the time for which communication link between them remains operable. The game terminates immediately when UAV$_1$ and UAV$_2$ lose their link. We need to compute the optimal strategy for each UAV.

In both problems, it is assumed that each UAV has complete knowledge about the state of the system.

In the next section, we analyze the first problem.

4.3 Analysis of Problem 1

We consider a situation in which UAV_1 and UAV_2 are not communicating initially in the presence of a jammer (UAV_j). The termination condition is defined as the first instant at which UAV_1 and UAV_2 are in a position to communicate. The cost function of the game is the time of termination of the game. The objective of the jammer is to maximize the time for which it can jam the communication between UAV_1 and UAV_2. The objective of UAV_1 and UAV_2 collectively is to minimize the time for which communication remains jammed.

In order to obtain the optimal strategies of the players we need to compute the *saddle-point strategies* since this is a zero-sum game. A set of strategies for the players is said to be in *saddle-point equilibrium* if no unilateral deviation in strategy by a player can lead to a better outcome for that player. Hence there is no motivation for the players to deviate from their equilibrium strategies. In scenarios where the players have no knowledge about each other's strategies, equilibrium strategies are important since they lead to a guaranteed minimum outcome for the players in spite of the other player's strategies.

For a point $\mathbf{x}$ in the state space, let $J(\mathbf{x})$ represent the outcome if the players implement their optimal strategies starting at the point $\mathbf{x}$. In this game, it is the time of termination of the game when the players implement their optimal strategies. It is also called the *value* of the game at $\mathbf{x}$.

Let $\nabla J = [J_{x_1} \quad J_{y_1} \quad J_{\phi_1} \quad J_{x_J} \quad J_{y_J} \quad J_{\phi_J}]^T$ denote the gradient of the value function. The Hamiltonian of the system is given by $H = 1 + \nabla J \cdot f(\mathbf{x}, \sigma_1^*, \sigma_j^*, \sigma_2^*, t)$. From the equations of motion of the system, the Hamiltonian is given by

$$H = 1 + J_{x_1}\dot{x}_1 + J_{y_1}\dot{y}_1 + J_{\phi_1}\dot{\phi}_1 + J_{x_j}\dot{x}_j + J_{y_j}\dot{y}_j + J_{\phi_j}\dot{\phi}_j$$

Rearranging the terms in the Hamiltonian we obtain

$$H = 1 + \sigma_2[J_{x_1}y_1 - J_{y_1}x_1 - J_{\phi_1} - J_{\phi_j} - J_{y_j}x_j + J_{x_j}y_j] +$$

$$\sigma_j J_{\phi_j} + \sigma_1 J_{\phi_1} + (J_{x_1}\cos\phi_1 + J_{y_1}\sin\phi_1) +$$

$$(J_{x_j}\cos\phi_j + J_{y_j}\sin\phi_j) - (J_{x_1} + J_{x_j})$$

Since the jammer wants to minimize the time of termination and the UAV's want to maximize the time of termination, we get the following expressions for the

controls from Isaacs' first condition:

$$(\sigma_1^*, \sigma_2^*, \sigma_j^*) = arg \max_{\sigma_j} \min_{\sigma_2 \sigma_1} H$$

Since the Hamiltonian is separable in its controls, the order of taking the extrema becomes inconsequential. Hence the optimal controls of the players are given as follows:

$$\sigma_2^* = -\text{sign}[J_{x_1} y_1 - J_{y_1} x_1 - J_{\phi_1} - J_{\phi_j} - J_{y_j} x_j + J_{x_j} y_j] \tag{4.4}$$

$$\sigma_j^* = \text{sign}(J_{\phi_j}) \tag{4.5}$$

$$\sigma_1^* = -\text{sign}(J_{\phi_1}) \tag{4.6}$$

The *retrogressive path equations* (RPE) for the system lead to the following equations:

$$\mathring{J}_{x_1} = -\sigma_2^* J_{y_1}, \quad \mathring{J}_{y_1} = \sigma_2^* J_{x_1} \tag{4.7}$$

$$\mathring{J}_{x_j} = -\sigma_2^* J_{y_j}, \quad \mathring{J}_{y_j} = \sigma_2^* J_{x_j} \tag{4.8}$$

$$\mathring{J}_{\phi_1} = -J_{x_1} \sin\phi_1 + J_{y_1} \cos\phi_1 \tag{4.9}$$

$$\mathring{J}_{\phi_j} = -J_{x_j} \sin\phi_j + J_{y_j} \cos\phi_j \tag{4.10}$$

where $^\circ$ denotes derivative with respect to retrograde time.

Figure 4.3 summarizes the entire control algorithm. The controller of each UAV takes as input the state variables and runs the RPE to compute the control. This control is then fed into the plant of the respective UAV. The plant updates the state variables based on the kinematic equations governing the UAV. Finally the sensors feed back the state variables into the controllers. In this case the sensors measure the position and the orientation of each UAV.

4.3.1 Termination situations

In order to compute the optimal strategies, we need to compute the boundary conditions for the dependent variables of the differential equation. In order to do so, we characterize the terminal conditions of the game in the state space and compute the value of ∇J at the terminal conditions. This section presents the computation of the terminal value of the dependent variables of the differential

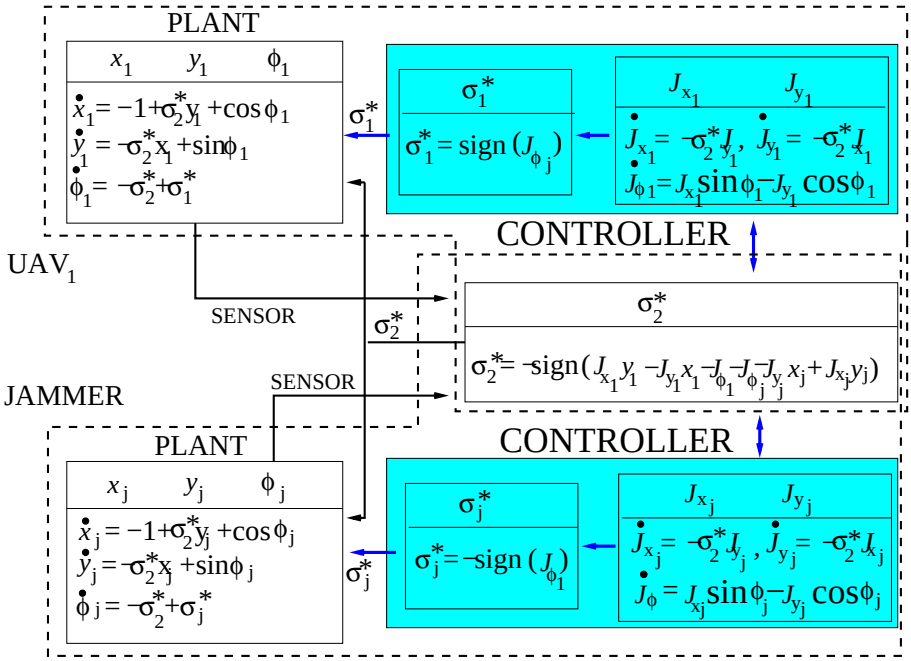

Figure 4.3: The control loop for the system.

equations governing the game.

From the communication model, we can conclude that UAV_1 can receive messages from UAV_2 when the following condition holds:

$$\eta d(\text{UAV}_J,\text{UAV}_1) \geq d(\text{UAV}_1,\text{UAV}_2)$$

where $d(\text{UAV}_i,\text{UAV}_j)$ is the Euclidean distance between UAV_i and UAV_j. Similarly, UAV_2 can receive messages from UAV_1 when the following condition holds:

$$\eta d(\text{UAV}_J,\text{UAV}_2) \geq d(\text{UAV}_1,\text{UAV}_2)$$

Hence we can conclude that the two nodes can communicate when the following condition holds:

$$\eta \min[d(\text{UAV}_J,\text{UAV}_1), d(\text{UAV}_J,\text{UAV}_2)] \geq d(\text{UAV}_1,\text{UAV}_2)$$

Hence the boundary of the game set is the set of positions of the UAVs that satisfies

the following condition:

$$\eta \min[d(\text{UAV}_J,\text{UAV}_1), d(\text{UAV}_J,\text{UAV}_2)] = d(\text{UAV}_1,\text{UAV}_2)$$

This leads to two termination manifolds in the state space.

1. The first terminal manifold is characterized by the positions of the UAVs such that UAV_1 is at the boundary of the *perception range* of UAV_2 and UAV_2 is inside the *perception range* of UAV_1. This is shown in Figure 4.4. In the coordinate system of UAV_2 the terminal manifold is represented by the hypersurface $F_1(x_1, y_1, \phi_1, x_j, y_j, \phi_j)$ which is given by the following expression:

$$(\sqrt{x_1^2 + y_1^2} - \eta\sqrt{x_j^2 + y_j^2} = 0) \cap ((x_1 - x_j)^2 + (y_1 - y_j)^2 - (x_j^2 + y_j^2) \leq 0)$$

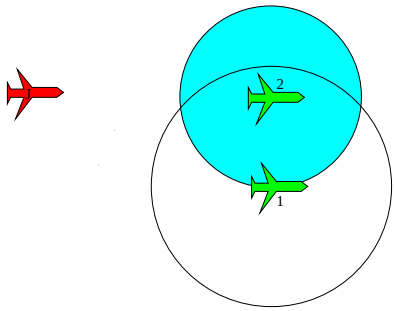

Figure 4.4: Termination situation 1.

2. The second terminal manifold is characterized by the positions of the UAVs such that UAV_2 is at the boundary of the *perception range* of UAV_1 and UAV_1 is inside the *perception range* of UAV_2. This is shown in Figure 4.5. In the coordinate system attached to UAV_2 this terminal manifold is represented by the hypersurface $F_2(x_1, y_1, \phi_1, x_j, y_j, \phi_j)$ which is given by the following expression:

$$(\sqrt{x_1^2 + y_1^2} - \eta\sqrt{x_j^2 + y_j^2} = 0) \cap ((x_1 - x_j)^2 + (y_1 - y_j)^2 - x_j^2 + y_j^2 \geq 0)$$

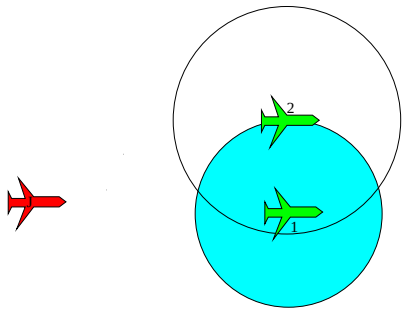

Figure 4.5: Termination situation 2.

Both the terminal surfaces are five-dimensional manifolds with boundary. Hence they can be parameterized using five independent variables x_1, y_1, x_j, ϕ_1 and ϕ_j. Since $J \equiv 0$ on the terminal manifold, ∇J satisfies the following equations at an interior point in the manifold:

$$\begin{aligned} J^0_{x_1} + J^0_{y_j}\frac{\partial y_j}{\partial x_1} = 0, \quad J^0_{y_1} + J^0_{y_j}\frac{\partial y_j}{\partial y_1} = 0 \\ J^0_{x_j} + J^0_{y_j}\frac{\partial y_j}{\partial x_j} = 0, \quad J^0_{\phi_1} = 0, \quad J^0_{\phi_j} = 0 \end{aligned} \tag{4.11}$$

In addition to the above equations, Isaacs' second condition leads to the following equation:

$$H(\mathbf{x}, \nabla J, f(\mathbf{x}, \sigma_1^*, \sigma_2^*, \sigma_j^*)) = 0 \tag{4.12}$$

The value of ∇J at the terminal manifold can be obtained from Equations (4.11) and (4.12). Since there are two different terminal manifolds, we have to analyze both of them separately. At first, we compute the value of ∇J on terminal manifold 1.

Substituting the expression for $F_1(x_1, y_1, \phi_1, x_j, y_j, \phi_j)$ in Equations (4.11) and (4.12), we obtain the following value of J_{y_j}:

$$J^0_{y_j} = y^0_j[\sqrt{(x^0_j)^2 + (y^0_j)^2}(\frac{1}{\eta} - 1) + (x^0_j - \frac{x^0_1}{\eta^2})]^{-1} \tag{4.13}$$

The superscript ^{0} is used to denote the value of the variables as the terminal conditions. The terminal values of the remaining components of ∇J can be computed from Equation (4.11). From the values of ∇J at the terminal manifold, the optimal

controls of the UAVs at termination can be computed. An elaborate computation of the optimal control of the UAVs is shown in the appendix.

4.4 Analysis of Problem 2

For Problem 2 as described in Section 4.2, Isaacs' first condition leads to the following optimal strategies for the players:

$$(\sigma_1^*, \sigma_2^*, \sigma_j^*) = arg \max_{\sigma_1,\sigma_2} \min_{\sigma_j} H$$

Hence the optimal controls of the players are given as follows:

$$\sigma_2^* = \text{sign}[J_{x_1} y_1 - J_{y_1} x_1 - J_{\phi_1} - J_{\phi_j} - J_{y_j} x_j + J_{x_j} y_j]$$
$$\sigma_j^* = -\text{sign}(J_{\phi_j})$$
$$\sigma_1^* = \text{sign}(J_{\phi_1})$$

The retrogressive path equations remain the same as in the previous problem. The terminal conditions also remain the same. Analysis done in the previous section can be extended to this problem. The results obtained by simulating the differential equations governing the optimal control laws and the trajectories are presented in the next section.

4.5 Results

Figures 4.6, 4.7, 4.8 and 4.9 show trajectories of the players for both problems along with their optimal controls for various terminal conditions and different values of η. The position of the players corresponding to the termination situation is shown by a small circle in the plots showing the trajectories of the players. Each figure shows the trajectory of the players just before termination for a small time interval. From the expression of the optimal controls in Equations (4.4), (4.5) and (4.6), we can infer that the controls of the players are bang-bang. This is also verified from the simulation results. From the nature of the controls and kinematics of the system, we can infer that the optimal paths comprise arcs of circles and straight line trajectories as motion primitives. Arcs of circles are generated when

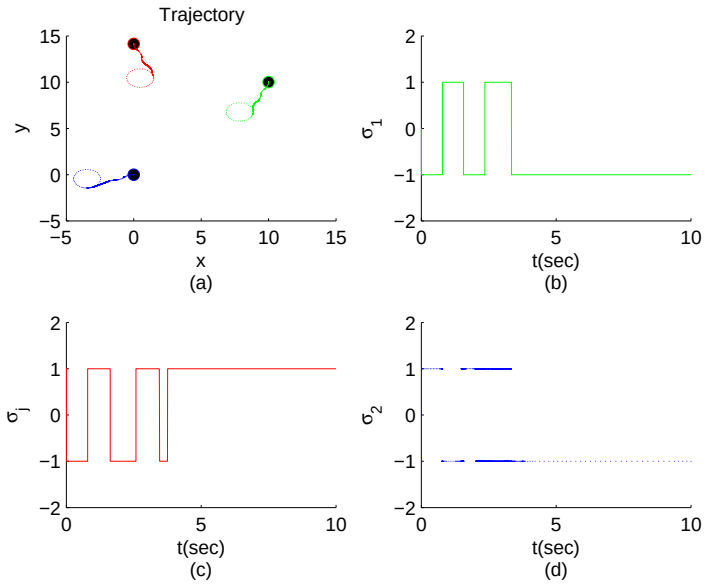

Figure 4.6: The players leading to termination condition 1 for Problem 1. The value $\eta = 1$. The player in red is the jammer. The players in green and blue are UAV_1 and UAV_2 respectively. Panel (b) shows the control of the UAV_1, (c) shows the control of the UAV_J, (d) shows the control of the UAV_2.

the UAV keeps its angular velocity saturated at one extrema for a non-zero interval of time. Straight line segments are obtained due to rapid switching between the extremum value of the controls (chattering). An instance of such a behavior is exhibited by UAV_2 in Figure 4.6.

Future work will prevent such undesired behavior by adding the derivative of the controls in the cost function of the game by considering a dynamic extension of the original system.

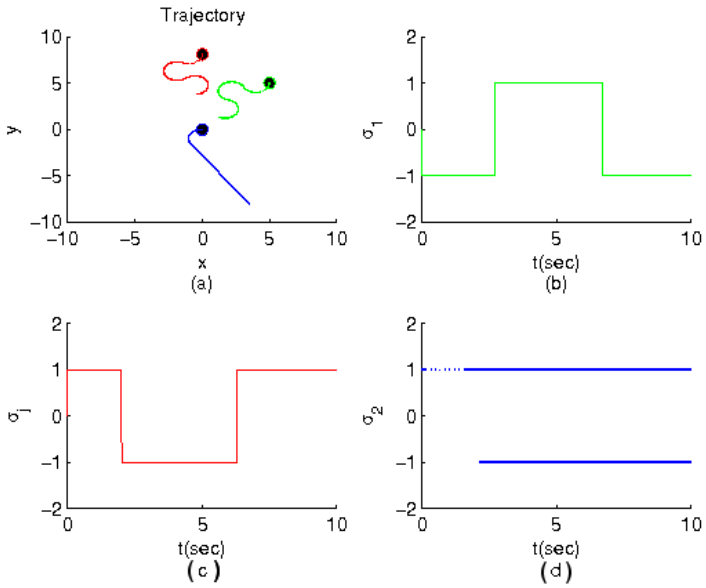

Figure 4.7: The players leading to termination condition 1 for Problem 2. The value $\eta = 2$. The player in red is the jammer. The players in green and blue are UAV_1 and UAV_2 respectively. Panel (b) shows the control of the UAV_1, (c) shows the control of the UAV_J, (d) shows the control of the UAV_2.

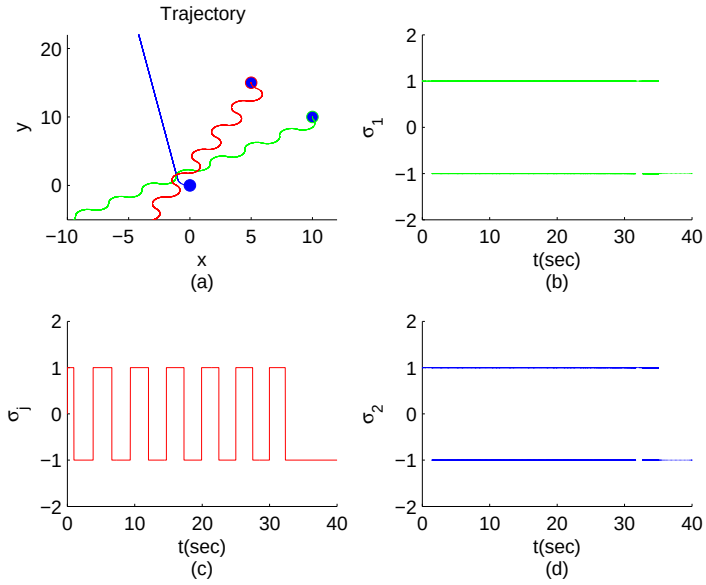

Figure 4.8: The players leading to termination condition 2 for Problem 1. The value $\eta = 1$. The player in red is the jammer. The players in green and blue are UAV_1 and UAV_2 respectively. Panel (b) shows the control of the UAV_1, (c) shows the control of the UAV_J, (d) shows the control of the UAV_2.

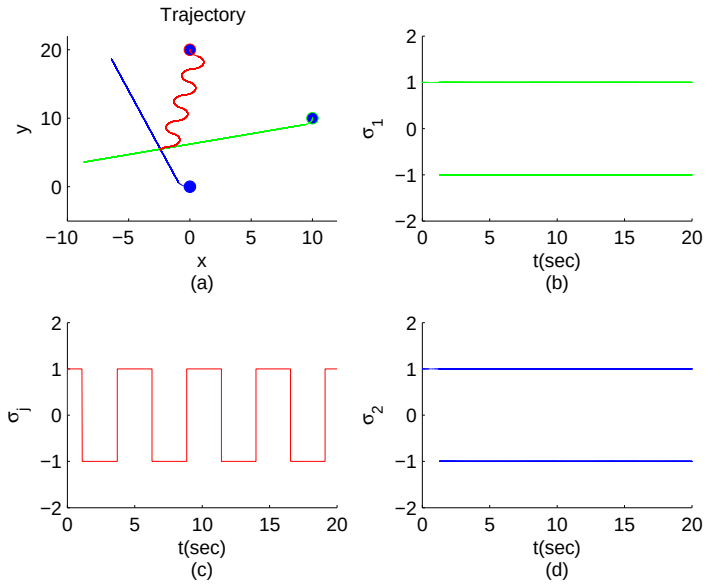

Figure 4.9: The players leading to termination condition 2 for Problem 2. The value $\eta = 1$. The player in red is the jammer. The players in green and blue are UAV_1 and UAV_2 respectively. Panel (b) shows the control of the UAV_1, (c) shows the control of the UAV_J, (d) shows the control of the UAV_2.

CHAPTER 5

JAMMING IN HETEROGENEOUS NETWORKS

In this chapter, we extend our work in Chapter 4 to address the jamming problem in a mobile network containing heterogeneous vehicles. In combat scenarios, teams of vehicles are deployed having different communication and motion constraints. Our interest lies in understanding the interplay between constraints in the communication posed by an intruder in a network and the constraints in the mobility inherent in the dynamics of the vehicles. In order to introduce heterogeneity in the problem, we assume that the nodes of the mobile network and the jammer can be aerial as well as ground vehicles.

Section 5.2 presents the problem formulation. The mobility models for the nodes are presented. Based on the aforementioned models, a multi-player pursuit-evasion game is analyzed in Section 5.3. Section 5.4 presents the optimal strategies for a special class of vehicles. Section 5.5 presents the conclusions.

5.1 Problem Formulation

In this section, we present the mobility models for the nodes. The communication and jamming model used in this chapter is the same as that introduced in Section 4.3. We conclude the section by formulating the problems.

5.1.1 System model

We now describe the kinematic model of the nodes. In this chapter, we analyze a network of heterogeneous vehicles that differ from each other in their dynamic models. Since we are interested in real scenarios, we choose the nodes as well as the jammer to resemble the dynamics of terrestrial or aerial vehicles. We use the motion models of UAVs (Unmanned Air Vehicles) and AGVs (Autonomous Ground Vehicles) to model the dynamics of the nodes. By neglecting the detailed

description of the real system that might render the complete solution to be numerical in nature, the dynamical models are simplified to a level that captures the essential kinematic constraints of the system.

We assume the following motion models for the nodes:

1. UAV: We use the five state model [105] for the UAV that takes into account the course angles, the flight path angles and the height of the UAV from the ground during its flight. The dynamic equations are given below:

$$\begin{aligned} \dot{x} &= W\cos\psi\cos\theta, \quad \dot{y} = W\sin\psi\cos\theta \\ \dot{z} &= W\sin\theta, \quad \dot{\psi} = \frac{g}{W}\eta\tan\phi, \quad \dot{\theta} = \frac{g\cos\theta}{W}(\eta - 1) \end{aligned}$$

   where W_i represents velocity, ψ_i the heading angle, θ_i the pitch angle, g the gravitational acceleration, ϕ_i the roll angle and η_i the load factor of the UAV$_i$. The geometry of the coordinate system is shown in Figure 5.1. W, ϕ and η, satisfying the constraints $\mid W \mid \leq W_{max}, \mid \phi \mid \leq \phi_{max}$ and $\mid \eta \mid \leq \eta_{max}$, are the controls of the UAV. The configuration space of the UAV is $X \simeq \mathbb{R}^3 \times S^1 \times S^1$.

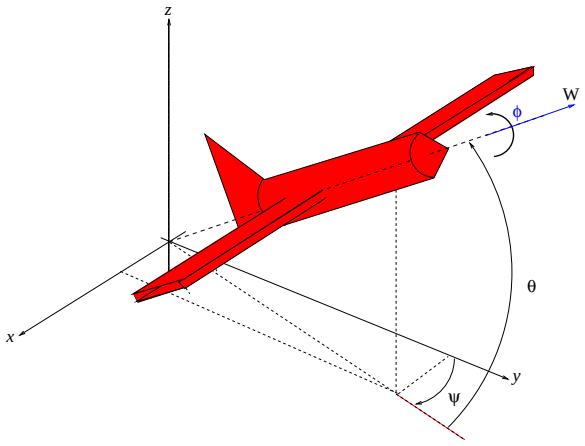

Figure 5.1: UAV model.

2. AGV: From [106], we model the AGV as a car-like robot with five-dimensional configuration space using the following dynamic equations:

$$\begin{aligned} \dot{x} &= v\cos\theta\cos\zeta, \quad \dot{y} = v\sin\theta\cos\zeta \\ \dot{\theta} &= v\sin\zeta, \quad \dot{v} = u_1, \quad \dot{\zeta} = u_2 \end{aligned}$$

where u_1 and u_2, satisfying $\mid u_1 \mid \leq u_{1max}$ and $\mid u_2 \mid \leq u_{2max}$, denote respectively the linear and angular accelerations of the vehicles. We also consider the fact that the car has a bound on the steering angle, i.e. $\mid \zeta \mid \leq \zeta_{max}$. The geometry of the coordinate system is shown in Figure 5.2. The state space of the system $X \subset \mathbb{R}^3 \times S^1 \times S^1$.

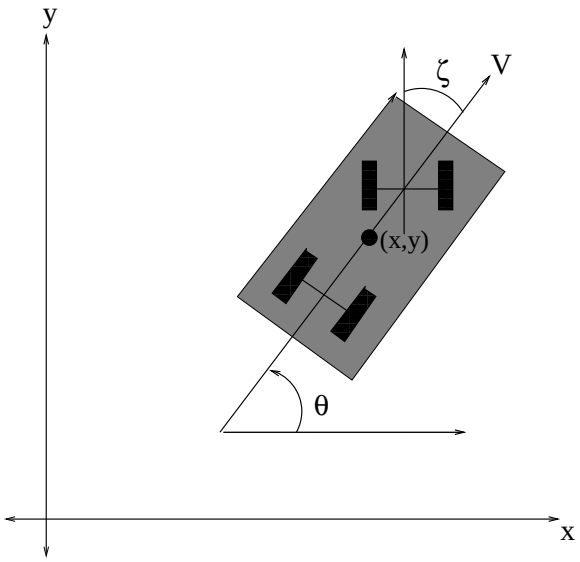

Figure 5.2: AGV model.

5.1.2 Problem statement

From the mobility models proposed in the previous section and the communication model proposed in the previous chapter, we formulate the following problems.

- *Problem 1*: Consider a situation in which two nodes are not communicating initially because of the presence of a jammer. The objective of the jammer is to maximize the time for which it can jam the communication between the two nodes. The objective of two nodes is to minimize the time for which communication remains jammed. The game terminates at the first instant at which two nodes are in a position to communicate. We need to compute the optimal strategy for each node.

- *Problem 2*: Now consider a situation in which the two nodes are communicating initially in the presence of a jammer. The objective of the jammer is

to minimize the time it takes to jam the communication channel between the two nodes. The objective of the two nodes is to maximize the time for which communication link between them remains operable. The game terminates immediately when the two nodes lose their link. We need to compute the optimal strategy for each node.

In both problems, it is assumed that each node has complete knowledge about the state of the system, i.e., the position of the other node and the jammer. Moreover the equations governing the dynamics of the nodes and the jammer are of the following form:

$$\dot{x} = f(x, u, t)$$

where $x \in X$ is an n-dimensional manifold, the controls $u \in \mathcal{U}$ are a class of functions of t taking their values in some compact subdomain $\mathcal{K} \in R^n$. Later in the chapter, we analyze the situation when $f(x, u, t)$ represents the dynamics of a UAV or a car-like robot.

In the next section, we analyze the first problem.

5.2 Analysis of Problem 1

We consider a situation in which the two nodes are not communicating initially because of the presence of a jammer. The termination condition is defined as the first instant at which two nodes are in a position to communicate. The cost function of the game is the time of termination of the game. The objective of the jammer is to maximize the time for which it can jam the communication between the nodes. The objective of the two nodes collectively is to minimize the time for which communication remains jammed.

In order to obtain the optimal strategies of the players we need to compute the *saddle-point strategies* since this is a zero-sum game. A set of strategies for the players is said to be in *saddle-point equilibrium* if no unilateral deviation in strategy by a player can lead to a better outcome for that player. Hence there is no motivation for the players to deviate from their equilibrium strategies. In scenarios where the players have no knowledge about each other's strategies, equilibrium strategies are important since they lead to a guaranteed minimum outcome for the players in spite of the other player's strategies.

WLOG we assume that vehicles 1 and 2 are the nodes in the formation and

vehicle 3 is the jammer. The state-space of the system is $\mathbf{X} \simeq \mathrm{X}_1 \times \mathrm{X}_2 \times \mathrm{X}_3$, where $\mathbf{X}_i$ is the state-space of the ith vehicle. For a point $\mathbf{x} \in \mathbf{X}$ in the state space, let $J(\mathbf{x})$ represent the outcome if the players implement their optimal strategies starting at the point $\mathbf{x}$. In this game, it is the time of termination of the game when the players implement their optimal strategies. It is also called the *value* of the game at $\mathbf{x}$.

Let us assume that the player i has state space of dimension n_i. Let $\nabla J = [J_{x_1}, \cdots, J_{x_n}]^T$, where $n = n_1 + n_2 + n_3$, denote the gradient of the value function. Let $u = [u_1 \quad u_2 \quad u_3]^T$ denote the controls for all the players. Since this is a minimum time problem, the Hamiltonian of the system is given by $H = 1 + \nabla J \cdot f(\mathbf{x}, u, t)$. From the equations of motion of the system, the Hamiltonian is given by the following expression:

$$H = 1 + \sum_{j=1}^{3} \sum_{i=1}^{n_j} J_{x_i^j} \dot{x}_i^j$$

In the above expression, the outer summation is over the number of vehicles and the inner summation is over the number of states of each vehicle. Rearranging the terms in the Hamiltonian we obtain

$$H = 1 + \sum_{j=1}^{3} u^j \sum_{i=1}^{n_j} J_{x_i^j} f_i^j(x)$$

Since the jammer wants to maximize the time of termination and the nodes want to minimize the time of termination, the Hamiltonian of the system satisfies the following Isaacs conditions along the optimal trajectories [9]:

1. $(u^{1*}, u^{2*}, u^{3*}) = arg \max_{(u^{1*}, u^{2*})} \min_{u^{3*}} H$
2. $H(\mathbf{x}, \nabla J, u^{1*}, u^{2*}, u^{3*}) = 0$

Condition 1 implies that when the players implement their optimal strategies, any unilateral deviation by the pursuer might lead to a smaller value for the Hamiltonian and any unilateral deviation by the evader might lead to a larger value of the Hamiltonian. Moreover condition 2 implies that when the players implement their optimal controls, the Hamiltonian of the system is zero. The Isaacs conditions are an extension of Pontryagin's principle to optimization in a differential game [10].

Since the Hamiltonian is separable in its controls, the order of taking the extrema becomes inconsequential. Hence the optimal control of nodes 1 and 2 is

given as follows:

$$u^{j*} = u^j_{max}\text{sign}[\sum_{i=1}^{n_j} J_{x_i^j} f_i^j(x)] \quad j = 1, 2$$

The optimal control for node 3 is given as follows:

$$u^{3*} = -u^3_{max}\text{sign}[\sum_{i=1}^{n_j} J_{x_i^j} f_i^j(x)]$$

The *retrogressive path equation* (RPE) is given by

$$(\overset{\circ}{\nabla} J) = -\nabla H$$

where $^\circ$ denotes derivative with respect to inverse time. This leads to the following system of equations for the nodes:

$$\overset{\circ}{J}_{x_i^j} = u^{j*} \sum_{i=1}^{n_j} J_{x_i^j} [f_i^j(x)]_{x_i^j}$$

where $[f_i^j(x)]_{x_i^j}$ represents the derivative of $f_i^j(x)$ w.r.t. x_i^j. Figure 5.3 summarizes the entire control algorithm. The controller of each node takes as input the state variables and runs the RPE to compute the control. This control is then fed into the plant of the respective node. The plant updates the state variables based on the kinematic equations governing the node. Finally the sensors feed back the state variables into the controllers. In this case the sensors measure the state variable associated with each node.

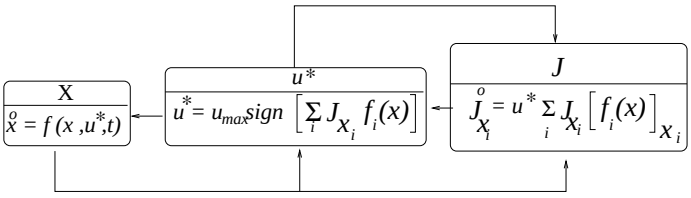

Figure 5.3: The control loop for each vehicle.

5.2.1 Termination situations

In order to compute the optimal strategies, we need to compute the boundary conditions for the dependent variables of the differential equation. In order to do so, we characterize the terminal conditions of the game in the state space and compute the value of ∇J at the terminal conditions. This section presents the computation of the terminal value of the dependent variables of the differential equations governing the game.

From the communication model, we can conclude that node 1 can receive messages from node 2 when the following condition holds:

$$\eta d(\text{Jammer,node 1}) \geq d(\text{node 1, node 2})$$

where $d(\cdot, \cdot)$ is the Euclidean distance between the two vehicles. Similarly, node 2 can receive messages from node 1 when the following condition holds:

$$\eta d(\text{Jammer,node 2}) \geq d(\text{node 1,node 2})$$

Hence we can conclude that the two nodes can communicate when the following condition holds:

$$\begin{aligned} \eta \min[d(\text{Jammer,node 1}), d(\text{Jammer,node 2})] \\ \geq d(\text{node 1,node 2}) \end{aligned}$$

Hence the boundary of the game set is the set of positions of the UAV's that satisfy the following condition:

$$\begin{aligned} \eta \min[d(\text{Jammer,node 1}), d(\text{Jammer,node 2})] \\ = d(\text{node 1,node 2}) \end{aligned}$$

This leads to two termination manifolds in the state space.

1. The first terminal manifold is characterized by the positions of the nodes such that node 1 is at the boundary of the *perception range* of node 2, and node 2 is inside the *perception range* of node 1. This is shown in Figure 5.4.

2. The second terminal manifold is characterized by the positions of the nodes such that node 2 is at the boundary of the *perception range* of node 1, and

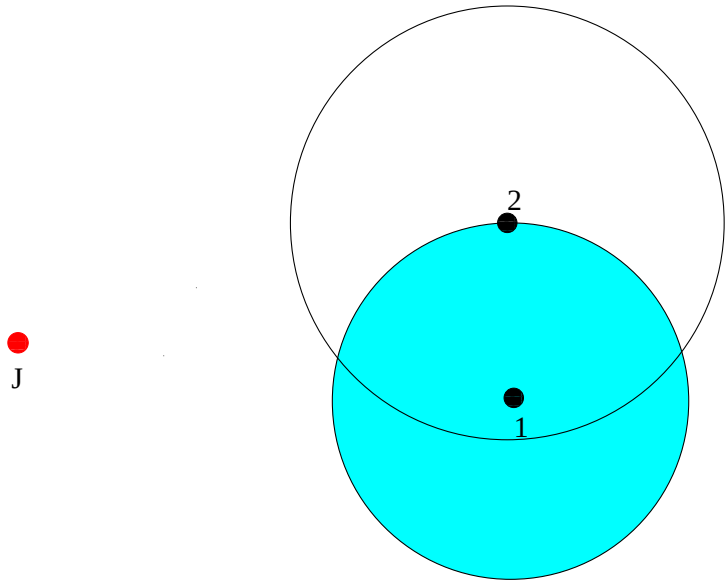

Figure 5.4: Termination situation 1.

node 1 is inside the *perception range* of node 2. This is shown in Figure 5.5.

Since $J \equiv 0$ on the terminal manifold ($\mathcal{M}$), ∇J satisfies the following equations at an interior point x in the terminal manifold:

$$\nabla J \cdot t_i = 0 \tag{5.1}$$

where t_i is the basis vector of $T_x\mathcal{M}$

Since both terminal surfaces are 14-dimensional manifolds with boundary, this leads to a system of 14 simultaneous non-linear equations for the value of ∇J. In addition, ∇J also satisfies the second Isaacs condition that leads to the following equation:

$$H(\mathbf{x}, \nabla J, f(\mathbf{x}, u_1^*, u_2^*, u_3^*)) = 0 \tag{5.2}$$

∇J at the terminal manifold has 15 unknown variables corresponding to the directional derivative of ∇J in each direction constituting the basis of the configuration space. From Equations (5.1) and (5.2), we get a set of 15 simultaneous equations. Since there are two different terminal manifolds, we have to analyze them separately. From the values of ∇J at the terminal manifold, the optimal controls of the nodes at termination can be computed using Equations (5.1) and

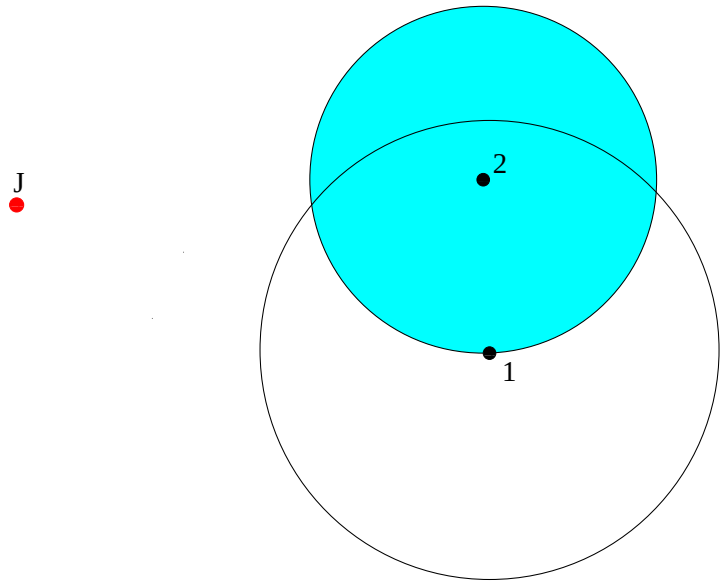

Figure 5.5: Termination situation 2.

(5.2).

5.3 Analysis of Problem 2

For Problem 2 as described in Section 5.2, Isaacs' first condition leads to the following optimal strategies for the players:

$$(u^{1*}, v^{1*}, u^{2*}, v^{2*}, u^{3*}, v^{3*}) = arg \min_{(u^{1*}, v^{1*}, u^{2*}, v^{2*})} \max_{(u^{3*}, v^{3*})} H$$

The retrogressive path equations remain the same as in the previous problem. The terminal conditions also remain the same. Analysis done in the previous section can be extended to this problem.

5.4 Analysis for UAV and AGV

The equations of motion of a given vehicle depend only on its individual controls. For a UAV the controls are V, η and ϕ. For an AGV the controls are v and w. Substituting the equations of motion in the expression for the Hamiltonian gives

us the following:

$$H = 1 + \sum_{i=1}^{3} J_{x_i} f_i(x_i, u_i)$$

From the above expressions we can see that the Hamiltonians are *separable* in their controls. Hence each player maximizes or minimizes the part of the Hamiltonian associated with his controls without any interference from the other players. Finding the optimal control for each player therefore reduces to the following optimization problem:

$$\max_{u_i} J_{x_i} f_i(x_i, u_i) \quad \text{or} \quad \min_{u_i} J_{x_i} f_i(x_i, u_i)$$

Now we consider both vehicles and compute their extremum seeking control. The control laws depend on the objective function of the vehicle. We present the analysis for the scenario in which the optimal controls of the vehicles maximize the Hamiltonian.

1. AGV: Using the kinematic equations for car-like robot we arrive at the following optimization problem:

$$\max_{u_1, u_2} [J_v u_1 + J_\zeta u_2]$$

In case $\mid \zeta \mid < \zeta_{max}$, the optimal controls of the vehicle are given by the following expression:

$$u_1 = \begin{cases} u_{1max} & J_v > 0 \\ -u_{1max} & J_v < 0 \end{cases}$$

$$u_2 = \begin{cases} u_{2max} & J_\zeta > 0 \\ -u_{2max} & J_\zeta < 0 \end{cases}$$

In case $\mid \zeta \mid = \zeta_{max}$, $u_2 = 0$. The retrogressive path equations associated

with a car-like robot are as follows:

$$\begin{aligned}
\mathring{J}_x &= 0, \quad \mathring{J}_y = 0 \\
\mathring{J}_\theta &= -vJ_x \sin\theta\cos\zeta + vJ_y \cos\theta\cos\zeta \\
\mathring{J}_v &= J_x \cos\theta\cos\zeta + J_y \sin\theta\cos\zeta + J_\theta \sin\zeta \\
\mathring{J}_\zeta &= -vJ_x \cos\theta\sin\zeta - vJ_y \sin\theta\sin\zeta + vJ_\theta \cos\zeta
\end{aligned}$$

2. UAV: The Hamiltonian associated with the UAV is given by the following expression:

$$H_{UAV} = J_x W\cos\psi\cos\theta + J_y W\sin\psi\cos\theta$$

$$+J_z W\sin\theta + J_\psi \frac{g}{W}\eta\tan\phi + J_\theta \frac{g\cos\theta}{W}(\eta - 1)$$

In case the UAV is the maximizer of the Hamiltonian we obtain the following optimization problem:

$$(W^*, \eta^*, \phi^*) = \max_{V,\eta,\phi} H_{UAV}$$

Since the Hamiltonian is non-linear in the controls, the optimal controls are obtained by solving a non-linear program with bounded control inputs. Due to the special form of the Hamiltonian in terms of the control ϕ we can compute an analytical expression for the optimal value of ϕ. In case $\mid \phi \mid \leq \phi_{max}$ the expression above leads to the following value of ϕ:

$$\phi = \begin{cases} \phi_{max} & \frac{J_\psi g\eta}{W} > 0 \\ -\phi_{max} & \frac{J_\psi g\eta}{W} < 0 \end{cases}$$

The retrogressive path equations associated with a car-like robot are then as follows:

$$\begin{aligned}
&\mathring{J}_x = 0, \quad \mathring{J}_y = 0, \quad \mathring{J}_z = 0 \\
&\mathring{J}_\psi = -WJ_x \sin\psi\cos\theta + WJ_y \cos\psi\cos\theta \\
&\mathring{J}_\theta = -WJ_x \cos\psi\sin\theta + WJ_y \sin\psi\sin\theta + W\cos\theta
\end{aligned}$$

$$-\frac{g\sin\theta(\eta-1)}{W}$$

If the vehicles are minimizing their respective Hamiltonian, the sign of the optimal controls get reversed. The retrogressive path equations remain the same.

In Chapter 7, we present some future research directions regarding jamming in hetergoneous networks.

CHAPTER 6

GRAPH-THEORETIC TECHNIQUES FOR NETWORK CONNECTIVITY

In this chapter, we analyze the problem of maintaining connectivity in a network of mobile agents in the presence of a jammer. This is a variation of the standard connectivity maintenance problem which arises due to limitations in communications and sensing model for each agent. In our work, the limitations in communications are due to the presence of a jammer in the vicinity.

The rest of the chapter is organized as follows. Section 6.2 presents the dynamic model associated with the nodes in the network. Section 6.3 presents a differential game formulation of the problem and presents necessary conditions for optimal strategies for the nodes as well as the jammer. Section 6.4 presents a state-dependent graph formulation for our system. Section 6.5 presents some important results in case of static networks. Section 6.6 presents control laws for the agents in case of a dynamic network using tools from algebraic graph theory. Section 6.7 presents some simulations based on the control laws proposed for the agents.

6.1 Introduction

In the past two decades, extensive research on cooperative control of multi-agent systems has been driven by military as well as civilian applications. Civilian applications range from search and rescue missions for disaster management to deployment of swarms of robots in the ocean to contain oil spills. Military applications range from deployment of sensor networks for surveillance and reconnaissance in urban warfare to utilization of a network of autonomous robotic tanks on battlefronts. In such scenarios, autonomous agents are deployed in teams to carry out a specific mission. The agents communicate among themselves in order to make decisions. Since the mode of communication is wireless, it is susceptible to malicious attacks. In this work, we investigate such a scenario in which a mobile

intruder jams the communication channel in a vehicular network.

In this chapter, we formulate the problem of jamming in a mobile network as a problem of maintaining connectivity in a dynamic graph in the presence of an intruder. Substantial research has been done in the recent past to address the problem of maintaining connectivity in mobile networks. Based on tools from potential field methods and algebraic graph theory, centralized algorithms have been proposed in [107] and [108] to maintain connectivity in mobile networks. The authors use the dynamics of the Laplacian matrix in order to obtain feasible controls that maintain connectivity in addition to satisfying the differential constraints on the motion of each agent. In [109], the notion of *geometric connectivity robustness* is introduced as a measure of the local connectedness of a network. Furthermore, the authors show that under special conditions the new notion provides a sufficient condition for global connectedness of the network. In [110], the authors use the weighted graph Laplacian technique proposed in [111] to guarantee connectedness while achieving formation stabilization. In [112], a decentralized algorithm is presented for maintaining connectivity using the Laplacian of the proximity graph. In [113], the problem of maintaining connectivity is addressed for agents having second-order dynamics. The authors establish an existence theorem for connectivity maintenance and present optimal controls to maintain connectivity in a distributed fashion. In [114], [115], the authors propose a distributed feedback and *provably correct* control framework for connectivity maintenance in addition to accounting for communication delays as well as collision avoidance. Most of the prior work deals with the problem of maintaining connectivity due to the distributed architecture of sensing and communication in multi-agent systems which provides increased efficiency, performance, scalability and robustness. In contradistinction, our work focuses on maintaining connectivity of a mobile network in the presence of an adversarial agent.

In this work, we generalize the work in Chapters 4 and 5 to networks having an arbitrary number of agents possessing different dynamics. We model the problem as a problem of maintaining connectivity in a dynamic graph in which the existence of an edge between two nodes depends on the state of the nodes as well as the jammer. Due to the dependence of the combinatorial structure of the graph on the continuous-time dynamics of the nodes we use the notion of *state-dependent graphs*, introduced in [116], to model the problem. Applying tools from algebraic graph theory on the state-dependent graphs provides us with locally optimal control strategies for the agents as well as the jammer.

The communication model between the nodes and the jamming model are the same as those proposed in Chapter 4. In the next section, we present the dynamics associated with the nodes.

6.2 Dynamic Model of the Nodes

We assume that there are m agents in the network in the presence of a jammer. Let the dynamics associated with the ith agent be given by the following equation:

$$\dot{x}_i = f_i(x_i, u_i) \tag{6.1}$$

where $x_i \in \mathbb{R}^{n_i}$, $u_i \in \mathcal{U}_i \simeq \{\phi : [0,t] \rightarrow \mathcal{A}_i \mid \phi(\cdot) \quad \text{is measurable}\}$, where $\mathcal{A}_i \subset \mathbb{R}^{p_i}$. $f_i : \mathbb{R}^n \times \mathcal{A}_i \rightarrow \mathbb{R}$ is uniformly continuous, bounded and Lipschitz continuous in x_i for fixed u_i. Consequently, given a fixed $u_i(\cdot)$ and initial point, there exists a unique trajectory solving Equation (1) [117]. Let the state of node i be denoted as $x_i \in \mathbf{X}_i \subset \mathbb{R}^{n_i}$.

Let $\mathbf{X}_\bullet$ denote the state-space of the jammer. We assume that the jammer has the following dynamics associated with itself:

$$\dot{x}_\bullet = f_\bullet(x_\bullet, u_\bullet) \tag{6.2}$$

where $x_\bullet \in \mathbb{R}^{n_\bullet}$, $u_\bullet \in \mathcal{U}_\bullet \simeq \{\phi : [0,t] \rightarrow \mathcal{A}_\bullet \mid \phi(\cdot) \quad \text{is measurable}\}$, where $\mathcal{A}_\bullet \subset \mathbb{R}^{p_\bullet}$. $f_\bullet : \mathbb{R}^{n_\bullet} \times \mathcal{A}_\bullet \rightarrow \mathbb{R}$ is uniformly continuous, bounded and Lipschitz continuous in $x_\bullet$ for fixed $u_\bullet$.

Let $\mathbf{X} = \mathbf{X}_1 \times \cdots \times \mathbf{X}_m \times \mathbf{X}_\bullet \subset \bigoplus_i \mathbb{R}^{n_i} \times \mathbb{R}^{n_\bullet}$ represent the entire state of the system, where $\bigoplus$ represents the Cartesian product of the Euclidean spaces $\mathbb{R}^{n_i}$. Let $u = [u_1^T \cdots u_m^T]^T$ be a column vector that represents the control of all the nodes in the network.

We define the *workspace* [118] as the ambient space in which the agents exist. Since we are interested in vehicular networks, the ambient space of the nodes is either $\mathbb{R}^2$ or $\mathbb{R}^3$. As a simple example to highlight the difference between the state space and the workspace, consider the following second order agent that moves in a straight line with u as its control input:

$$\begin{aligned} \dot{x}_1 &= x_2 \\ \dot{x}_2 &= u \end{aligned}$$

where the state-space $[x_1 \quad x_2]^T$ is two-dimensional but the agent can only move on a straight line and hence the workspace is one-dimensional. Since all the agents reside in the same ambient space, we use Ω to denote the workspace for all agents.

In the next section, we present a differential game formulation for the problem of maintaining connectivity among the agents in the presence of the jammer.

6.3 A Differential Game Formulation

The network connectivity maintenance problem can be formulated as the following zero-sum differential game between the jammer and the nodes in the network. Consider a situation in which the network is initially connected in the presence of a jammer. The objective of the jammer is to minimize the time it takes to disconnect the communication network by jamming the communication channel between agents. The objective of the agents is to maximize the time for which the communication link between them remains operable. The game terminates immediately when the agents lose their link. We need to compute the optimal strategy for each agent. In this problem, *disconnection* refers to a situation in which there are agents i and j such that there is no path in the communication network to transmit messages between them. In [6], we address a special case of the above problem in which the network contains two nodes and their dynamics are modeled to resemble those of UAVs and the jammer is another aerial vehicle modeled as a UAV.

In order to compute optimal strategies of the players we need to compute the *saddle-point strategies* since this is a zero-sum game. A set of strategies for the players is said to be in *saddle-point equilibrium* if no unilateral deviation in strategy by a player can lead to a better outcome for that player. Hence there is no motivation for the players to deviate from their equilibrium strategies. In scenarios where the players have no knowledge about each other's strategies, equilibrium strategies are important since they lead to a guaranteed outcome for the players in spite of the other player's strategies.

For a point $\mathbf{x}$ in the state space, let $J(\mathbf{x})$ represent the outcome if the players implement their optimal strategies starting at the point $\mathbf{x}$. In this game, it is the time of termination of the game when the players implement their optimal strategies. It is also called the *value* of the game at $\mathbf{x}$. Assuming that $J(\mathbf{x})$ exists and is

at least $C^2(\mathbf{x})$, we formulate the Hamiltonian of the system:

$$H(\mathbf{x}, \nabla \mathbf{J}, u, u_\bullet) = 1 + \sum_{i=1}^{m} J_{x_i} f_i(x_i, u_i) + J_{x_\bullet} f_\bullet(x_\bullet, u_\bullet) \tag{6.3}$$

Let u^* and $u_\bullet^*$ be the optimal controls used by the agents in the network and the jammer respectively. Since the agents are the maximizer and the jammer is the minimizer, the Hamiltonian of the system satisfies the following conditions along the optimal trajectories [9]. These are the Isaacs conditions.

1. $(u^*, u_\bullet^*) \equiv \arg\max_{u^*} \min_{u_\bullet^*} H(\mathbf{x}, \nabla J, u, u_\bullet)$
2. $H(\mathbf{x}, \nabla J, u^*, u_\bullet^*) = 0$

Since the Hamiltonian is separable in the controls of the individual agents, Isaacs' second condition leads to the following expression for the optimal controls:

1. $u_i^* = \max_{u_i} J_{x_i} f_i(x_i, u_i)$
2. $u_\bullet^* = \min_{u_\bullet} J_{x_\bullet} f_\bullet(x_\bullet, u_\bullet)$

The *retrogressive path equations* [9] for the agents are given as follows:

$$\mathring{J}_{\mathbf{x}} = \frac{\partial H(x, u^*, u_\bullet^*, J_{\mathbf{x}})}{\partial \mathbf{x}} \tag{6.4}$$

The termination conditions are the states of the nodes and the jammer such that the network is disconnected.

The above partial differential equation along with the boundary conditions form the Hamilton-Jacobi-Isaacs (HJI) equations [48]. It is difficult to obtain analytical solutions even for low dimensional systems except for special circumstances. It is a well known fact that these equations suffer from the *curse of dimensionality*. Many computational techniques have been proposed to compute the optimal trajectories for such problems, but they are computationally intensive even for systems evolving in low dimensions [98], [99], [100]. Due to the inherent difficulty in solving the above differential game we formulate the network problem as a game of maintaining connectivity in a dynamic graph. In the next section, we present a transformation from the state space to a state-dependent graph.

6.4 State-Dependent Graphs

In this section, we present a graph-theoretic formulation for the jamming problem under consideration.

The connectivity of the network can be modeled using graphs. In our problem, the connectivity of the network of agents depends on the position of the agents relative to the jammer. Since the agents and the jammer are assumed to be mobile, the connectivity of the network evolves in time, rendering the graph to be a dynamic graph. Since the topology of the graph depends on the state of the nodes, we can use the framework of state-dependent graphs introduced in [116] to map the state of the system to a graph. A state-dependent graph is a mapping, g_c, from the state $\mathbf{X}$, to the set of all labeled graphs on m vertices, $G(m)$, i.e.,

$$g_c : \mathbf{X} \to G(m)$$

It is assumed that the order of these graphs at all times is m since the number of agents is independent of time. Let $E(g_c(x))$ denote the edge-set of the graph under consideration. Now we specify how the existence of a communication link dictates the existence of an edge between a pair of vertices in the state-dependent graph G. For nodes i and j with states $x_i \in \mathbf{X}_i$ and $x_j \in \mathbf{X}_j$ respectively, we consider the subset $S_{ij} \subset \mathbf{X}_i \times \mathbf{X}_j$ to define the edge between i and j if the following condition is satisfied:

$$ij \in E(g_c(x)) \quad \text{if and only if} \quad (x_i, x_j) \in S_{ij} \tag{6.5}$$

The jamming model proposed in Section 6.2 leads to the following definition of S_{ij}. Let $d = \rho(\bar{x}_i, \bar{x}_j)$, where $\bar{x}_i$ and $\bar{x}_j$ are the coordinates of the nodes i and j in the workspace Ω equipped with a distance metric $\rho : \Omega \times \Omega \to \mathbb{R}$. Let $B_r[p] = \{y \in \Omega \mid \rho(y, p) \leq r\}$. From the above discussion we can conclude the following:

$$S_{ij} = \{(x_i, x_j) \mid \bar{x}_\bullet \notin B_{\eta d}[\bar{x}_i] \cup B_{\eta d}[\bar{x}_j]\} \tag{6.6}$$

The above statement along with (5) means that if the jammer lies within a distance ηd from either of the nodes, then the communication channel is assumed to be jammed. The collection of edge states is denoted as

$$\mathcal{S} = \{S_{ij}\}_{i,j\in[N],i\neq j} \quad \text{with} \quad S_{ij} \subset \mathbf{X}_i \times \mathbf{X}_j$$

From [116], the state dependent graph is defined as follows:

Definition: Given the set system $\mathcal{S}$, the map g_c :$\mathbf{X}\rightarrow G_m$ with an image consisting of graphs of order m, having an edge between vertex i and j iff $(x_i, x_j) \in S_{ij}$, is defined as a state-dependent graph with respect to $\mathcal{S}$.

Now that we have a mapping g_c from the state of the system to a graph on m vertices, we can study the properties of the graphs from the properties of the system. In the next section, we provide some properties of the static network that help the agents to localize the jammer using G.

6.5 Jammer Localization in Static Networks

Before moving on to dynamic nodes it is useful to investigate some properties of the mapping g_c for the static case, i.e., when $\dot{x}_i = 0$ for all agents. Our motivation arises from the fact that the jammer does not broadcast its position. Although the location of the jammer can be estimated using on-board sensors, its location can also be estimated using the connectivity of G. According to the communication model, in the absence of the jammer any two nodes in the network can communicate. This implies that the graph G is K_m, i.e., the complete graph on m vertices. In the presence of the jammer in the vicinity, some edges of the graph disappear due to the loss of communication link between specific nodes.

In reference to the state-dependent graph, our interest lies in finding a solution to the following graphical equation:

$$g_c(x) = G \tag{6.7}$$

where the set $\mathcal{S}$ and the function g_c are defined in the previous sections. We assume that each agent knows the position of the other nodes as well as the connectivity of the network. This is a reasonable assumption in a connected communication network in which one node can transmit messages to another node using a single hop or multiple hops. Hence from the known variables x_i and G we want to estimate $x_\bullet$.

The following Lemma provides an estimate of the possible positions of the

jammer.

Lemma 12: Given a state-dependent graph G, the set of possible positions of the jammer is given by the following semi-algebraic set:

$$\bigcup_{ij \notin G} [B_{\frac{\rho(\bar{x}_i, \bar{x}_j)}{\eta}}(\bar{x}_i) \cup B_{\frac{\rho(\bar{x}_i, \bar{x}_j)}{\eta}}(\bar{x}_j)]/$$

$$\bigcup_{ij \in G} [B_{\frac{\rho(\bar{x}_i, \bar{x}_j)}{\eta}}(\bar{x}_i) \cup B_{\frac{\rho(\bar{x}_i, \bar{x}_j)}{\eta}}(\bar{x}_j)]$$

Proof. If $ij \notin G$, the jammer lies in $\bigcup_{ij \notin G}[B_{\frac{\rho(\bar{x}_i, \bar{x}_j)}{\eta}}(\bar{x}_i) \cup B_{\frac{\rho(\bar{x}_i, \bar{x}_j)}{\eta}}(\bar{x}_j)]$. If $ij \in G$, the jammer lies outside $\bigcup_{ij \notin G}[B_{\frac{\rho(\bar{x}_i, \bar{x}_j)}{\eta}}(\bar{x}_i) \cup B_{\frac{\rho(\bar{x}_i, \bar{x}_j)}{\eta}}(\bar{x}_j)]$. Hence the result follows from the two expressions. □

In the next section, we address the case in which the nodes of the network are dynamic.

6.6 Dynamic Networks

In Section 6.4, we presented a graph-theoretic framework to model the connectivity of the dynamic network. In this section, we present control strategies for connectivity maintenance based on the algebraic properties of graphs. In order to do so, we need to define the following mathematical objects associated with a graph G having m nodes:

1. Adjacency matrix : It is an $m \times m$ matrix with entries given as follows:

$$a_{ij} = \begin{cases} 1 & \text{if an edge exists between } i \text{ and } j \\ 0 & \text{if no edge exists between } i \text{ and } j \end{cases}$$

2. Laplacian of a graph ($\mathcal{L}$(G)) : It is an $m \times m$ matrix with entries given as follows:

   (a) $a_{ij} = \begin{cases} -1 & \text{if an edge exists between } i \text{ and } j \\ 0 & \text{if no edge exists between } i \text{ and } j \end{cases}$

   (b) $a_{ii} = -\sum_{k=1, k \neq i}^{m} a_{ik}$

In a dynamic network, since G is a function of **x** its adjacency matrix is also a function of the state **x**. Let **A**(x) denote the adjacency matrix of the graph G.

The element $a_{ij} = 1$ if an edge exists between nodes i and j; otherwise, it is zero. Stated symbolically, $a_{ij} = 1$ *iff* $(x_i, x_j) \in S_{ij}$. Let $d_i = \rho(\bar{x}_\bullet, \bar{x}_i)$, $d_j = \rho(\bar{x}_\bullet, \bar{x}_j)$ and $d_{ij} = \rho(\bar{x}_i, \bar{x}_j)$.

Changes in the adjacency occur at discrete points in time. On the other hand, the dynamics of the nodes and the jammer are continuous in time. In order to relate the discrete-time dynamics of the adjacency matrix to the continuous-time dynamics of the nodes, we use the following continuous approximation for a_{ij}:

$$a_{ij}(\mathbf{x}) = \hat{u}(d_i - \eta d_{ij}) \cdot \hat{u}(d_j - \eta d_{ij})$$

where $\hat{u}(\cdot)$ is a continuous approximation to the Heaviside step function given by the following logistic function:

$$\hat{u}(y) = \frac{1}{1 + e^{-ky}}$$

As $\lim_{k\to\infty}$, the logistic function takes the following form:

$$\hat{u}(y) = \begin{cases} 1 & \text{y}\geq 0 \\ 0 & \text{otherwise} \end{cases}$$

Hence k can be used as a parameter to vary the rate at which the exponential function decays in the neighborhood of zero. The dynamics of the $a_{ij}(\mathbf{x})$ can be written as follows:

$$\dot{a}_{ij}(\mathbf{x}) = \nabla_{\mathbf{x}} a_{ij}(\mathbf{x}) \cdot \dot{\mathbf{x}} \tag{6.8}$$

where $\nabla_{\mathbf{x}} a_{ij}(\mathbf{x})$ denotes the $mn \times 1$ vector which is the gradient of $a_{ij}(\mathbf{x})$ w.r.t. $\mathbf{x}$.

The four important parameters that model the connectivity of a graph G are the following:

1. The minimum degree of G, $d_{min}(G)$
2. The vertex connectivity of G, $\kappa_1(G)$
3. The edge connectivity of G, $\kappa_0(G)$
4. The second smallest eigenvalue of the Laplacian of G, $\lambda_2(\mathcal{L}(G))$ (Fiedler value)

The four quantities are related in the following manner:

$$\lambda_2(\mathcal{L}(G)) \leq \kappa_0(G) \leq \kappa_1(G) \leq d_{min}(G)$$

In this chapter, we use the parameter $\lambda_2(\mathcal{L}(G))$ to study the connectivity maintenance problem.

The second-smallest eigenvalue of $\mathcal{L}(G)$ is called the *Fiedler value*, denoted as $\lambda_2(\mathcal{L}(G))$. It is also called the algebraic connectivity of G. It has emerged as an important parameter in many systems problems defined over networks. In [119], [120], [121], it has also been shown to be a measure of the stability and robustness of the networked dynamic system. Since this chapter deals with connectivity maintenance in the presence of a malicious intruder, $\lambda_2(\mathcal{L}(G))$ arises as a natural parameter of interest for both players.

For a graph G to be connected, $\lambda_2(\mathcal{L}(G)) > 0$ [122]. Therefore, in order to maintain connectivity the nodes in the network must move in the presence of a jammer so as to satisfy the above condition. On the other hand, the jammer must move in such a way to make $\lambda_2(\mathcal{L}(G)) = 0$. In the remainder of this section, we assume that the network is initially connected.

From the above discussion a control law can be designed for the nodes so as to keep $\lambda_2(\mathcal{L}(G))$ a non-decreasing function of time $\implies \frac{\partial(\lambda_2(\mathcal{L}(G)))}{\partial t} \geq 0$. Since $\frac{\partial(\lambda_2(\mathcal{L}(G)))}{\partial t}$ is also a function of the controls of the jammer it might not be possible for the nodes to satisfy the above condition at all times. Instead the following objective leads to a feasible control for the nodes at all times:

$$\text{Maximize} : \quad \frac{\partial(\lambda_2(\mathcal{L}(G)))}{\partial t} \tag{6.9}$$

On the other hand, the jammer must move so as to make $\lambda_2(\mathcal{L}(G)) = 0$. Therefore, a plausible strategy for the jammer is to keep $\lambda_2(\mathcal{L}(G))$ a decreasing function at all times. As in the previous case, such an objective might not lead to a feasible control strategy at all times. Therefore, the jammer can have the following objective in order to yield a feasible control at all times:

$$\text{Minimize} : \quad \frac{\partial\lambda_2(\mathcal{L}(G))}{\partial t} \quad \text{if} \quad \lambda_2 \neq 0 \tag{6.10}$$

Since $\mathcal{L}(G)$ is a symmetric positive semi-definite matrix, all its eigenvalues are non-negative. Therefore the jammer cannot decrease $\lambda_2(\mathcal{L}(G))$ once it reaches 0.

This leads to the additional constraint on its objective.

In order to satisfy the above objective for the players we need a relation between the control of the agents and $\frac{\partial \lambda_2(\mathcal{L}(G))}{\partial t}$. Since $\lambda_2(\mathcal{L}(G))$ is a function of the relative positions of the agents in a network we can get a relation between $\lambda_2(\mathcal{L}(G))$ and the u_i. From [123], we get the following expression:

$$\frac{\partial \lambda_2(\mathcal{L}(G))}{\partial \mathcal{L}} = \frac{v_2 v_2^T}{v_2^T v_2} \tag{6.11}$$

where v_2 is the eigenvalue corresponding to the $\lambda_2(\mathcal{L}(G))$.

Consider agent i having state space $x_i \in \mathbb{R}^{n_i}$. Let $x_i = [x_i^{(1)}, \cdots, x_i^{(n_i)}]^T$. Let $f_i = [f_i^{(1)}, \cdots, f_i^{(n_i)}]^T$. We can use the chain rule to obtain the following expression:

$$\frac{\partial \lambda_2(\mathcal{L}(x))}{\partial x_i^{(k)}} = \langle \frac{\partial \lambda_2(\mathcal{L})}{\partial \mathcal{L}}, \frac{\partial \mathcal{L}}{\partial x_i^{(k)}} \rangle \tag{6.12}$$

where $\langle A, B \rangle \triangleq tr(A^T B)$, an inner product for the space of matrices. Hence we obtain the following relation between $\frac{\partial \lambda_2(\mathcal{L}(G))}{\partial t}$ and the control u_i of each agent:

$$\begin{aligned}\frac{\partial \lambda_2(\mathcal{L}(G))}{\partial t} = \sum_{i=1}^{m} \sum_{k=1}^{n_i} \langle \frac{\partial \lambda_2(\mathcal{L})}{\partial \mathcal{L}}, \frac{\partial \mathcal{L}}{\partial x_i^{(k)}} \rangle f_i^k(x_i^{(k)}, u_i) + \\ \sum_{k=1}^{n_\bullet} \langle \frac{\partial \lambda_2(\mathcal{L})}{\partial \mathcal{L}}, \frac{\partial \mathcal{L}}{\partial x_\bullet^{(k)}} \rangle f_j^{(k)}(x_\bullet^{(k)}, u_\bullet)\end{aligned}$$

Therefore, a locally optimal control law for the agents is a solution of the following optimization problem:

1. Node i: $u_i^* = \max_{u_i} \sum_{k=1}^{n_i} \langle \frac{\partial \lambda_2(\mathcal{L})}{\partial \mathcal{L}}, \frac{\partial \mathcal{L}}{\partial x_i^{(k)}} \rangle f_i^k(x_i^{(k)}, u_i)$

2. Jammer: $u_\bullet^* = \min_{u_\bullet} \sum_{k=1}^{n_\bullet} \langle \frac{\partial \lambda_2(\mathcal{L})}{\partial \mathcal{L}}, \frac{\partial \mathcal{L}}{\partial x_\bullet^{(k)}} \rangle f_j^{(k)}(x_\bullet^{(k)}, u_\bullet)$

In the next section, we present some simulations based on the above control law for the agents.

6.7 Results

We consider a network of agents moving in a plane in the vicinity of a jammer. All the agents, including the jammer, are holonomic kinematic agents with fixed speeds. The differential equation governing the motion of agent i is as follows:

$$x_i = u_i \cos\theta_i$$
$$y_i = u_i \sin\theta_i$$

The differential equation governing the motion of agent i is as follows:

$$x_\bullet = u_\bullet \cos\theta_\bullet$$
$$y_\bullet = u_\bullet \sin\theta_\bullet$$

Using the control laws from the previous section, we obtain the following controls for the agents and the jammer:

1. Node i:
$$(\cos\theta_i, \sin\theta_i) \;||\; (\langle\frac{\partial\lambda_2(\mathcal{L})}{\partial\mathcal{L}}, \frac{\partial\mathcal{L}}{\partial x_i}\rangle, \langle\frac{\partial\lambda_2(\mathcal{L})}{\partial\mathcal{L}}, \frac{\partial\mathcal{L}}{\partial y_i}\rangle)$$

2. Jammer:
$$(\cos\theta_\bullet, \sin\theta_\bullet) \;||\; -(\langle\frac{\partial\lambda_2(\mathcal{L})}{\partial\mathcal{L}}, \frac{\partial\mathcal{L}}{\partial x_\bullet}\rangle, \langle\frac{\partial\lambda_2(\mathcal{L})}{\partial\mathcal{L}}, \frac{\partial\mathcal{L}}{\partial y_\bullet}\rangle)$$

Figures 6.1 and 6.2 show simulations in which the control scheme is implemented. In Figure 6.1, we have 20 agents in a communication network in the presence of a jammer. Half of the agents have speed more than the jammer and rest have speeds less than the jammer. In Figure 6.2, we have 15 agents in a communication network in the presence of a jammer. All the agents have the same speed as the jammer. The simulation continues until the jammer succeeds in disconnecting the network for the first time.

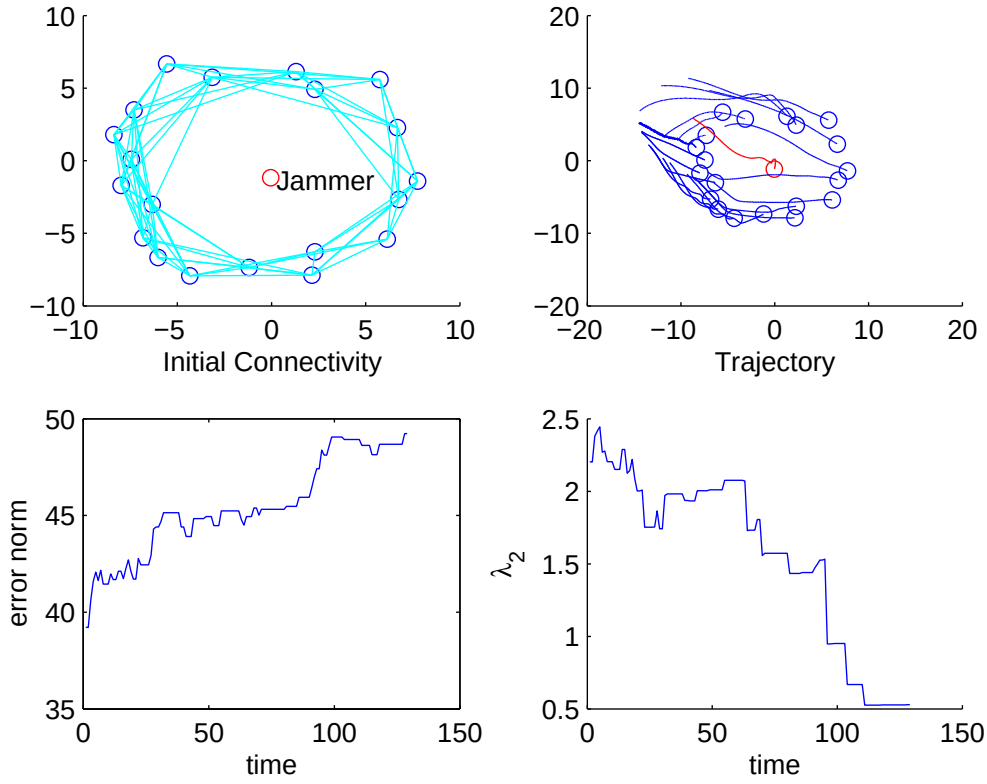

Figure 6.1: Simulation results for twenty agents having the same speed.

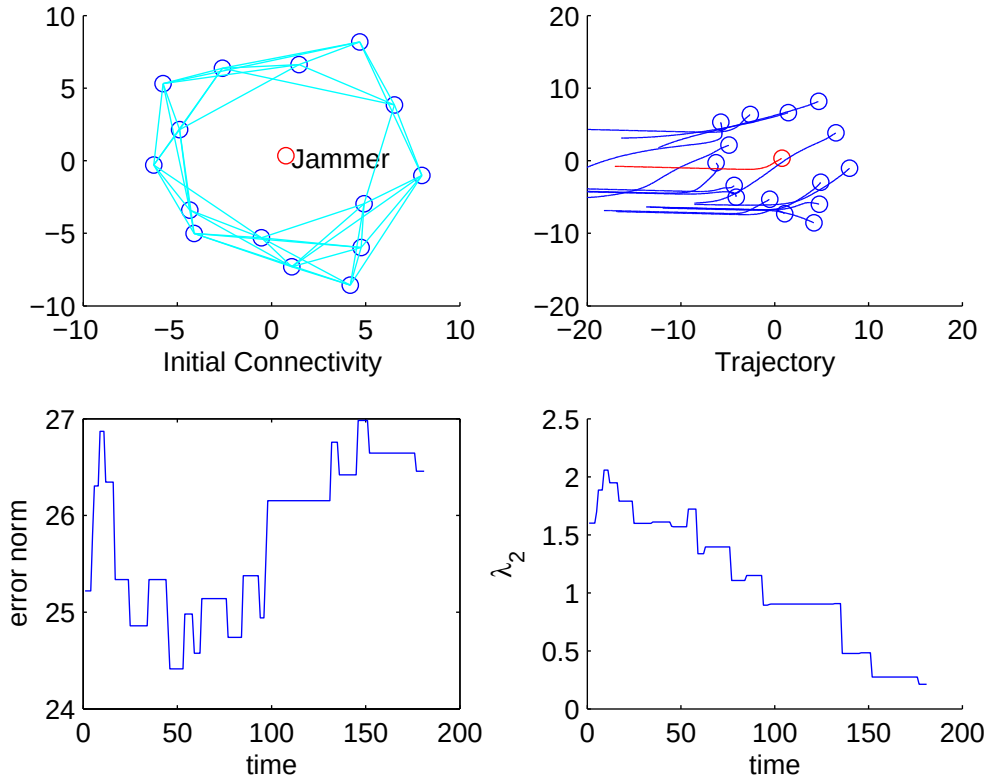

Figure 6.2: Simulation results for fifteen agents having different speeds.

CHAPTER 7

FUTURE RESEARCH

In this chapter, we propose some problems for future research related to each chapter.

7.1 Chapter 2

In Chapter 2, we analyzed the problem of visibility-based pursuit-evasion as a game of kind. We provided a lower bound on the size of the *escape set* and *capture set*. A problem that still remains open is to find an algorithm to completely partition the workspace into *escape set* and *capture set* in the presence of polygonal obstacles. This in turn provides an algorithm to construct the exact barrier surface that separates the two sets.

Another future problem of algorithmic nature that extends the visibility-based pursuit-evasion problem in case of multiple pursuers is the following:

Modified Art Gallery Problem

Consider k pursuers and one evader in a planar environment having polygonal obstacles. The maximum speeds of the pursuers and the evader are $\bar{v}_p$ and $\bar{v}_e$ respectively. The pursuer and the evader are holonomic.

1. All the pursuers and the evader know each other's instantaneous position. All the pursuers know the instantaneous velocity of the evader. Given the initial positions of the pursuers and the evader, does there exist a motion strategy for the pursuers such that at any given time, the evader is visible to at least one pursuer?

2. A pursuer can only know the instantaneous position and velocity of other pursuers in its visibility polygon. Only those pursuers that can see the

evader have the knowledge of evader's instantaneous velocity. Given the initial positions of the pursuers and the evader, does there exist a motion strategy for the pursuers such that at any given time, the evader is visible to at least one pursuer for all future times?

The answers to the above questions will be functions of $\bar{v}_p$ and $\bar{v}_e$. Now we want to answer the following question: What is the minimum number of pursuers sufficient to maintain the visibility of the evader as the function of the ratio of their velocities? The current upper bound is $\lceil \frac{n}{3} \rceil$ for any speed of the pursuers and the evader. An important problem is to reduce this bound as a function of $\bar{v}_p$ and $\bar{v}_e$.

7.2 Chapter 3

In Chapter 3, we used differential game theory to analyze the visbility based pursuit-evasion problem as a game of degree. In addition to the regular analysis, we presented the singular analysis and provided the construction of dispersal surfaces. A future problem is to extend the singular analysis and explore all the possible singular surfaces that occur in the game in order to complete the construction of the optimal trajectories into the entire phase space.

7.3 Chapter 4

In Chapter 4, we considered a differential game theoretic approach to compute optimal strategies by a team of UAVs to evade the attack of an aerial jammer on the communication channel. We considered two variants of the problem in this paper. We formulated the problem as a zero-sum pursuit-evasion game and used Isaacs' approach to derive the necessary conditions to arrive at the equations governing the saddle-point strategies of the players. The cost function was picked as the termination time of the game. We illustrated the results through simulations.

Future work will extend the problem to analyze multiple jammers and multiple UAVs in the formation. Another direction of future research is to extend the locally optimal trajectories presented in this dissertation into the entire phase space. In order to do so, construction of various types of singular surfaces [72] is needed.

7.4 Chapter 5

In Chapter 5, we considered a differential game theoretic approach to compute optimal strategies by a team of vehicles to evade the attack of a jammer on the communication channel. We considered two variants of the problem. We formulated the problem as a zero-sum pursuit-evasion game and used Isaacs' approach to derive the necessary conditions to arrive at the equations governing the saddle-point strategies of the players. The cost function was picked as the termination time of the game. Finally, we derived the equations governing the optimal controls for the vehicles in the case of a UAV and an AGV.

A possibility for future work is to simulate the differential equations governing the evolution of the game for the following cases.

1. UAV jamming a team of AGVs.
2. UAV jamming a team of AGVs and UAVs.
3. AGV jamming a team of AGVs and UAVs.

Further, these problems can be extended to multiple jammers and formations having more than two vehicles. Moreover, restrictions on the proximity of the vehicles can also be included in order to avoid collision.

7.5 Chapter 6

In Chapter 6, we generalized our previous work in [6] to networks having an arbitrary number of agents possessing different dynamics. We modeled the problem from the perspective of maintaining connectivity in a dynamic graph in which the existence of an edge between two nodes depends on the state of the nodes as well as the jammer. Due to the dependence of the combinatorial structure of the graph on the continuous-time dynamics of the nodes, we used the notion of *state-dependent graphs* to model the problem. Applying tools from algebraic graph theory to the state-dependent graphs provided us with locally optimal control strategies for the agents as well as the jammer.

A future research direction is to extend the techniques to agents with non-Euclidean state space. This includes vehicles that have non-holonomic constraints on their motion. Another future research direction is to look into a differential

game-theoretic formulation of the problem in which the payoff of the players is related to the Fiedler value of the proximity graph. Finally, one can extend the techniques to the problems of delay and consensus that arise in cooperative networks in the presence of an antagonistic agent like a jammer.

APPENDIX A

CONSTRUCTION OF THE U SET

Algorithm CONSTRUCTUSET(S,a, e_0)

Input: A set S of disjoint polygonal obstacles, the initial evader position e_0, ratio of maximum evader speed to maximum pursuer speed a

Output: The coordinates of the vertices of the *U set*

for all $E_i \in S$ **do**

l_1 =DIJKSTRA(MVGCONSTRUCT(S,$\mathbf{e}_0$),$\mathbf{e}_0$,E_i)

$h_i(\mathbf{x}) = \hat{\mathbf{n}}_i \cdot (\mathbf{x} - v_i) + \frac{l_1}{a} = 0$

INTERSECTHALFPLANES($h_1^-, ...h_n^-$)

end for

The subroutine DIJKSTRA(G,I,F) computes the least distance between nodes I and F in graph G. The subroutine INTERSECTHALFPLANES($h_1^-, ..., h_n^-$) computes the intersection of the half planes $h_1^-, ..., h_n^-$ [41]. The time complexity of the above algorithm is $O(n^3 \log n)$, where n is the number of edges in the environment.

The subroutine MVGCONSTRUCT(S,$\mathbf{e}_0$) constructs the Modified Visibility Graph of the environment including the initial position of the evader. In addition to the usual Visibility Graph, the Modified Visibility Graph includes for each vertex, v, a list of all edges visible to v and the minimum distance v to the edge. The shortest path from v to an edge E is computed using the $\min\{d(v, E), \min_k\{d_{VG}(v, v_k)+$

$d(v_k, E)\}\}$, where $d_{VG}(v, v_k)$ represents the least distance in the visibility graph between v and v_k [118].

A.1 Boundedness of U Set

For sake of convenience, we restate Lemma 4 from Section 2.2.

Lemma 4: For every edge E_i, there exists a line h_i parallel to E_i and a corresponding half-space h_i^+ such that the pursuer loses the game if $\mathbf{p}_0 \in h_i^+$.

Given an edge E_i and the initial position of the evader, proof of Lemma 4 provides an algorithm to find the line h_i and the corresponding half-plane h_i^+. Now we present some geometrical constructions required to prove the next proposition. Refer to Figure A.1. Consider a convex obstacle. Consider a point c strictly inside the obstacle. For each i, extend the line segment v_ic to infinity in the direction $\vec{v_ic}$ to form the ray cv_i'. Define the region bounded by rays cv_i' and cv_{i+1}' as *sector* $v_i'cv_{i+1}'$. The $sectors$ possess the following properties

1. Any two sectors are mutually disjoint.

2. The union of all the sectors is the entire plane.

We can extend the above idea to any n-sided convex polygon. We use the construction to prove the following proposition.

Proposition 9: In an environment containing a single convex polygonal obstacle, given the initial position of the evader, the initial positions of the pursuer from which it can win the game constitute a bounded subset of the free workspace.

Proof. Refer to Figure A.2. Consider an edge E_i of the convex obstacle with end points v_i and v_{i+1}. WLOG, the obstacle lies below l_{E_i}. Let c be a point strictly

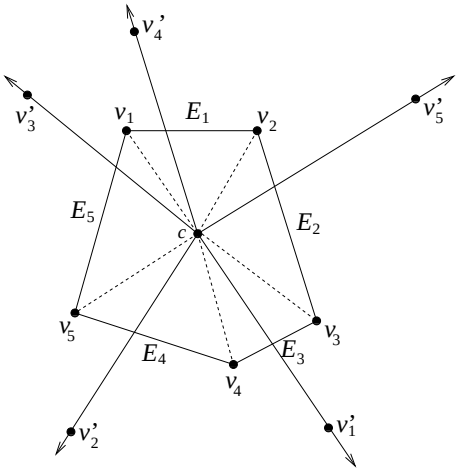

Figure A.1: A polygon and its sectors.

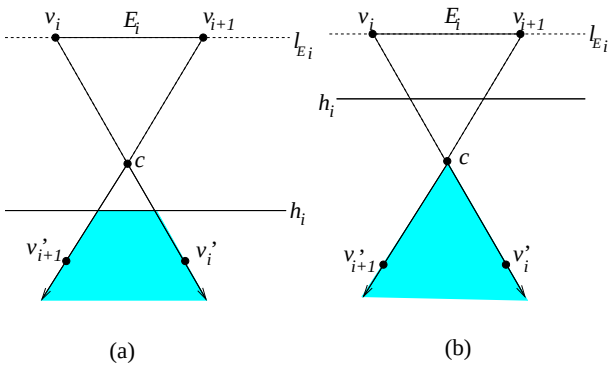

Figure A.2: Proof of Proposition 9.

inside the convex polygon. Extend the line segments v_ic and $v_{i+1}c$ to form *sector* $v'_icv'_{i+1}$. Using Lemma 1, given the initial position of the evader, we can construct a line h_i parallel to E_i such that if the initial pursuer position lies below h_i, the evader wins the game. In case the line h_i intersects the *sector* $v'_icv'_{i+1}$, as shown in Figure A.2(a), the evader wins the game if the initial pursuer position lies in the shaded region. In case the line h_i does not intersect the *sector* $v'_icv'_{i+1}$, as shown in Figure A.2(b), the evader wins the game if the initial pursuer position lies anywhere in the sector. Hence for every sector, there is a region of finite area such that if the initial pursuer position lies in it then it might win the game. Every edge of the polygon has a corresponding sector associated with it. Since each sector has a region of finite area such that if the initial pursuer position lies in it, the pursuer might win the game, the union of all these regions is finite. Hence the proposition follows. □

In the proof of Proposition 9, we generate a bounded set for each convex polygonal obstacle such that the evader wins the game if the initial position of the pursuer lies outside this set. In a similar way, we can generate a bounded set for a non-convex obstacle. Given a non-convex obstacle, we construct its convex-hull. We can prove that Lemma 1 holds true for the convex-hull. Finally, we can use Proposition 9 to prove the existence of a bounded set. For any polygon in the environment, let us call the bounded set generated from Proposition 9 the *B set*.

Recall from Section 2.2 that the *U set* is defined as $\cap_{i=1}^{n} h_i^-$. The next theorem proves that the *U set* generated by a single obstacle is a subset of the *B set* and hence bounded.

Proposition 10: For a given convex obstacle, the *U set* is a subset of the *B set* and hence bounded.

Proof. Consider a point q that does not lie in the *B set*. From the construction of

the *B set*, q must belong to some half-plane h_j^+. If $q \in h_j^+$, then $q \notin h_j^- \implies q \notin \cap_{i=1}^n h_i^-$. This implies that the complement of the *B set* is a subset of the complement of the *U set*. This implies that the *U set* is a subset of the *B set*. □

APPENDIX B

TERMINAL VALUE OF CONTROLS

From the expressions for the optimal controls in Equations (4.4), (4.5) and (4.6) and the terminal values of ∇J, it can be inferred that the value of the optimal controls might not be unique due to the argument of the sign function vanishing at termination. In order to compute the values of optimal control of the players just before termination, we need to compute higher derivatives of the arguments of the sign function till it becomes non-zero.

The optimal control for the players and their higher derivatives at termination are given as follows:

- σ_1^*:

$$\sigma_1^* = -\text{sign}(J_{\phi_1}^0)$$

$$J_{\phi_1}^0 = 0$$

$$\dot{J}_{\phi_1}^0 = 0$$

$$\ddot{J}_{\phi_1}^0 = -\frac{\sigma_1^*}{\eta^2}\sqrt{(x_1^0)^2 + (y_1^0)^2}[\sqrt{(x_j^0)^2 + (y_j^0)^2}(\frac{1}{\eta} - 1) + (x_j^0 - \frac{x_1^0}{\eta^2})]^{-1}$$
$$= \sigma_1^* c_1(\mathbf{x^0}) \tag{B.1}$$

- σ_j^*

$$\sigma_j^* = \text{sign}(J_{\phi_j}^0)$$

$$J^0_{\phi_j} = 0$$

$$\dot{J^0}_{\phi_j} = 0$$

$$\ddot{J^0}_{\phi_j} = -\sigma^*_j \sqrt{(x^0_j)^2 + (y^0_j)^2}[\sqrt{(x^0_j)^2 + (y^0_j)^2}(\frac{1}{\eta} - 1) + (x^0_j - \frac{x^0_1}{\eta^2})]^{-1}$$
$$= \sigma^*_j c_j(\mathbf{x^0}) \tag{B.2}$$

- σ^*_2

$$\sigma^*_2 = -\text{sign}[J_{x_1} y_1 - J_{y_1} x_1 - J_{\phi_1} - J_{\phi_j} - J_{y_j} x_j + J_{x_j} y_j]$$

$$(J_{x_1} y_1 - J_{y_1} x_1 - J_{\phi_1} - J_{\phi_j} - J_{y_j} x_j + J_{x_j} y_j) = 0$$

$$(J_{x_1} y_1 - J_{y_1} x_1 - J_{\phi_1} \dot{-} J_{\phi_j} - J_{y_j} x_j + J_{x_j} y_j) =$$

$$(y^0_j - \frac{y^0_1}{\eta^2})[\sqrt{(x^0_j)^2 + (y^0_j)^2}(\frac{1}{\eta} - 1) + (x^0_j - \frac{x^0_1}{\eta^2})]^{-1} \tag{B.3}$$

From Equation (B.1) we can conclude the following:

- $\ddot{J}^0_{\phi_1} > 0 \Rightarrow \dot{J}^0_{\phi_1} < 0 \Rightarrow J^0_{\phi_1} > 0 \Rightarrow \sigma^*_1 < 0 \Rightarrow c_1(\mathbf{x^0}) < 0$
- $\ddot{J}^0_{\phi_1} < 0 \Rightarrow \dot{J}^0_{\phi_1} > 0 \Rightarrow J^0_{\phi_1} < 0 \Rightarrow \sigma^*_1 > 0 \Rightarrow c_1(\mathbf{x^0}) < 0$

From Equation (B.2) we can conclude the following:

- $\ddot{J}^0_{\phi_j} > 0 \Rightarrow \dot{J}^0_{\phi_j} < 0 \Rightarrow J^0_{\phi_j} > 0 \Rightarrow \sigma^*_j > 0 \Rightarrow c_j(\mathbf{x^0}) > 0$
- $\ddot{J}^0_{\phi_j} < 0 \Rightarrow \dot{J}^0_{\phi_j} > 0 \Rightarrow J^0_{\phi_j} < 0 \Rightarrow \sigma^*_j < 0 \Rightarrow c_j(\mathbf{x^0}) > 0$

From the expressions of σ^*_1 and σ^*_j, we can conclude that $\text{sign}(c_1(\mathbf{x^0})) = \text{sign}(c_j(\mathbf{x^0}))$. This implies that if at termination $c_1(\mathbf{x^0}) < 0$ then $\ddot{J}_{\phi_1} = 0 \Rightarrow \sigma^*_j = 0$, and if $c_j(\mathbf{x^0}) < 0$ then $\ddot{J}_{\phi_j} = 0 \Rightarrow \sigma^*_1 = 0$.

Repeating the same analysis at terminal manifold 2 we get the following values for the $J^0_{y_j}$ and controls at termination:

$$J^0_{y_j} = (y^0_j - y^0_1)[\frac{\sqrt{(x^0_1)^2 + (y^0_1)^2}}{\eta^2} + (\sqrt{(x^0_1)^2 + (y^0_1)^2} +$$

$$\sqrt{(x^0_J)^2 + (y^0_J)^2})(\cos(\phi^0_1 - \phi^0_j) - 1) - \frac{x^0_1}{\eta^2})]^{-1}$$

- σ^*_1:

$$\sigma^*_1 = -\text{sign}(J_{\phi_1})$$

$$J^0_{\phi_1} = 0$$

$$\dot{J}_{\phi_1} = [y^0_j \cos\phi_1 - x^0_j \sin\phi_1]p(\mathbf{x^0})$$

- σ^*_j:

$$\sigma^*_j = \text{sign}(J_{\phi_j})$$

$$J^0_{\phi_j} = 0$$

$$\dot{J^0}_{\phi_j} = [y^0_j \cos\phi_1 - x^0_j \sin\phi_1]p(\mathbf{x^0})$$

- σ^*_2

$$\sigma^*_2 = -\text{sign}[J_{x_1}y_1 - J_{y_1}x_1 - J_{\phi_1} - J_{\phi_j} - J_{y_j}x_j + J_{x_j}y_j]$$

$$(J^0_{x_1}y^0_1 - J^0_{y_1}x^0_1 - J^0_{\phi_1} - J^0_{\phi_j} - J^0_{y_j}x^0_j + J^0_{x_j}y^0_j) = 0$$

$$(J^0_{x_1}y^0_1 - J^0_{y_1}x^0_1 - J^0_{\phi_1} \dot{-} J^0_{\phi_j} - J^0_{y_j}x^0_j + J^0_{x_j}y^0_j) =$$

$$-\frac{y_1}{\eta^2}p(\mathbf{x^0})$$

where $p(\mathbf{x^0}) = [\frac{\sqrt{(x_1^0)^2+(y_1^0)^2}}{\eta^2} + \sqrt{(x_J^0)^2+(y_J^0)^2}(\cos(\phi_1^0 - \phi_j^0) - 1) - \frac{x_1^0}{\eta^2})]^{-1}$.

REFERENCES

[1] S. Bhattacharya, S. Candido, and S. Hutchinson, "Motion strategies for surveillance," in *Robotics: Science and Systems - III*, W. Burgard, O. Brock, and C. Stachniss, Eds. Boston, MA: MIT Press, 2008, pp. 249–256.

[2] S. Bhattacharya and S. Hutchinson, "Approximation schemes for two-player pursuit evasion games with visibility constraints," in *Robotics: Science and Systems IV*, O. Brock, J. Trinkle, and F. Ramos, Eds. Boston, MA: MIT Press, 2009, pp. 81–88.

[3] S. Bhattacharya and S. Hutchinson, "On the existence of Nash equilibrium for a two player pursuit-evasion game with visibility constraints," in *Algorithmic Foundation of Robotics VIII*, G. S. Chirikjian, H. Choset, M. Morales, and T. Murphey, Eds. Berlin, Germany: Springer-Verlag, 2010, pp. 251–265.

[4] S. Bhattacharya, S. Hutchinson, and T. Başar, "Game-theoretic analysis of a visibility based pursuit-evasion game in the presence of obstacles," in *Proceedings of American Control Conference*, St. Louis, MO, June 2009, pp. 373–378.

[5] S. Bhattacharya and S. Hutchinson, "On the existence of Nash equilibrium for a two player pursuit-evasion game with visibility constraints," *International Journal of Robotics Research*, vol. 29, no. 7, pp. 831–839, June 2010.

[6] S. Bhattacharya and T. Başar, "Game-theoretic analysis of an aerial jamming attack on a UAV communication network," in *Proceedings of American Control Conference*, Baltimore, MD, June 2010, to appear.

[7] S. Bhattacharya and T. Başar, "Optimal strategies to evade jamming in heterogeneous mobile networks," in *Proceedings of Workshop on Search and Pursuit-Evasion*, Anchorage, AK, 2010, to appear.

[8] S. Bhattacharya and T. Başar, "Graph-theoretic approach to connectivity maintenance in mobile networks in the presence of a jammer," in *IEEE Conference on Decision and Control*, Atlanta, GA, Dec. 2010, submitted.

[9] R. Isaacs, *Differential Games*. New York, NY: Wiley, 1965.

[10] J. Lewin, *Differential Games: Theory and Methods for Solving Game Problems with Singular Surfaces*. London, England: Springer-Verlag, 1994.

[11] S. M. LaValle and J. Hinrichsen, "Visibility-based pursuit-evasion: The case of curved environments," *IEEE Transactions on Robotics and Automation*, vol. 17, no. 2, pp. 196–201, Apr. 2001.

[12] O.Tekdas, W.Yang, and V.Isler, "Robotic routers: Algorithms and implementation," *International Journal of Robotics Research*, to be published.

[13] A. J. Briggs and B. R. Donald, "Robust geometric algorithms for sensor planning," in *Proceedings of Second Workshop on Algorithmic Foundations of Robotics*, J.-P. Laumond and M. Overmars, Eds. Wellesley, MA: A. K. Peters Ltd., 1996, pp. 197–212.

[14] D. Hsu, W. Lee, and N. Rong, "A point-based POMDP planner for target tracking," in *Proceedings of IEEE International Conference on Robotics and Automation*, 2008, pp. 2644–2650.

[15] T. Y. Li, J. M. Lien, S. Y. Chiu, and T. H. Yu, "Automatically generating virtual guided tours," in *Computer Animation Conference*, 1997, pp. 99–106.

[16] T. L. Sung and T. Y. Um, "Practical guidance for homing missiles with bearings-only measurements," *IEEE Transactions on Aerospace and Electronic Systems*, vol. 32, no. 1, pp. 434–443, Jan. 1996.

[17] B. Espiau, F. Chaumette, and P. Rives, "A new approach to visual servoing in robotics," *IEEE Transactions on Robotics and Automation*, vol. 8, no. 3, pp. 313–326, 1992.

[18] E. Malis, F. Chaumette, and S. Boudet, "2D 1/2 visual servoing," *IEEE Transactions on Robotics and Automation*, vol. 15, no. 2, pp. 238–250, 1999.

[19] E. Marchand, P. Bouthemy, F. Chaumette, and V. Moreau, "Robust real-time visual tracking using a 2d-3d model-based approach," in *IEEE International Conference on Computer Vision*, vol. 1, 1999, pp. 262–268.

[20] S. A. Hutchinson, G. D. Hager, and P. I. Corke, "A tutorial on visual servo control," *IEEE Transactions on Robotics and Automation*, vol. 12, no. 5, pp. 651–670, 1996.

[21] A. Efrat, H. Gonzalez-Banos, S. Kobourov, and L. Palaniappan, "Optimal strategies to track and capture a predictable target," in *Proceedings of IEEE International Conference on Robotics and Automation*, vol. 3, 2003, pp. 411–423.

[22] S. M. LaValle, H. H. Gonzalez-Banos, C. Becker, and J. C. Latombe, "Motion strategies for maintaining visibility of a moving target," in *Proceedings of IEEE International Conference on Robotics and Automation*, vol. 1, Albuquerque, NM, USA, Apr. 1997, pp. 731–736.

[23] W. Cheung, "Constrained pursuit-evasion in the plane," M.S. thesis, University of British Columbia, September 2005.

[24] M. Sipser, *Introduction to Theory of Computation*. Boston, MA: PWS, 1997.

[25] R. Murrieta-Cid, B. Tovar, and S. Hutchinson, "A sampling based motion planning approach to maintain visibility of unpredictable moving targets," *Journal on Autonomous Robots*, vol. 19, no. 3, pp. 285–300, Dec. 2005.

[26] H. Gonzalez-Banos, C. Lee, and J. Latombe, "Real-time combinatorial tracking of a target moving unpredictably among obstacles," in *Proceedings of IEEE International Conference on Robotics and Automation*, vol. 2, 2002, pp. 1683–1690.

[27] T. Bandyopadhyay, Y. Li, M. Ang Jr., and D. Hsu, "A greedy strategy for tracking a locally predictable target among obstacles," in *Proceedings of IEEE International Conference on Robotics and Automation*, 2006, pp. 2342–2347.

[28] T. Bandyopadhyay, Y. Li, M. Ang Jr., and D. Hsu, "Stealth tracking of an unpredictable target among obstacles," in *Algorithmic Foundations of Robotics VI*, M. O. M. Erdmann, D. Hsu and A. F. van der Stappen, Eds. Berlin, Germany: Springer-Verlag, 2004, pp. 43–58.

[29] T. Bandyopadhyay, N. Rong, M. Ang Jr., D. Hsu, and W. Lee, "Motion planning for people tracking in uncertain and dynamic environments," presented at the Workshop on People Detection and Tracking, IEEE International Conference on Robotics and Automation, 2009.

[30] P. Fabiani and J. Latombe, "Tracking a partially predictable object with uncertainty and visibility constraints: A game-theoretic approach," in *International Joint Conference on Artificial Intelligence*, vol. 2, 1999, pp. 942–947.

[31] R. Murrieta-Cid, H. H. Gonzalez-Banos, and B. Tovar, "A reactive motion planner to maintain visibility of unpredictable targets," in *Proceedings of IEEE International Conference on Robotics and Automation*, vol. 4, 2002, pp. 4242–4248.

[32] R. Murrieta-Cid, T. Muppirala, A. Sarmiento, S. Bhattacharya, and S. Hutchinson, "Surveillance strategies for a pursuer with finite sensor

range," *International Journal of Robotics Research*, vol. 26, no. 3, pp. 1548–1553, March 2007.

[33] J. Schwartz and M. Sharir, "On the piano mover's problem: I. The case of a two-dimensional rigid polygonal body moving amidst polygonal barriers," *Communications on Pure and Applied Mathematics*, vol. 36, no. 3, pp. 345–398, 1983.

[34] R. Murrieta-Cid, R. Monroy, S. Hutchinson, and J. P. Laumond, "A complexity result for the pursuit-evasion game of maintaining visibility of a moving evader," in *Proceedings of IEEE International Conference on Robotics and Automation*, 2008, pp. 2657–2664.

[35] L. Parker, "Algorithms for multi-robot observation of multiple targets," *Journal on Autonomous Robots*, vol. 12, pp. 231–255, 2002.

[36] B. Jung and G. Sukhatme, "Tracking targets using multiple robots: The effect of environment occlusion," *Autonomous Robots*, vol. 13, no. 3, pp. 191–205, 2002.

[37] A. Kolling and S. Carpin, "Multirobot cooperation for surveillance of multiple moving targets: A new behavioral approach," in *Proceedings of IEEE Conference on Robotics and Automation*, 2006, pp. 1311–1316.

[38] A. Kolling and S. Carpin, "Cooperative observation of multiple moving targets: An algorithm and its formalization," *International Journal of Robotics Research*, vol. 26, no. 9, pp. 935–953, 2007.

[39] Z. Tang and U. Ozguner, "Motion planning for multitarget surveillance with mobile sensor agents," *IEEE Transactions on Robotics and Automation*, vol. 21, no. 5, pp. 898–908, Oct. 2005.

[40] S. Luke, K. Sullivan, L. Panait, and G. Balan, "Tunably decentralized algorithms for cooperative target observation," in *International Joint Conference on Autonomous Agents and Multiagent Systems*, July 2005, pp. 911–917.

[41] M. de Berg, M. van Kreveld, M. Overmars, and O. Schwarzkopf, *Computational Geometry: Algorithms and Applications*. Berlin, Germany: Springer-Verlag, 1997.

[42] J. E. Goodman and J. O. Rourke, *Handbook of Discrete and Computational Geometry*. New York, NY: CRC Press, 1997.

[43] J. V. Breakwell and A. W. Merz, "Towards a solution of the homicidal chauffeur game," presented at the First International Conference of the Theory and Application of Differential Games, Amherst, MA, 1969.

[44] J. V. Breakwell, "Some differential games with interesting discontinuities," University of Stanford, Stanford, CA, Tech. Rep., 1973.

[45] D. Leshem, "Composite barriers and corner conditions in differential games," Ph.D. dissertation, Stanford University, Stanford, CA, 1985.

[46] J. R. Isbell, "Pursuit around a hole," *Naval Research Logistics Quarterly*, vol. 14, no. 4, pp. 569–571, Aug. 2006.

[47] A. Blaquière, F. Gerard, and G. Leitmann, *Quantitative and Qualitative Games*. New York, NY: Academic Press, 1969.

[48] T. Başar and G. J. Olsder, *Dynamic Noncooperative Game Theory*, 2nd ed. Philadelphia, PA: SIAM, 1999.

[49] T. Başar and P. Bernhard, *H-infinity Optimal Control and Related Minimax Design Problems: A Dynamic Game Approach*. Boston, MA: Birkhauser, August 1995.

[50] Y. C. Ho and G. J. Olsder, "Differential games: Concepts and applications," in *Mathematics of Conflict*, M. Shubik, Ed. North-Holland, Amsterdam, The Netherlands: Elsevier, 1983, pp. 127–186.

[51] H. E. Scarf, "On differential games with survival payoff," *Annals of Mathematical Studies*, vol. 3, no. 39, pp. 393–406, 1957.

[52] W. Fleming, "A note on differential games of prescribed duration," *Annals of Mathematical Studies*, vol. 13, no. 39, pp. 407–416, 1957.

[53] W. H. Fleming, "The convergence problem for differential games," *Journal for Mathematical Analysis and Applications*, vol. 3, pp. 102–116, 1961.

[54] W. H. Fleming, "The convergence problem for differential games," in *Annals of Mathematics*. Princeton, NJ: Princeton University Press, 1964, no. 52, pp. 195–210.

[55] P. P. Varaiya, "On the existence of solutions to a differential game," *SIAM Journal on Control*, vol. 5, no. 1, pp. 153–162, 1967.

[56] P. Varaiya and J. Lin, "Existence of saddle points in differential games," *SIAM Journal on Control*, vol. 7, no. 1, pp. 141–157, 1969.

[57] R. J. Elliott, N. J. Kalton, and L. Markus, "Saddle points for linear differential games," *SIAM Journal on Control*, vol. 11, no. 1, pp. 100–112, 1973.

[58] R. J. Elliott and N. J. Kalton, "The existence of value in differential games of pursuit and evasion," *Journal of Differential Equations*, vol. 12, pp. 504–523, 1972.

[59] W. Fleming, "The cauchy problem for degenerate parabolic equations," *Journal of Mathematical Mechanics*, vol. 13, pp. 987–1008, 1964.

[60] A. Friedman, *Differential Games*. New York, NY: Wiley, 1971.

[61] R. J. Elliott and N. J. Kalton, "Cauchy problems for certain Isaacs-Bellman equations and games of survival," *Transactions of American Mathematical Society*, vol. 198, pp. 45–72, 1974.

[62] R. J. Elliott and N. J. Kalton, "Boundary value problems for nonlinear partial differential operators," *Journal of Mathematical Analysis and Applications*, vol. 46, pp. 228–241, 1974.

[63] N. Krassovski and A. Subbottin, *Jeux Differentiels*. Moscow, Russia: Mir Press, 1977.

[64] A. Subbottin, "A generalization of the basic equation of the theory of differential games," *Soviet Mathematics Doklady*, no. 22, pp. 358–362, 1980.

[65] M. G. Crandall and P. L. Lions, "Viscosity solutions of Hamilton-Jacobi equations," *Transactions of the American Mathematical Society*, vol. 277, no. 1, pp. 1–42, 1976.

[66] P. L. Lions, *Generalized Solutions of Hamilton-Jacobi Equations*. Boston, MA: Pitman, 1982.

[67] P. E. Souganidis, "Approximation schemes for viscosity solutions of Hamilton-Jacobi equations," Ph.D. dissertation, University of Wisconsin-Madison, 1983.

[68] L. C. Evans and P. E. Souganidis, "Differential games and representation formulas for solutions of Hamilton-Jacobi-Isaacs equations," *Indiana University Mathematics Journal*, vol. 33, no. 5, pp. 773–797, 1984.

[69] M. Bardi, M. Falcone, and P. Soravia, "Numerical methods for pursuit-evasion games via viscosity solutions," in *Stochastic and Differential Games: Theory and Numerical Methods*. Boston, MA: Birkhauser, 1999, pp. 105–176.

[70] I. M. Mitchell, "Application of level set methods to control and reachability problems in continuous and hybrid systems," Ph.D. dissertation, Stanford University, Stanford, CA, August 2002.

[71] I. M. Mitchell, A. M. Bayen, and C. J. Tomlin, "A time-dependent Hamilton-Jacobi formulation of reachable sets for continuous dynamic games," *IEEE Transactions on Automatic Control*, vol. 50, no. 7, pp. 947–957, July 2005.

[72] A. A. Melikyan, *Generalized Characteristics of First Order PDEs: Applications in Optimal Control and Differential Games*. Boston, MA: Birkhauser, 2000.

[73] P. Bernhard, "Singular surfaces in differential games: An introduction," in *Differential Games and Applications*. Berlin, Germany: Springer-Verlag, 1977, pp. 1–33.

[74] A. A. Melikyan and N. V. Hovakimyan, "Singular trajectories in the game of simple pursuit in the manifold," *Journal of Applied Mathematics and Mechanics*, vol. 55, no. 1, pp. 42–48, 1991.

[75] A. A. Melikyan and N. V. Hovakimyan, "Game problem of simple pursuit on a two-dimensional cone," *Journal of Applied Mathematics and Mechanics*, vol. 55, no. 5, pp. 607–618, 1991.

[76] A. A. Melikyan, N. V. Hovakimyan, and L. Harutunian, "Games of simple pursuit and approach on a two-dimensional cone," *Journal of Optimization Theory and Applications*, vol. 98, no. 3, pp. 515–543, 1998.

[77] N. V. Hovakimyan and L. Harutunian, "Game problems on rotation surfaces," *International Journal of Game Theory*, vol. 9, no. 2, pp. 117–129, 1999.

[78] X. C. Ding, A. Rahmani, and M. Egerstedt, "Optimal multi-UAV convoy protection," in *Conference on Robot Communication and Configuration*, vol. 9, no. 5, April 2009, pp. 1–6.

[79] J. Tisdale, Z. Kim, and J. Hedrick, "Autonomous UAV path planning and estimation," *IEEE Robotics and Automation Magazine*, vol. 16, pp. 35–42, 2009.

[80] C. G. Valicka, S. R. Bieniawski, J. Vian, and D. M. Stipanović, "Cooperative avoidance control for UAVs," in *Proceedings of the Tenth International Conference on Control, Automation, Robotics and Vision*, 2008, to appear.

[81] M. Pavone, K. Savla, and E. Frazzoli, "Sharing the load: Mobile robotic networks in dynamic environments," *IEEE Robotics and Automation Magazine*, vol. 16, pp. 52–61, 2009.

[82] T. Samad, J. S. Bay, and D. Godbole, "Network-centric systems for military operations in urban terrian: The role of UAVs," *Proceedings of the IEEE*, vol. 95, no. 1, pp. 92–107, 2007.

[83] W. Xu, T. Wood, W. Trappe, and Y. Zhang, "Channel surfing and spatial retreats: Defenses against wireless denial of service," in *3rd ACM Workshop on Wireless Security*, 2004, pp. 80–89.

[84] A. D. Wood, J. A. Stankovic, and S. H. Son, "Jam: A jammed-area mapping service for sensor networks," in *Proceedings of 24th IEEE Real-Time Systems Symposium*, December 2003, pp. 286–297.

[85] M. Cagalj, S. Capcun, and J. P. Hubaux, "Wormhole-based anti-jamming techniques in sensor networks," *IEEE Transactions on Mobile Computing*, vol. 6, pp. 100–114, January 2007.

[86] A. D. Wood, J. A. Stankovic, and G. Zhou, "Deejam: Defeating energy-efficient jamming in IEEE 802.15.4 based wireless networks," in *4th Annual IEEE Conference on Sensor, Mesh and Ad Hoc Communications and Networks (SECON 07)*, 2007, pp. 60–69.

[87] L. Chen, "On selfish and malicious behaviours in wireless networks - a non-cooperative game theoretic approach," Ph.D. dissertation, Ecole Nationale Superieure des Telecommunications, Paris, France, October 2008.

[88] A. G. Pashkov and S. D. Terekhov, "A differential game of approach with two pursuers and one evader," *Journal of Optimization Theory and Applications*, vol. 55, pp. 303–311, July 1987.

[89] A. Y. Levchenkov and A. G. Pashkov, "Differential game of optimal approach of two inertial pursuers to a noninertial evader," *Journal of Optimization Theory and Applications*, vol. 65, pp. 501–518, June 1990.

[90] P. Hagedorn and J. V. Breakwell, "A differential game of approach with two pursuers and one evader," *Journal of Optimization Theory and Applications*, vol. 18, pp. 15–29, 1976.

[91] J. V. Breakwell and P. Hagedorn, "Point capture of two evaders in succession," *Journal of Optimization Theory and Applications*, vol. 27, pp. 89–97, 1979.

[92] S. Shankaran, D. Stipanović, and C. Tomlin, "Collision avoidance strategies for a three player game," *Annals of International Society of Dynamic Games*, 2010, to appear.

[93] J. V. Breakwell and P. Hagedorn, "Further properties of non-zereo sum differential games," *Journal of Optimization Theory and Applications*, vol. 3, pp. 207–219, 1969.

[94] E. M. Vaisbord and V. I. Zhukovskiy, *Introduction to Multi-Player Differential Games and their Applications*. New York, NY: Gordon and Breach, 1988.

[95] V. I. Zhukovskiy and M. E. Salukvadze, *The Vector Valued Maxmin*. San Diego, CA: Academic Press, 1994.

[96] D. M. Stipanović, A. A. Melikyan, and N. V. Hovakimyan, "Some sufficient conditions for multi-player pursuit evasion games with continuous and discrete observations," *Annals of the International Society of Dynamic Games*, vol. 10, pp. 133–145, 2009.

[97] D. Stipanović, A. Melikyan, and N. Hovakimyan, "Guaranteed strategies for nonlinear multi-player pursuit-evasion games," *International Game Theory Review*, 2010, to appear.

[98] I. M. Mitchell and C. J. Tomlin, "Overapproximating reachable sets by Hamilton-Jacobi projections," *Journal of Scientific Computing*, vol. 19, pp. 323–346, 2003.

[99] D. M. Stipanović, I. Hwang, and C. J. Tomlin, "Computation of an overapproximation of the backward reachable set using subsystem level set functions," *Dynamics of Continuous, Discrete and Impulsive Systems*, vol. 11, pp. 399–411, 2004.

[100] D. M. Stipanović, S. Shankaran, and C. Tomlin, "Strategies for agents in multi-player pursuit-evasion games," presented at the Eleventh International Symposium on Dynamic Games and Applications, Tucson, AZ, 2006.

[101] P. Papadimitratos and Z. J. Haas, "Secure routing for mobile ad-hoc networks," in *Communication Networks and Distributed Systems Modeling and Simulation Conference*, January 2002, pp. 27–31.

[102] G. Noubir and G. Lin, "Low power denial of service attacks in data wireless LANs and countermeasures," *Mobile Computing and Communications Review*, vol. 7, pp. 29–30, July 2003.

[103] R. A. Poisel, *Modern Communication Jamming Principles and Techniques*. Norwood, MA: Artech, 2004.

[104] J. J. Proakis and M. Salehi, *Digital Communications*. New York, NY: McGraw-Hill, 2007.

[105] P. B. Sujit and R. Beard, "Multiple UAV path planning using anytime algorithms," in *Proceedings of American Control Conference*, St. Louis, MO, June 2009, pp. 2978–2983.

[106] J. P. Laumond, S. Sekhavat, and F. Lamiraux, *Guidelines in Nonholonomic Motion Planning for Mobile Robots*. Berlin, Germany: Springer, 1998.

[107] M. M. Zavlanos and G. J. Pappas, "Potential fields for maintaining connectivity of mobile networks," *IEEE Transactions on Robotics*, vol. 23, pp. 812–816, August 2007.

[108] M. M. Zavlanos and G. J. Pappas, "Controlling connectivity of dynamic networks," in *IEEE Conference on Decision and Control*, Seville, Spain, December 2005, pp. 6388–6393.

[109] D. P. Spanos and R. M. Murray, "Robust connectivity of networked vehicles," in *IEEE Conference on Decision and Control*, Bahamas, December 2004, pp. 2893–2898.

[110] M. Ji and M. Egerstedt, "Distributed formation control while preserving connectedness," in *IEEE Conference on Decision and Control*, San Diego, CA, December 2006, pp. 5962–5967.

[111] M. Ji and M. Egerstedt, "Connectedness preserving distributed coordination control among dynamic graphs," in *Proceedings of American Control Conference*, Portland, OR, June 2005, pp. 93–98.

[112] M. C. DeGennaro and A. Jadbabaie, "Decentralized control of connectivity for multiagent systems," in *IEEE Conference on Decision and Control*, San Diego, CA, December 2006, pp. 3628–3633.

[113] G. Notarstefano, K. Savla, F. Bullo, and A. Jadbabaie, "Maintaining limited-range connectivity among second order agents," in *Proceedings of American Control Conference*, Minneapolis, MN, June 2006, pp. 2124–2129.

[114] M. M. Zavlanos and G. J. Pappas, "Distributed connectivity control of mobile networks," in *IEEE Conference on Decision and Control*, New Orleans, LA, December 2007, pp. 3591–3596.

[115] M. M. Zavlanos and G. J. Pappas, "Distributed connectivity control of mobile networks," *IEEE Transactions on Robotics*, vol. 24, pp. 1416–1428, 2008.

[116] M. Mesbahi, "On state-dependent dynamic graphs and their controllability properties," *IEEE Transactions on Automatic Control*, vol. 50, pp. 387–392, 2005.

[117] V. I. Arnold, *Geometric Method in the Theory of Ordinary Differential Equations*. New York, NY: Springer-Verlag, 1983.

[118] H. Choset, K. Lynch, S. Hutchinson, G. Kantor, W. Burgard, L. Kavraki, and S. Thrun, *Principles of Robot Motion: Theory, Algorithms, and Implementations*. Cambridge, MA: The MIT Press, 2005.

[119] J. A. Fax and R. M. Murray, "Information flow and cooperative control of vehicle formations," *IEEE Transactions on Automatic Control*, vol. 9, pp. 1465–1474, 2004.

[120] R. Olfati-Saber and R. M. Murray, "Consensus problems in networks of agents with switching topology and time delay," *IEEE Transactions on Automatic Control*, vol. 49, no. 9, pp. 1520–1533, 2004.

[121] H. Tanner, A. Jadbabaie, and G. Pappas, "Flocking in fixed and switching networks," *IEEE Transactions on Automatic Control*, vol. 5, pp. 863–868, May 2007.

[122] N. Biggs, *Algebraic Graph Theory*. Cambridge, U.K.: Cambridge University Press, 1993.

[123] E. Stump, A. Jadbabaie, and V. Kumar, "Connectivity management in mobile robot teams," in *Proceedings of IEEE International Conference on Robotics and Automation*, vol. 9, May 2008, pp. 1525–1530.